MASTER THESIS

The impact of overnutrition and oxidative stress on Apolipoprotein O

Theresa Hohl, BSc

under the supervision of

Ao. Univ.-Prof.in Mag.a Dr.in rer.nat.techn. Hilde Laggner

Univ.Prof. Mag. Dr.rer.nat.Robert Mach

Center for Pathobiochemistry and Genetics

Medical University Vienna

January 2023

Acknowledgments

First of all, I would like to express my deepest gratitude to Dr. Hilde Laggner. Besides enabling me to be part of the interesting research at the Center for Pathobiochemistry and Genetics, she offered the best possible supervision. I want to thank her for guiding me individually through my practical work and the process of thesis writing. I especially appreciate her expertise, enthusiasm, patience, and trust in me.

Moreover, I am grateful to Dr. Robert Mach for guiding me through administrative responsibilities and always being open to my suggestions and questions, thus helping me greatly with my thesis.

Also, many thanks to the colleagues of the institute for their open kind, and successful cooperation. I could not have imagined a better place and atmosphere for performing my thesis.

Finally, I want to acknowledge the immense support from my family for always believing in and bringing out the best in me. Without them, I would not be where I am today, both academically and personally.

Abstract

Today's fast-paced lifestyle has a major impact on human health and is the source of several disorders. Together with the obesity epidemic, the prevalence of non-alcoholic fatty liver disease, NAFLD, has become a worldwide challenge for modern medicine. Thus, it is crucial to gain a better understanding of NAFLD and its effect on lipid metabolism, in which apolipoproteins are of considerable physiological importance. A recently discovered apolipoprotein, apolipoprotein O, appears to be involved in lipid metabolism and consequently in the pathobiochemistry of NAFLD.

In this thesis, the effect of overnutrition on liver cells was simulated by treating HepG2 cells, a human hepatoma cancer cell line, with oleic acid. Hence, lipid accumulation – as it occurs in NAFLD – is mediated. Furthermore, a more progressive form of NAFLD, which is characterized by inflammation, was mimicked by the addition of tumor necrosis factor α and menadione. Within this setting, the protein production of apolipoprotein O was studied.

After exposing the cells for 24 h to 0.5 mM and 1 mM oleic acid, an estimated 3-fold increase of intracellular triglyceride content was observed. However, the cytotoxic impact on the cells drastically increased by the incubation with concentrations higher than 0.5 mM oleic acid. Furthermore, it was observed that serum starvation for 24 h before the treatment might support triglyceride accumulation.

Even though only small effects of oleic acid on apolipoprotein O protein production were measured, it seems to be promoted by triglyceride deposition after 24 h of incubation with oleic acid. While tumor necrosis factor α and menadione did not affect the intracellular triglyceride level, contradictory outcomes were recorded regarding the effect on the protein content of apolipoprotein O. Overall, the data suggest a small decrease of apolipoprotein O protein production after the addition of the two stress factors. Moreover, the activation of the nuclear factor-kappa B pathway, monitored by two transcription factors, was achieved by tumor necrosis factor α and to a smaller extent also by menadione.

When oleic acid and stress factors were simultaneously added to the cells, a slightly inhibited apolipoprotein O protein production might have been examined. However, the results do not reflect a uniform phenomenon. Nevertheless, possible protective properties of oleic acid in the inflammatory process have to be considered.

Overall, assessing the impact of overnutrition and oxidative stress on the production of apolipoprotein O remains difficult. Further research on finding the balance between lipid accumulation and lipotoxicity as well as the reflection of the biochemical processes inside liver cells is required.

Zusammenfassung

Der Lebensstil der mit unserer schnelllebigen Welt einhergeht beeinflusst maßgebend die Gesundheit der Menschen. Nicht nur die Adipositas-Epidemie, sondern auch die Verbreitung der nicht-alkoholischen Fettleber-Erkrankung, NAFLD, stellen weltweite Herausforderungen für die moderne Medizin dar. Um ein besseres Verständnis über NAFLD zu bekommen werden die Effekte von NAFLD auf den Lipidstoffwechsel, in dem Apolipoproteine eine wesentliche physiologische Bedeutung einnehmen, untersucht. Ein kürzlich entdecktes Apolipoprotein, Apolipoprotein O, scheint im Lipidstoffwechsel eine Rolle zu spielen, und dadurch möglicherweise in der Pathobiochemie von NAFLD.

Im Rahmen dieser Arbeit wurde der Effekt von Überernährung in Leberzellen simuliert. Dafür wurden HepG2 Zellen, eine humane Leberkrebszelllinie, herangezogen und mit Ölsäure inkubiert. Es erfolgte eine Lipidanreicherung, ähnlich wie bei NAFLD. Darüber hinaus wurde eine progressivere und fortgeschrittenere Form von NAFLD untersucht. Für dieses Stadium sind Entzündungen charakteristisch, die hier durch die Zugabe von Tumornekrosefaktor α und Menadion ausgelöst wurden. Schließlich wurde innerhalb dieser Bedingungen die Produktion von Apolipoprotein O untersucht.

Eine Inkubation der Zellen mit 0.5 mM und 1 mM Ölsäure für 24 h Stunden führte zu einem etwa dreifach höheren Triglycerid-Spiegel verglichen mit der Kontrollprobe. Allerdings wurden deutlich erhöhte cytotoxische Effekte beobachtet, wenn die Zellen mit Ölsäure Konzentrationen über 0.5 mM versetzt wurden. Außerdem wurde festgestellt, dass ein Serumentzug von 24 h vor der Inkubation mit der Ölsäure die Triglycerid-Anreicherung möglicherweise fördert.

Allgemein konnten nur geringe Effekte auf die Apolipoprotein O-Produktion gemessen werden. Trotzdem scheint eine Triglycerid-Anreicherung, wie sie nach 24 h Inkubation mit Ölsäure erreicht wurde, die Proteinproduktion zu fördern. Der Einsatz der zwei Stressfaktoren, Tumornekrosefaktor α und Menadion, beeinflusste den Triglycerid-Gehalt nicht, lieferte jedoch widersprüchliche Ergebnisse in Bezug auf die Apolipoprotein O-Synthese. Die ermittelten Daten deuten auf einen verringerten Gehalt an intrazellulären Apolipoprotein O durch die Anwesenheit der Stressfaktoren hin. Des Weiteren wurde die Aktivierung des nuklearfaktor kappa B Signalwegs durch Tumornekrosefaktor α und, zu einem kleineren Ausmaß, durch Menadion nachgewiesen.

Schließlich wurden die Zellen mit einer Kombination aus Ölsäure und Stressfaktoren inkubiert, wodurch vermutlich eine geringe Inhibierung der Apolipoprotein O-Produktion stattfand. Darüber hinaus wurden mögliche protektive Effekte der Ölsäure beobachtet, die bei einer Simulation von Entzündungsreaktionen zu hinterfragen sind.

Insgesamt bleibt es weiterhin schwierig eindeutige Aussagen über dem Zusammenhang von Überernährung und oxidativen Stress auf die Apolipoprotein O-Produktion zu treffen. In Zukunft gilt es das Gleichgewicht zwischen Lipidanreicherung und Lipidtoxizität zu finden, sowie geeignete Bedingungen zu definieren, die möglichst genau die zellulären Prozesse der Leber wiedergeben.

Table of contents

1 Introduction

1.1 Lipoproteins

1.1.1 Structure

Lipoproteins are soluble complexes consisting of proteins and lipids [1] and are crucial for the transportation of lipids through the blood. For transportation, lipids can either be bound to specific proteins, like steroid hormones to sex hormone-binding globulin, or be enclosed in a micellar complex, forming lipoproteins [2].

Lipids of the blood plasm can generally be divided into hydrophobic and amphiphilic lipids. Fatty acids, phospholipids, and free cholesterol belong to the latter lipids. Most fatty acids are bound to albumin, while phospholipids, mainly lecithin and sphingomyelin, are surface-active substances and can therefore keep hydrophobic substances in solution. Phospholipids can be synthesized in all organs, serving as emulsifiers [2]. Together with free cholesterol, they form the shell of lipoproteins. Polar portions face outwards, making lipoproteins soluble in an aqueous environment, like blood. In contrast, the core of lipoproteins is hydrophobic and consists of esterified cholesterol and triglycerides [3], which make up the majority of transported lipids [4]. Moreover, lipophilic vitamins like vitamin A, D, E, and K can be present in the core as well [5]. Triglycerides (TGs) can either be taken up through food or are synthesized in the liver [2]. They function as an energy source for various organs and are stored in fatty tissue. Cholesterol on the other hand is necessary for the production of steroid hormones, cell membranes, and bile acids [6]. Even though cholesterol can be formed in all human cells, it is preferably taken up into cells from the pool of circulating lipoproteins through specific mechanisms due to energy-saving [2]. The general structure of lipoproteins can be seen in Figure 1 [7].

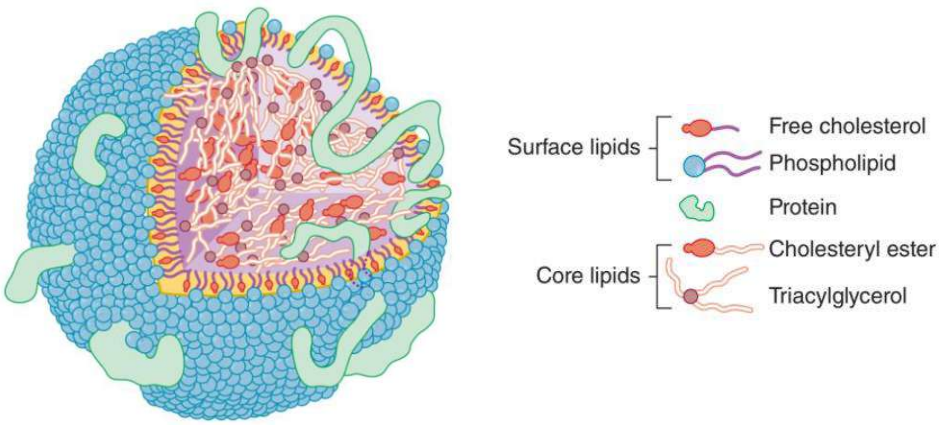

Figure 1: Illustration of the structure of lipoproteins [7]

1.1.2 Classes

As illustrated in Figure 1 [7], the hydrophilic shell of lipoproteins also contains proteins, which are called apolipoproteins. These proteins show both hydrophobic and hydrophilic portions, allowing interactions with lipid components and with the aqueous environment, simultaneously [3]. Therefore, apolipoproteins are of considerable importance and their functions are further described in *1.2.2 Functions of apolipoproteins*. Nevertheless, lipoproteins are not distinguished by their apolipoprotein compositions, but by their hydrated density [1], being dependent on the lipid-to-protein ratio. Therefore, lipoproteins can be separated and classified by ultracentrifugation. Other ways to categorize lipoproteins are by their diameter using size exclusion chromatography, or by their charge density which leads to different electrophoretic mobility on agarose gel electrophoresis [8].

Generally, lipoproteins can be divided into chylomicrons (CM), very low density (VLDL), low density (LDL), and high density (HDL) lipoproteins according to increasing density, ranging from larger to smaller sizes. For instance, the relative protein content of CM amount to 1-2 %, compared to HDL having approximately 50 %. The mentioned classes can be further divided into subclasses and have certain functions, which depend on the apolipoprotein component [1]. The following Table 1 summarises the physical properties, chemical composition as well as apolipoprotein content of the mentioned four main classes [9].

	CM	VLDL	LDL	HDL
Density (g/mL)	0.93	0.93-1.006	1.019-1.063	1.063-1.21
Diameter (nm)	75-1200	30-80	18-25	5-12
Triglycerides (%)	86	55	6	4
Cholesterol and cholesteryl ester (%)	5	19	50	19
Phospholipids (%)	7	18	22	34
Apolipoproteins (%)	2	8	22	42

Table 1: Physical properties, chemical composition, and apolipoprotein content of CM, VLDL, LDL, HDL [9]

The respective classes of lipoproteins display significant heterogeneity, marking their role in metabolism. Substantial alternation concerning the distribution or assembly of lipoproteins classes can imply pathological conditions [8].

1.1.3 Lipoprotein metabolism

Lipoproteins typically comprise various types of apolipoproteins [8]. The general function of lipoprotein classes results from their apolipoprotein and lipid composition. CM are formed in the intestine and are crucial for the delivery of dietary TGs to different tissues [1], which is called exogenous metabolism. On the other hand, the function of the endogenous pathway is to pass on endogenous TGs [4]. Therefore, VLDL, which originates from the liver, is used. Its transported TGs are hydrolyzed by lipoprotein lipase (LPL) located in the vascular bed to generate free fatty acids (FFAs). FFAs can then be metabolized or stored in muscle and fatty tissues [10]. As

listed in Table 1, both CM and VLDL, which are essential for TG transport, consisting of a large part of TGs [9]. Moreover, VLDL can be metabolized to intermediate-density lipoprotein (IDL) and to LDL [10], which is necessary to bring cholesteryl ester to the liver as well as peripheral tissues [1]. The role of the third major pathway is the reverse cholesterol transport, for which HDL is responsible. HDL mainly compromises phospholipids and apolipoprotein A-1 but contains little amounts of cholesterol. Thus it is designated to carry excess cholesterol from cells to the liver [4]. Initially, nascent HDL-3 is formed in the liver and the small intestine and is subsequently esterified to HDL-2 [10]. Figure 2 [10] gives an overview of the three described pathways.

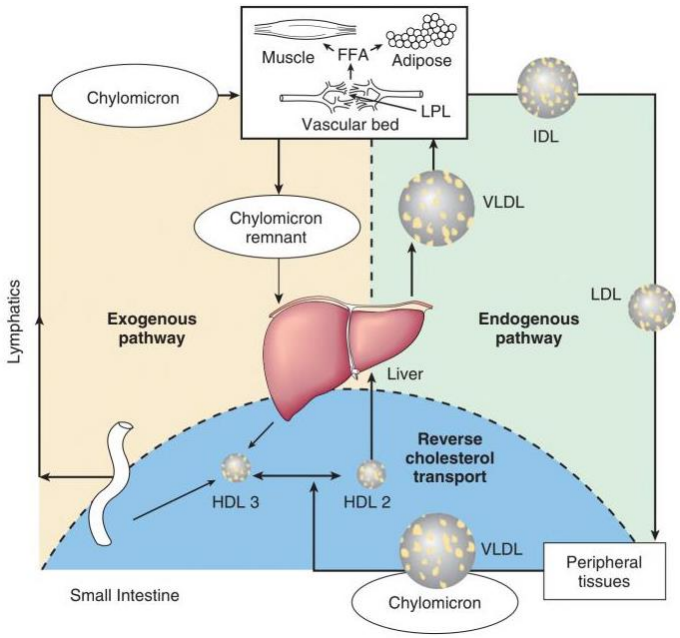

Figure 2: Illustration of the exogenous, endogenous, and reverse cholesterol pathway [10]

1.2 Apolipoproteins, APOs

As mentioned above (see *1.1.2 Classes*), the shell of lipoproteins comprises inter alia of proteins also referred to as apolipoproteins (APOs) [3]. The main production site of APOs is the liver, but small amounts can be formed by almost every organ [11]. Overall, the human gene family of APOs contains 22 members, which can be organized into 10 subfamilies, from ApoA to ApoE, ApoH, ApoJ, ApoL, ApoM, and ApoO. Depending on the type of lipoproteins, different APOs are bound to them. Certain APOs are associated with various lipoproteins, as shown in Figure 3 [12].

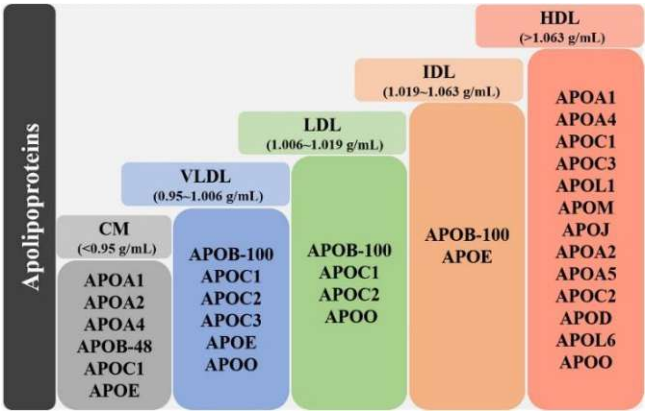

Figure 3: Lipoprotein classes and associated APOs [12]

1.2.1 Soluble and insoluble apolipoproteins

Generally, APOs can be divided into two groups: soluble and insoluble proteins. Since the latter cannot exist independently in plasma, they are reliant on lipoproteins and are non-exchangeable between plasma lipoprotein molecules. Representatives of the class of insoluble APOs are apolipoprotein B-100 (ApoB-100) and apolipoprotein B-48 (ApoB-48). In contrast, soluble proteins can move freely as well as be bound to lipoproteins, where they can be exchanged [13]. Exchangeable proteins share a similar genetic pattern, including 11-mer tandem repeats, which encode amphipathic α-helices. These α-helices represent an essential motif both structurally and functionally [14]. Therefore, the interchangeability of APOs is reflected by the amount and/or structure of such amphipathic helical motifs [15]. Even though 90 % of all APOs are associated with lipoproteins, a small part of the soluble APOs can be temporarily separated from them, for example during inflammation [14]. Furthermore, it has been shown that exchangeable APOs are not only indispensable for the modulation of TG and cholesterol in plasma but also have essential roles in intracellular lipid regulation [15]. For example, soluble APOs cover apolipoprotein A-I (ApoA-I), apolipoprotein C-II (ApoC-II), apolipoprotein C-III (ApoC-III), and apolipoprotein E (ApoE). Apolipoprotein(a) can exist independently in plasma too and is covalently attached to ApoB-100 to generate lipoprotein(a), abbreviated as Lp(a). The just-mentioned APOs are clinically relevant, linked to lipid metabolism and atherogenesis [13].

1.2.2 Functions of apolipoproteins

Previously, APOs were claimed to be an agent only for lipid transportation, but are actually essential for many roles in the body, such as ensuring stability during plasma lipid transport. Furthermore, APOs act as cofactors of particular enzymes involved in the metabolism of lipoprotein particles. Most importantly, APOs mediate the uptake of plasma lipoprotein particles and their followed catabolism within cells by recognizing their specific membrane receptors [16]. However, APOs seem to be Janus-faced. APOs also affect vascular biology as well as atherosclerotic disease pathophysiology by controlling lipoprotein metabolism. For example,

ApoB-100 is crucial for the structure of VLDL as well as the metabolic remnants of VLDL, which are IDL and LDL. Moreover, ApoB-100 is involved in withholding LDL particles in the arterial wall, but also in initiating atherosclerosis. On the other hand, Apo-A1, which is mainly bound to HDL, plays an essential role in reverse cholesterol transport, an anti-atherosclerotic effect of HDL [13].

Mutations in APO genes with different allelic polymorphisms and phenotypes can lead to uncommon blood lipid metabolism and utilization. They are therefore not only involved in atherosclerosis and cardiovascular diseases but also in hyperlipidemia and tumors [12]. One APO that reflects the variety of roles in the body is ApoE, which exists in three isoforms: ApoE2, ApoE3, and ApoE4 [17]. The isoforms vary by one or two amino acids [13]. ApoE is almost exclusively necessary for lipid transportation in the central nervous system and is also generally important in lipoprotein metabolism, cell growth, immune regulation, and inflammation [18]. But it can also be linked to Alzheimer's disease, Parkinson's disease, multiple sclerosis, vascular dementia, cardiovascular disease, type 2 diabetes mellitus (T2DM), and further disorders [17]. As mentioned above, ApoE is a soluble APO and is mainly formed in the liver and brain. ApoE can be bound to CM, CM remnants, VLDL, IDL, and HDL [13].

1.3 Apolipoprotein O, ApoO

1.3.1 Discovery of ApoO

One characteristic of obesity is a profuse accumulation of fat in adipose as well as in nonadipose tissues, which leads to lipotoxicity and lipoapoptosis in nonadipose tissues. At least to some extent, lipotoxicity is responsible for changes in cardiac functions. Therefore, the heart has to be shielded from excessive lipid deposition [19]. In transgenic mice, it was proven that the expression of *APOB* displays such protective effects [20], which indicates that the production of lipoproteins by the heart is a protective process to unload excessive cellular lipids. The analysis of the heart transcriptome of dogs fed a hypercaloric high-fat diet revealed differentially expressed genes in comparison to animals with a regular diet. Furthermore, cDNAs representing proteins of unidentified functions were found, including a new apolipoprotein whose expression is dependent on obesity in hearts and was designated apolipoprotein O (ApoO) in 2006 [19].

1.3.2 Characteristics of ApoO

ApoO consists of 198 amino acids, whereof 23 amino acids form a signal peptide. It is conserved among species, expressed in several human tissues, and colocalized to perilipins, which mark lipid droplets in cells. Just like for the ApoA1, ApoA-IV, and ApoE family, the polypeptide motif pfam01442, forming a pair of α-helices, was found in the corresponding cDNA sequence of ApoO. It is assumed that ApoO is an exchangeable APO since it is mainly

found on HDL, and to a smaller extent also on LDL, and VLDL. Moreover, its secretion is suppressed by microsomal triglyceride transfer protein (MTTP) inhibitors [19]. Generally, ApoO comes in three different isoforms: *(i)* a 55 kDa glycosylated, form located in light membranes, like endoplasmic reticulum or Golgi apparatus, *(ii)* a 55 kDa glycosylated form, secreted into the extracellular matrix and *(iii)* as a 22 kDa from, which is not glycosylated and present in mitochondria [21].

1.3.3 Properties of ApoO

Because of the discovery of ApoO in the hearts of dogs with obesity and the finding of upregulated levels of ApoO in the hearts of humans with diabetes, it is indicated that ApoO might be part of myocardium-protective processes against lipid deposition [19]. Protective properties were also suggested by Yu et al., who found elevated ApoO levels of 4.94 ± 1.59 µg/mL in the plasma of patients with acute coronary syndrome (ACS). In healthy subjects, the mean ApoO plasma level was 2.21 ± 0.83 µg/mL [22]. ACS describes an umbrella term, including all conditions identified by signals of abrupt myocardial ischemia, which is a sudden decrease in the bloodstream towards the heart [23]. The significantly increased ApoO levels in subjects with ACS might represent an inflammatory predictor, whereby inflammation is greatly involved in the development of ACS [22]. A connection between ApoO and inflammation as well as lipid metabolism was also observed in HepG2 cells, a human liver cancer cell line, by a microarray analysis [24].

Furthermore, several publications claim that ApoO plays an important role in the function of mitochondria [25, 26, 21]. More precisely, Koob et al. described that ApoO is part of the MICOS complex. The inner mitochondrial membrane can be split into the inner boundary membrane and the cristae membrane, which are connected by so-called crista junctions. The mentioned MICOS complex is essential for the cristae structure and the generation of crista junctions. The overall mitochondrial membrane architecture is crucial for the function of mitochondria and alternations are associated with several human disorders, such as diabetes or cardiomyopathy [21]. However, Tian et al. found that overexpression of *APOO* in the liver of mice can lead to impaired mitochondrial function [27] and Turkieh et al. assumed that a slight *APOO* overexpression influences mitochondrial uncoupling and respiration [28].

Turkieh et al. also reported that ApoO increases lipotoxicity in mice and rat cardiac myoblasts cells, assuming that *APOO* overexpression supports apoptosis [28]. Possible activation of autophagy and apoptosis was also reported by Liu et al. after *APOO* expression was elevated both in mouse and cellular myocardial infarction models. It is assumed that ApoO affects the p38MAPK pathway, which regulates inflammation, apoptosis, autophagy, and oxidative stress, thereby intensifying myocardial damage [29].

Alternations of ApoO levels in the context of lipid metabolism were observed several times. For example, it was proven that a TG accumulation led to increased ApoO levels in the liver of chicken and in LMH, chicken hepatoma cells [25], as well as in HepG2 cells [26]. Mostofa et al. found that the MicroRNA miR200c directly targets ApoO and is therefore part of fat accumulation in the liver [30]. Moreover, it was shown, that overexpression of *APOO* in the liver of mice resulted in liver damage and caused TG deposition in mice and human hepatoma L02 cells. Furthermore, the extent of mRNA expression of genes involved in fatty acid oxidation was altered in mice. For example, a significant reduction of CPT1 was examined, suggesting that fatty acid metabolism is inhibited. Therefore, it is hypothesized that overexpression of *APOO* might play a part in the development of NAFLD, non-alcoholic fatty liver disease [27]. CPT1 and its connection to lipid metabolism is further described in *1.4.3.3 Fatty acid oxidation, FAO*.

1.4 Non-alcoholic fatty liver disease, NAFLD

NAFLD is a global health problem, which encompasses a spectrum of diseases marked by fatty accumulation in the liver. Generally, the liver is essential to maintain metabolic homeostasis, such as lipid metabolism. However, the human liver appears not to be intended for much lipid storage and chronic fatty accumulation is considered a pathological condition [31].

In NAFLD, a minimum of 5 % of hepatocytes display lipid droplets that surpass 5-10 % of liver weight [27]. Currently, it is estimated that 25-30 % of the world's population is affected by NAFLD, but the prevalence is drastically increasing with similar rates for obesity and T2DM. Moreover, NAFLD is the most common chronic liver disorder in industrialized regions and pertains to the major reasons for liver transplantation [32]. Paik et al. analyzed mortality data from the United States during the period 2007 to 2016 and revealed that the six most common causes of death (cirrhosis, cardiovascular disease, non-liver cancer, hepatocellular carcinoma, diabetes mellitus, and lung disease – ordered from highest to lowest frequency) constitute 67.5 % of NAFLD-related deaths [33].

1.4.1 Stages of NAFLD

In 1980, Ludwig et al. depicted an until then unnamed liver disease, non-alcoholic steatohepatitis (NASH), that is histologically similar to alcoholic hepatitis [34]. NASH is one of the two major subgroups of NAFLD and characterizes a more advanced and aggressive state of NAFLD, compared to NAFL, non-alcoholic fatty liver [35]. NASH can be marked with inflammation, hepatocyte damage, and pericellular fibrosis [36], and long-term NASH most likely develops into hepatocellular carcinoma (HCC) [35]. In subjects with NASH, the leading causes of mortality are cardiovascular disease and cancer. According to population-based studies, about 25 % of patients with NAFLD will develop NASH [37]. Globally, HCC is the fourth most common reason for cancer death [35], and NAFLD is the most rapidly growing reason for HCC

in the USA. Similar trends were observed in Europe, South Korea, and southeast Asia. Due to the advancing obesity epidemic, NAFLD-related HCC incidences are expected to rise concomitantly [38].

The other major subtype of NAFLD is NAFL, also known as simple steatosis, which is a nonprogressive type of NAFLD and rarely progresses to cirrhosis. NAFL and NASH are both reversible, while liver cirrhosis and HCC are irreversible [35]. In NAFL, the hepatic lipid accumulation does not cause lipotoxicity, since only inert kinds of lipids, such as TGs and cholesterol esters, are stored. However, it is indicated that they do not keep their neutral character in lipid droplets, since NASH often comes with increased levels of free cholesterol, diacylglycerols, and ceramides. The two latter forms can promote insulin resistance, and free cholesterol and ceramides can induce cellular stress reactions, cell death, inflammation, and fibrosis [5].

1.4.2 Risk factors for NAFLD

Up to now, there is insufficient knowledge of the course of NAFLD, its pathogenic driving force, and adequate *in vitro* and animal models to simulate NAFLD. Nevertheless, metabolic syndrome (MetS) represents the main risk factor for NAFLD and NASH. MetS usually covers obesity, hyperglycemia, dyslipidemia, and systematic hypertension. However, the link between NAFLD and characteristics of MetS seem to be bidirectional: On the one hand, MetS rises the risk of NAFLD, and on the other hand, NAFLD may promote various characteristics and accompanying illnesses of MetS. T2DM, one attribute of MetS, has the clearest connection to the development of NAFL, and up to 75 % of subjects living with T2DM suffer from NAFLD. Moreover, MetS enhances cardiovascular diseases and total mortality in NAFLD patients [36].

1.4.2.1 Obesity and NAFLD

As mentioned, MetS also includes obesity [36], the result of a disequilibrium between energy inflow and outflow in adipose tissue. Obesity is especially characterized by excessively increased TG storage in adipose tissue, which predominantly consists of adipocytes. However, adipocytes do not only accumulate lipids as an energy depot but also secrete hormones and molecules called adipokines, just as an endocrine cell. For example, FFAs as well as FFA metabolites, and other pro-inflammatory adipokines can be secreted, activating various inflammatory pathways. Dysfunctional adipocytes result in changes in adipose tissue, which in turn can lead to displaced fat accumulation. Thus, selective insulin resistance in e.g. liver or pancreatic beta cells is triggered, making them vulnerable to lipoapoptosis. Since the equilibrium between adipose tissue and the liver considerably affects the energy homeostasis of the whole body, imbalances result in disease development of obesity and NAFLD [15].

1.4.2.2 Oxidative stress and NAFLD

Generally, it is indicated that NAFLD might be a mitochondrial-related disorder since almost all individuals with NAFLD display liver mitochondrial dysfunction [27]. One critical element that is associated with impaired mitochondrial functions is oxidative stress [39]. Normally, oxidative and antioxidative mechanisms are balanced [40]. Thus, the equilibrium between ROS-forming processes and antioxidative activities to remove ROS is maintained [41]. ROS stands for reactive oxygen species, which are characterized by an unpaired electron and are therefore highly reactive [39]. When ROS overcome the intracellular antioxidative response, oxidative stress occurs [41], and lipid peroxides are generated. NAFLD conditions lead to an elevation of mitochondrial ROS formation and ROS-eliminating actions are downregulated [40].

To regulate antioxidant defense mechanism and detoxication, nuclear factor erythroid-derived 2-like 2 (Nrf2) is essential. In the presence of oxidative stress or toxic molecules, Nrf2 is activated [42]. Subsequently, antioxidative genes are transcribed, resulting in decreased intracellular ROS levels and restrained oxidative stress. Hence, it seems that activating Nrf2 can shield hepatocytes from oxidative damage and lipotoxicity, which can relief NAFLD [40].

1.4.3 Formation of NAFLD

The formation of NAFLD is primarily linked to three metabolic pathways: *(i)* assembling and excreting of VLDL-TG in the liver, *(ii)* upregulated adipogenesis and *de novo* lipogenesis in the liver, and *(iii)* enhanced lipid uptake and suppression of fatty acid oxidation (FAO) [27]. However, the cause of NAFLD is still not well understood. Nevertheless, it can be concluded that NAFLD can be traced back to a net retention of lipids in hepatocytes, in particular TGs. In individuals with NAFLD, lipolysis of fatty tissue is the major source of hepatic lipid content, followed by *de novo* lipogenesis. Only 15 % derive from dietary fatty acids [31].

Both generations as well as lipolysis of TGs can create FFAs, but also toxic lipid intermediates. Intracellularly, such intermediates can promote inflammatory pathways, like the nuclear factor-kappa B (NF-κB) pathway [25]. The NF-κB pathway is involved in usual physiology but also inflammation, cancer, and autoimmune diseases. The signaling can be activated by several influences like inflammatory cytokines, microbial outputs, and immune or stress signals [43]. If the FA metabolism is impaired, like in NAFLD, the cellular inflammatory condition is consequently affected, which in turn might promote the pathogenesis of NAFLD [25].

1.4.3.1 Assembly and secretion of Very Low Density Lipoprotein

The function of the endogenous pathway is to move hepatic TGs with VLDL, which originate from the liver [4], as described in *1.1.3 Lipoprotein metabolism*. The secretion rate of VLDL is linked to the accessibility of TGs in the liver and the general capacity for the assembling of VLDL. The construction of VLDL consists of two steps requiring microsomal triglyceride

transfer protein (MTTP): First, a new ApoB-100 molecule is formed and followingly, partial lipidation leads to a small and tight precursor of VLDL. Then, the precursor develops into a mature TG-rich VLDL by merging with a TG droplet. Every VLDL comprises one ApoB-100 molecule, which is crucial for exporting the mature particle from the liver. In NAFLD patients, the secretion of VLDL-TG is impaired, but the responsible mechanisms are unrevealed. However, the secretion rate is elevated compared to healthy subjects, while the size of the secreted VLDL particles remains equal or slightly greater, implying that VLDL particles consist of more TGs. According to animal studies, very large VLDL complexes cannot export from the liver, leading to superfluous intra-hepatic TGs and thus to hepatic steatosis [44].

1.4.3.2 Adipogenesis and de novo lipogenesis

As previously mentioned, the formation of NAFLD is inter alia linked to enhanced adipogenesis and *de novo* lipogenesis (DNL) [27]. Adipogenesis refers to the multi-step generation of preadipocytes into mature adipocytes comprising lipids. Two phases of adipogenesis have been described. First, multipotent stem cells differentiate into unipotent preadipocytes, thus becoming incapable of developing into other cell types. Then, the final differentiation into adult adipocytes occurs [45].

By DNL, saturated fatty acids and monounsaturated fatty acids are generated by acetyl-coenzyme A (CoA). Usually, only a small part of about 5 % of fatty acids in the liver and VLDL constitute fatty acids formed by DNL. In contrast, hepatic DNL is elevated in subjects with NAFLD, whereby more than 25 % of VLDL TGs are traced back to DNL. This raise primarily originates from the induction of enzymes participating in DNL, which are activated by insulin signaling and enhanced glucose flux stemming from energy excess [5].

1.4.3.3 Fatty acid oxidation, FAO

Imbalances of the third mentioned pathway, FAO, can be linked to obesity, insulin resistance, and diabetes. Furthermore, FAO and CPT1A affect cell growth in cancer cells, as well as their survival and drug resistance. CPT1, carnitine palmitoyltransferase-1, belongs to the human L-carnitine acyltransferases, just as carnitine acetyl-transferase (CRAT), carnitine-octanolyltransferase (CROT), and carnitine-palmitoyltransferase-2 (CPT2). L-carnitine acyltransferases are crucial for carrying fatty acids into mitochondria [46]. Before entering into mitochondria, a thioesterification is necessary, whereby fatty acids and CoA react to fatty acyl-CoA esters [47]. Subsequently, L-carnitine acyltransferases support the reversible conversion of acyl-CoA esters into acyl-carnitine esters and vice versa [46], as illustrated in Figure 4 [48].

Due to the high range of fatty acid chain lengths, the enzymes of L-carnitine acyltransferases favor certain chain length esters. CPT1, situated in the outer mitochondrial membrane, and CPT2 carry medium and long acyl-CoA chains into the mitochondrial matrix. Even though CPT1 is the rate-limiting enzyme of FAO, L-carnitine must be available for the carnitine shuttle

to work and to balance the contents of acyl-CoA and acyl-carnitine. For human CPT1, three forms exist: CPT1A, CPT1B, and CPT1C, located in the liver, muscle, and brain, respectively.

Besides the regulation of FAO, CPT1A supports adjustments to the surroundings, in health as well as in disease. If CPT1A activity decreases, the generation of acyl-carnitines transported into mitochondria for oxidation is impaired. In turn, glucose production and gluconeogenesis are deficient. Furthermore, a reduced CPT1A expression damages the production of aspartate which is necessary for the synthesis of DNA [46].

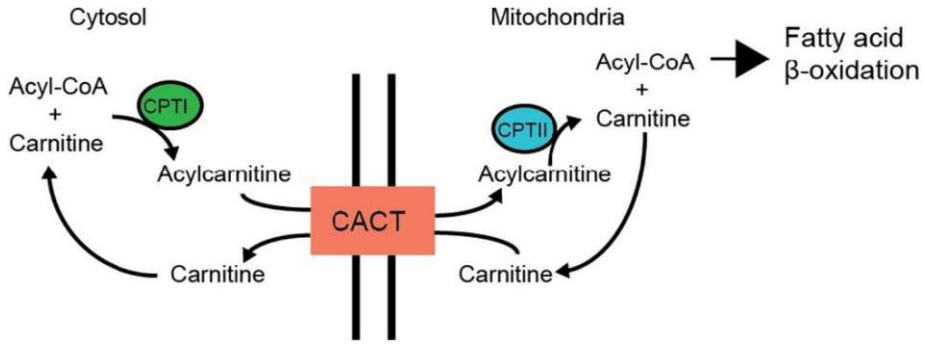

Figure 4: Visual representation of the carnitine shuttle system [48]

Inside the mitochondria, fatty acid β-oxidation takes place. β-Oxidation is the utmost pathway to catabolize FA and is responsible for the maintenance of the energy homeostasis of the whole body [46]. To metabolize saturated fatty acyl-CoA esters, β-oxidation occurs in repeated rounds, each consisting of oxidation, hydration, oxidation, and tocolysis. Within one cycle acetyl-CoA, a unit of two carbon atoms, dissociates from the acyl-CoA ester chain. Therefore, the fatty acyl-CoA ester is reduced by two carbon atoms each round, until the whole chain is transformed into acetyl-CoA molecules [47].

1.4.3.4 Lipolysis

As stated before, the major part of hepatic lipid content is generated by lipolysis [31], the hydrolysis of TGs. During intracellular lipolysis, FAs are formed from TGs associated with lipid droplets in the cytosol or from lipoprotein-associated TGs in lysosomes. This process is catalyzed by lipases, which can be divided into two subgroups: lipases with an optimal pH value of around 7, or around 5. The former are called neutral lipases and degrade cytosolic lipid droplets, while the latter represent the acid lipases that are based in lysosomes. Therefore, the two intracellular pathways for TG transformation are referred to as neutral and acid lipolysis. Because of the importance of lipases, their dysfunction can lead to various pathologies, like dyslipidemia or lipid-storage diseases. Indirectly, the activity of lipases and lipolytic processes influence several factors of homeostasis, linking them inter alia to obesity, T2DM, cancer, and NAFLD [49].

1.4.4 Apolipoproteins and NAFLD

Generally, it has been shown that patients with NAFLD exhibit increased serum ApoB contents, which is crucial for the structure of VLDL and LDL. Since the protein responsible for the structure of HDL, ApoA1, has antioxidative effects, protective properties against NAFLD are assigned to it [26]. Nevertheless, the function of ApoO in the context of NAFLD remains uncertain.

In adipocytes, intracellular soluble APOs are attributed to different roles. ApoE may function to keep ideal TG contents, a process in which ApoO and internalized ApoA5 appear to be implicated as well. Furthermore, ApoA4, ApoA5, ApoC3, and ApoE are involved in the assembly and secretion of VLDL in hepatocytes, participating in the regulation of TG homeostasis in the liver. Hence, intracellular soluble APOs are involved in lipid metabolism both in adipose tissue and in the liver [15]. Moreover, hepatocytes and adipocytes are the primary origins of exchangeable APOs [50]. Therefore, it is indicated that these metabolically active cells communicate *via* soluble APOs, concerning the relation between NAFLD and obesity. Hence, APOs might be a suitable target for therapeutic agents in obesity and NAFLD [15].

1.4.5 Treatment of NAFLD

In 2019, the global NASH market has attributed a value of USD 2.94 billion and in 2027 it is predicted to grow to USD 54 billion [37]. Even though a changing lifestyle, weight loss, and exercise are ways to cope with NAFLD, it becomes more widespread and modifications of eating habits as well as sporting activities are hard to maintain. Since T2DM and insulin resistance are closely linked to NAFLD development, anti-diabetic medications might show curative potential [51]. A major issue regarding the development of medication targeting NASH is its complexity. Instead of one pathogenic pathway, NASH is affected by both, extrinsic and internal, like dietary and genetic factors, respectively. Furthermore, the course of NASH is irregular and non-linear along the spectrum and commonly happens over a few decades [37].

2 Objective

NAFLD is a common disorder and its incidence as well as its prevalence are rapidly growing worldwide. Hence, there is a great demand to better understand the pathogenesis of NAFLD and to determine critical points. What triggers inflammation, the formation of cirrhosis, or HCC? When will the time point be reached, at which only two options are left for patients: liver transplantation or death? Considering that obesity is a disorder closely linked to NAFLD and that the obesity epidemic is also on the march, the need for liver transplants is expected to rise. Therefore, it is important to have the ability to treat NAFLD before irreversible states – cirrhosis and HCC – are reached. Unfortunately, there is a lack of animal and cell models mimicking NAFLD. Regarding animal models, both ethnic aspects and questions of utility have to be taken into account. A suitable *in vivo* model should develop a fatty liver that is histologically and biochemically similar to human ones, to achieve results that can be related to the human body and its mechanisms. *In vitro,* other problems emerge. When simulating NAFLD, cells need to be exposed to a fatty acid (FA) overload, which can result in negative effects like lipotoxicity. Furthermore, it is challenging to reach elevated levels of fatty acids, since they are poorly soluble and thus need to be complexed to bovine serum albumin (BSA). Additionally, the right type of BSA, preparation of FA/BSA, and FA:BSA ratios have to be studied.

This thesis aims to simulate overnutrition by elevating the intracellular triglyceride content through the incubation with oleic acid complexed to BSA and thus mimicking NAFLD. In this context, a recently discovered apolipoprotein, ApoO, is investigated. Currently, the knowledge of ApoO is limited and due to the physiological importance of apolipoproteins, the effect of overnutrition on ApoO protein production is examined by Western blot analysis. Moreover, the impact of chemical inducers of oxidative stress and inflammation on ApoO levels is evaluated.

3 Materials and Methods

3.1 Cell culture

HepG2 cells, a human hepatocyte carcinoma cell line (from ATCC), with the reference number 85011430 were obtained from Sigma-Aldrich (St. Louis, USA). Unless otherwise stated, the cells were cultured in 75 cm^2 tissue culture flasks (T75) from TPP (Trasadingen, Switzerland), using Dulbecco's Modified Eagle's Medium/Nutrient Mixture F-12 Ham with phenol red (DMEM:F12, Gibco, Carlsbad, USA) complemented with 10 % fetal bovine serum, 100 units/mL penicillin and 0,1 mg/mL streptomycin, 2 mM L-glutamine solution from Sigma-Aldrich (St. Louis, USA), and 0.2 % Plasmocin (InvivoGen, San Diego, USA) as growth medium in a humified environment with 5 % CO_2/95 % air and 37 °C in a Galaxy 170 S incubator from Eppendorf (Hamburg, Germany). To wash the cells, Dulbecco's Phosphate Buffered Saline (PBS) and to detach them, 0.25 % Trypsin-EDTA Solution, both from Sigma-Aldrich (St. Louis, USA), were applied.

3.1.1 Thawing of cells

1 vial with 1 mL of frozen cells was taken from the nitrogen tank, quickly thawed in a water bath at 37 °C and transferred into 10 mL growth medium, and then centrifuged at room temperature and 200 x g for 5 min, using an Eppendorf centrifuge 5810 R and an Eppendorf rotor A-4-62 (Hamburg, Germany). The supernatant was discarded and the pelleted cells were resuspended in 10 mL growth medium. The suspension was transferred into a 25 cm^2 tissue culture flask (T25) from Sarstedt (Nuembrecht, Germany), cultivated under the mentioned conditions, and transferred into T75 flasks as soon as possible.

3.1.2 Detaching and splitting of cells

When high cell densities (more than 80 % confluent) were reached, cells were split to maintain the exponential growth phase. The metabolized growth medium was aspirated and cells were washed with PBS. To detach the cells from T75 flasks, 2.5 mL of Trypsin was put on the cells and the flasks were placed in the incubator for 3 to 7 min until all cells were in suspension. Subsequently, growth medium was added and cells were diluted as needed, which was usually between 1:3 and 1:5.

3.1.3 Freezing of cells

Cells were first detached as described in *3.1.2 Detaching and splitting of cells*. Then, the homogenized cell suspension was divided and filled into 50 mL Centrifuge Tubes from Corning (Glendale, USA). After a centrifugation step at room temperature and 200 x g for 5 min using an Eppendorf centrifuge 5810 R and an Eppendorf rotor A-4-62 (Hamburg, Germany), the supernatants were discarded. To fill three 1.5 mL cryogenic vials, the pellet of one confluent T75 flask was resuspended with 1.5 mL ice-cold uncomplemented growth medium, and 1.5 mL

of the freezing medium was dropped in gently and mixed. The freezing medium consisted of Dulbecco's Modified Eagle's Medium/Nutrient Mixture F-12 Ham with phenol red supplemented with 50 % FCS and 20 % DMSO. Subsequently, portions of 1 mL of the cold cell suspensions were filled into cryogenic vials, placed in a Cool Cell LX Freezing Container (Merck, Darmstadt, Germany), and stored at -80 °C (GFL, Burgwedel, Germany). The next day, aliquots of the frozen cells were transferred into a nitrogen tank (-196°C) for longer storage.

3.2 Cell experiments

3.2.1 Pretreatment and treatment medium

Unless stated otherwise, Dulbecco's Modified Eagle's Medium (DMEM) with high glucose, and no phenol red from Gibco (Carlsbad, USA) and supplementary 100 units/mL penicillin and 0,1 mg/mL streptomycin, 2 mM L-glutamine from Sigma-Aldrich (St. Louis, USA), and 2 % of Bovine Serum Albumin from Sigma-Aldrich (St. Louis, USA) was used as pretreatment and treatment medium. Depending on the experiment, two different Bovine Serum Album were added: Either Bovine Serum Albumin (A4503 from Sigma-Aldrich), which was prepared by a modified method of the Cohn cold ethanol fractionation method and which was referred to as "Fraction V or BSA-V", or Bovine Serum Albumin (A6003 from Sigma-Aldrich), which also was purified by cold ethanol fractionation but was specifically tested for very low FA content/fatty acid free status and was therefore entitled "Fatty acid free or BSA-FAF".

3.2.2 Transfer on wells and pretreatment of cells

At the beginning of each cell experiment, cells had to be transferred from culture flasks into wells. Therefore, cells were detached as described in *3.1.2 Detaching and splitting of cells*, and counted, using the Olympus Cell Counter (Shinjuku, Japan). Subsequently, cells were diluted as needed and transferred into wells at a concentration of $0.4*10^6$ cells per mL. For the preparation of whole-cell lysates, the quantification of triglyceride content (TG quantification) and measurement of cell integrity with neutral red retention assays (NRR assays), cells were transferred onto 6-well plates. Each well had a diameter of 35 mm, an area of 9.6 cm^2, and was filled with 1.5 mL cell suspension. Only for cell fractionation, cells were exposed to treatments on cell culture petri dishes with a diameter of 100 mm and an area of 60.8 cm^2, using 9 mL cell suspension, respectively. Both 6-well plates and petri dishes were from Thermo Scientific (Waltham, USA).

48 h after the cells were transferred onto wells or dishes and became adherent, cells were exposed to a pretreatment for 24 h, if not otherwise specified. Thus, metabolized growth medium was aspirated, and cells were washed with PBS (2 mL/well or 15 mL/dish) before adding the pretreatment medium (1.5 mL/well or 9 mL/dish) and kept in the cell incubator for

24 h at 37 °C. When the pretreatment was over, the medium was aspirated and cells were again washed with PBS (2 mL/well or 15 mL/dish). If no pretreatment was performed, cells were washed two times with PBS (2 mL/well or 15 mL/dish) before adding the treatment medium. Finally, cells were ready for the respective treatments.

3.2.3 Treatment of cells

3.2.3.1 Testing of treatment condition of HepG2 cells

To assess the optimal treatment for the control group, a control experiment was conducted. Before the cells were exposed to a treatment, a pretreatment of 24 h with 2 % BSA-FAF was performed. This serum starvation of the cells was performed to synchronize the cells to the same cell cycle and to make the cell population more homogenous.

Afterward, the effects of the eight following treatments on cell integrity were investigated: DMEM, DMEM with 0.5 or 1 mM oleic acid complexed by BSA (OA; Oleic Acid-Albumin from bovine serum from Sigma-Aldrich, St. Louis, USA), DMEM with 2 % or 3.3 % BSA-FAF, DMEM with 2 % or 3.3 % BSA-V, or growth medium (DMEM:F12 with 10 % FCS). The pretreatment lasted 24 h as it is described in *3.2.2 Transfer on wells and pretreatment*, and after 4 and 24 h of treatment, cell viability assays (LDH and NRR assays) were performed (see *3.4.2 Lactate dehydrogenase assay (LDH* assay), *3.4.1 Neutral red retention assay (NRR* assay)).

3.2.3.2 Addition of oleic acid (OA)

For cell experiments with oleic acid, cells were pretreated with 2 % BSA-FAF as mentioned above, and washed once with PBS, or cells were not pretreated and washed twice with PBS. Then, oleic acid complexed by BSA (from Sigma-Aldrich, St. Louis, USA) was added to reach concentrations of 0, 0.125, 0.25, 0.5, 0.75 and 1 mM OA. The control group of the respective experiments was represented by the cells incubated with treatment medium (DMEM) containing 2 % of the BSA used (BSA-FAF for Western blot analysis, and BSA-V for TG quantification), and no oleic acid. The following Table 2 summarises the performed experiments.

The OA-Albumin complex contained 3 mM OA and 12 % BSA. For each experiment, a stock was prepared by diluting the complex 1:3 with treatment medium without BSA. Thus, the stock had a concentration of 1 mM OA with 4 % BSA. This stock was then further diluted with the treatment medium of the respective experiment, directly into the wells or dishes. It has to be noted that the BSA concentration of incubation with 1 mM OA contained 4 % BSA; and 0.75 mM included 3 % BSA, which differs from the other treatments with a final concentration of 2 % BSA.

Pretreatment (h)	Treatment (h)	OA (mM)	BSA	Method
24	24	0 - 0.5	FAF	WB (WCL)
24	24	0 - 0.5	FAF	WB (CF)
24	24	0 - 1	V	TG-Quantification
-	24	0 - 1	V	TG-Quantification

Table 2: Summary of the cell culture experiments with OA-concentration gradient

3.2.3.3 Addition of stress factors

To test the effect of induced experimental stress on cells, Tumor Necrosis Factor α (TNFα) and Menadione (or vitamin K3, abbreviated as Men), two stress factors from Sigma-Aldrich (St. Louis, USA), were used. Regarding TNFα, a stock of 10 µg/mL in PBS was prepared, portioned, and stored at -80 °C. For a 5 mM menadione stock, menadione was solved in 97 % ethanol, divided into aliquots, and stored protected from light and at -20 °C (Gorenje, Velenje, Slovenia).

For the treatment of HepG2 cells with menadione, a 50 or 10 µM working stock solution was prepared and protected from light, by slowly dropping 5 mM menadione into treatment medium with 2 % of the BSA used. Further dilutions were prepared directly in the cell culture wells to achieve final concentrations of 1, 5, or 10 µM menadione, respectively. TNFα was added to the cells in treatment medium with 2 % of the BSA used at a final concentration of 100 ng/mL. Table 3 gives an overview of all experiments performed with OA and the stress factors menadione and TNFα.

Pretreatment (h)	Treatment (h)	OA (mM)	TNFα (ng/mL)	Men (µM)	BSA	WB
24	24	1	100	10	FAF	WCL
2	4, 24	0.5, 1	100	5, 10	FAF	WCL

Table 3: Summary of the cell culture experiments with stress factors

3.2.3.4 Addition of OA plus stress factors

Further experiments, in which the stress factors were combined with 0.5 mM OA, were conducted. The applied concentration of TNFα was 100 ng/mL and for menadione 5 µM. The treatment medium consisted of DMEM with 2 % BSA-V.

Unlike the other experiments, no pretreatment was performed and cells were washed two times with PBS before starting the treatment. Furthermore, the treatment medium was not supplemented with glutamine. The control group was treated solely with treatment medium containing 2 % BSA-V and no glutamine. The performed experiments are listed in Table 4.

Pretreatment (h)	Treatment (h)	Combinations	BSA	Method
-	4, 24	OA+TNFα, OA+Men5	V	WB (WCL)
-	4, 24	OA+TNFα, OA+Men5	V	WB (CF)
-	24	OA+TNFα, OA+Men5	V	TG quantification

Table 4: Summary of the cell culture experiments with OA plus stress factors

3.3 Cell harvest and lysis

3.3.1 Whole-cell lysates

As already mentioned, cells were cultivated on wells of an area of 9.6 cm^2 for whole-cell lysates. As a lysis buffer, RIPA buffer was used. The components of the RIPA buffer are listed in Table 5.

Substance	Concentration	Manufacturer
NaCl	150 mM	Carl Roth (Karlsruhe, Germany)
NP-40	1.0 %	Sigma-Aldrich (St. Louis, USA)
NaDeoxycholate	0.5 %	Sigma-Aldrich (St. Louis, USA)
SDS	0.1 %	Carl Roth (Karlsruhe, Germany)
Tris	50 mM	Carl Roth (Karlsruhe, Germany)

adjusting the pH value to 8.0 with conc. HCl from Carl Roth (Karlsruhe, Germany)

Table 5: Contents of RIPA buffer

After HepG2 cells were exposed to various compounds for the indicated exposure time, plates were put on ice and 500 µL of each supernatant was transferred into reaction tubes (from Greiner Bio-One, Kremsmünster, Austria) and stored at -20 °C for LDH assays (see *3.4.2 Lactate dehydrogenase assay (LDH* assay)). The remaining supernatants were aspirated and cells were washed two times with ice-cold 2 mL PBS with 0.1 % Phenylmethanesulfonyl fluoride solution (PMSF) from Sigma-Aldrich (St. Louis, USA) per well. For cell lysis, 100 µL RIPA buffer with 1 % protease inhibitor cocktail (PIC) from Sigma-Aldrich (St. Louis, USA) was added and incubated for 5 min. Subsequently, cells were removed from the wells by scraping and transferred into reaction tubes on ice. After vortexing the suspension for 30 s every 10 min for 45 min, the lysates are centrifuged at 4 °C and 14000 x g for 30 min, using an Eppendorf centrifuge 5417 R with a 5417 C/R rotor (Hamburg, Germany). The supernatants were transferred into fresh reaction tubes and stored at -20 °C, the pellets were discarded.

3.3.2 Cell fractionation

To perform cell fractionation, cells were cultivated on dishes with an area of 60.8 cm^2 and a diameter of 100 mm from Thermo Scientific (Waltham, USA).

3.3.2.1 Abcam Kit – Separation of mitochondrial, cytosolic, and nuclear fraction

Buffers and Detergents were provided by the Standard Cell Fractionation Kit from Abcam (Cambridge, UK).

First, 2x Buffer A was diluted1:2 with ddH_2O to obtain Buffer A, and PIC was added. For each dish, 500 µL of supernatant was transferred into a reaction tube and stored at -20 °C for LDH assays (see *3.4.2 Lactate dehydrogenase assay (LDH* assay)). The remaining supernatants were aspirated. To collect the cells, 3 mL PBS with 0.1 % PMSF was put on them. After gently scraping, the suspensions were filled into 15 mL centrifugation tubes. The collection step was

repeated with 2 mL PBS with 0.1 % PMSF. Then, the samples were centrifuged at room temperature and 300 x g for 5 min, using an Eppendorf centrifuge and an Eppendorf rotor 16A4-44 (Hamburg, Germany). The supernatants were discarded and the pellets were resuspended in 5 mL of Buffer A. After taking 50 µL of each cell suspension, cell counting was performed with CASY (Omni Life Science, Bremen, Germany). Subsequently, the samples were centrifuged as before, the supernatants were discarded and the cell pellets were resuspended in the amount of Buffer A, which was needed to reach a concentration of $6.6*10^6$ cells/mL according to the average cell count. The same volume of Buffer B, which is prepared by diluting Detergent I 1:1000 in Buffer A, was then added and mixed by pipetting. The solutions were incubated for 7 min at room temperature on a rotator (REAX2 from Heidolph, Schwabach, Germany) and then centrifuged at 4 °C and 5000 x g for 1 min using an Eppendorf centrifuge 5417 R with a 5417 C/R rotor (Hamburg, Germany). The supernatants were transferred into a new set of reaction tubes and the pellets were saved on ice. The supernatants were recentrifuged at 4 °C and 10000 x g for 1 min with the same centrifuge as before. Finally, the resulting supernatants, containing cytosolic proteins, were filled into new reaction tubes. The pellets of the last two centrifugation steps were combined and resuspended in the same amount of Buffer A as used before the addition of Buffer B. This time, the same volume of Buffer C, a 1:25 dilution of Detergent II in Buffer A, was added and mixed by pipetting. After an incubation step of 10 min on the rotator at room temperature, the samples were centrifuged at 4 °C and 5000 x g for 1 min, using an Eppendorf centrifuge 5417 R with a 5417 C/R rotor. The supernatants were collected into a new set of reaction tubes and the pellets were saved on ice. The supernatants were again centrifuged at 4 °C and 10000 x g for 1 min with the same centrifuge as before, leading to the supernatants that contain mitochondrial proteins, which were transferred into new tubes. Again, the pellets of the last two centrifugation steps were combined and resuspended in Buffer A in the same volume as after the addition of Buffer C. These samples represented the nuclear fractions and were vortexed for 2 min at the highest setting. All fractions were stored at -80 °C.

3.3.2.2 Active Motif Kit – Separation of cytosolic and nuclear fractions

Buffers and used chemicals, except for PIC for the HB, were provided by the Active Motif Nuclear Extract Kit (Carlsbad, USA).

At first, all buffers were prepared according to the following Table 6 and stored on ice. It has to be noted that the kit contained 1 M DTT, which had to be diluted 1:1000 with ddH_2O before generating CLB.

Buffer	Components	Amount (%)
PBS/PI	ddH2O	85
	10x PBS	10
	Phosphatase Inhibitors	5
1x HB	ddH2O	89.5
	10x HB	10
	PIC	0.5
CLB	Lysis Buffer AM1	89
	10 mM DTT	10
	PIC	1

Table 6: Composition of needed buffers: PBS/Phosphatase Inhibitors (PBS/PI), 1x Hypotonic Buffer (HB), and Complete Lysis Buffer (CLB)

After cell treatment, the dishes were put on ice and 500 µL of each supernatant was transferred into reaction tubes and stored at -20 °C for LDH assays (see *3.4.2 Lactate dehydrogenase assay (LDH* assay)). The remaining supernatants were aspirated and cells were washed with ice-cold 5 mL PBS/PI. 3 mL of PBS/PI was then put on the adherent cells, removing them by gently scraping and transferring the cell suspensions into 15 mL centrifugation tubes. This step was repeated with 2 mL PBS/PI. Subsequently, the cells were centrifuged at 4 °C at 200 x g for 5 min using an Eppendorf centrifuge and an Eppendorf rotor 16A4-44. The resulting supernatants were discarded, and the cell pellets were put on ice and gently resuspended in 500 µL of HB by pipetting up and down several times. The suspensions were transferred into reaction tubes and incubated for 15 min on ice, before adding 25 µL Detergent and vortexing the solution at the highest setting for 10 s. All samples were centrifuged at 4 °C and 14000 x g for 30 s using an Eppendorf centrifuge 5417 R with a 5417 C/R rotor. The supernatants, representing the cytosolic fraction, were filled into new reaction tubes and stored at -80 °C. The cell pellets were resuspended in 50 µL of CLB and vortexed for 20 s at the highest setting. Afterward, the suspensions were incubated for 30 min on ice on a rocking platform (Rocky 3 D from Fröbel Labortechnik, Lindau, Germany) at level 1.5 and vortexed for 30 s at the highest setting. Finally, the samples were centrifuged at 4 °C and 14000 x g for 10 min with the centrifuge mentioned above. The supernatants, containing nuclear proteins, were transferred into new reaction tubes and stored at -80 °C.

3.3.3 Cell lysis for triglyceride quantification

To establish the intracellular triglyceride content, cells were cultivated on wells of an area of 9.6 cm^2 as well as on one T25 flask.

After the treatment time was over, cell number was determined, by detaching the cells from the T25 flask and analyzing the cell suspension with an Olympus Cell Counter. The plates were put on ice and 500 µL of the supernatants were transferred into reaction tubes and stored at -20 °C for LDH assays (see *3.4.2 Lactate dehydrogenase assay (LDH assay)*). The remaining supernatants were aspirated and cells were washed two times with 2 mL ice-cold

PBS per well. Subsequently, 5 % Igepal/ddH_2O from Sigma-Aldrich (St. Louis, USA) was added over two steps to reach 10^6 cells per mL. For each step, cells were scraped off the wells and transferred into reaction tubes. Then, all samples were put at 60 °C in a Thermomixer 5436 from Eppendorf (Hamburg, Germany) for 5 min, heating up to 80 °C. After cooling the samples back to room temperature, the samples were placed on the 80 °C Thermomixer and heated up to 95 °C for 5 min to solubilize all intracellular triglycerides. Followingly, samples were cooled down to room temperature, vortexed for 10 s at the highest setting, and centrifuged at room temperature and 14000 x g for 2 min using an Eppendorf centrifuge 5417 R with a 5417 C/R rotor. The resulting supernatants were transferred into a new set of reaction tubes. Small aliquots of the samples were further diluted 1:10 with ddH_2O and directly used for TG quantification Assay (see *3.5 Quantification of intracellular triglyceride content (TG quantification)*). The remaining solutions were stored at -20 °C.

3.4 Tests for measurement of cell integrity

3.4.1 Neutral red retention assay (NRR assay)

Neutral Red, a weakly positively charged dye, can be used as an indicator of cytotoxicity. The dye passes the cell membrane through non-ionic diffusion [52]. Healthy and uninjured cells take up neutral red into their lysosomal matrix where it accumulates due to the low pH value, while neutral red is washed out from damaged lysosomes. Therefore, the NRR assay determines the functionality of the lysozymes which helps to estimate the overall health condition of the cells [53].

Following the treatment, 500 µL of the supernatants were transferred into reaction tubes and stored at -20 °C to perform LDH assays (see *3.4.2 Lactate dehydrogenase assay (LDH assay)*), and the cells were washed two times with 2 mL PBS per well for a 6-well plate. The neutral red solution was prepared by mixing neutral red (0.4 % in ddH_2O) and high glucose Dulbecco's Modified Eagle's Medium without serum and phenol red (DMEM) in a ratio of 1:80. Then, 300 µL of this dilution was added to each well. After an incubation time of 3 h in the cell incubator at 37 °C, cells were washed twice with 2 ml PBS per well. An elution solution, containing 50 % ethanol from VWR (Radnor, USA) and 1 % acetic acid from Carl Roth (Karlsruhe, Germany), was prepared, and 1.5 mL was added to the cells and mixed by pipetting. The samples were incubated for 20 min on the Belly Dancer Platform Shaker from Stovall Life Science (Greensboro, USA), abbreviated as Belly Dancer, at room temperature. If the extraction solution was already saturated, another 1 mL of eluent was added per well. After 10 to 20 min all neutral red from within the cells was eluted and 200 µL of each reaction was transferred into a 96-well plate. The absorbance was measured on an iMark Microplate Reader at λ = 550 nm.

3.4.2 Lactate dehydrogenase assay (LDH assay)

As Alsabeeh et al. describe, cell viability has to be reviewed to determine if measured effects are rather traced back to cytotoxic impacts or to the treatment itself [54]. Therefore, LDH assays were performed concomitantly with each experiment. Lactate Dehydrogenase or LDH can be found in the cytoplasm of all body cells and catalyzes the formation of lactate to pyruvate, an oxidation, whereby NAD^+ is used as an acceptor of H^+ ions. In several pathological conditions, LDH levels are increased [55]. The LDH assay is based on the principle that cells with a damaged membrane release LDH, which generates NADH by oxidizing lactate. Then, NADH reduces the formazan dye INT, resulting in a change of color from yellow to red, which can be measured photometrically [56].

The Kit containing the necessary substances, which are the dye solution and the catalyst, was from Roche (Basel, Switzerland).

First, supernatants were thawed on ice and centrifuged at 4 °C, 14000 x g for 5 min, using an Eppendorf centrifuge 5417 R with a 5417 C/R rotor. Next, the working reagent was prepared, by mixing and vortexing the catalyst and the dye solution in a ratio of 1:45. 50 µL of the centrifuged supernatants were pipetted into a 96-well plate and 50 µL of the working reagent was added to each reaction. The samples were incubated for 20 to 40 min at room temperature on the Belly Dancer. Finally, absorbance was measured on an iMark Microplate Reader at λ = 490 vs 655 nm.

3.5 Quantification of intracellular triglyceride content (TG quantification)

With the help of microbial lipases, TGs are hydrolyzed to free fatty acids (FFAs) and glycerol, which can be determined with enzymatic methods [55]. The TG quantification is based on this principle, oxidizing glycerol into a product that reacts with the probe provided by the manufacturer. Hence, the color of the reaction changes to pink, which can be measured photometrically [57].

The TG Assay Buffer, TG Standard (1 mM), TG Probe, TG Enzyme Mix, and Lipase were provided by the ab65336 Triglyceride Quantification Assay Kit from Abcam (Cambridge, UK).

First, all substances were equilibrated to room temperature, keeping the TG Enzyme Mix and Lipase on ice. After cell lysis and 1:10 dilution with ddH_2O (see *3.3.3 Cell lysis for triglyceride quantification*), the TG Standard was diluted 1:5 with TG Assay Buffer, resulting in a stock of 0.2 mM. The TG quantification assay itself was performed in a 96-well plate. Each well was filled with 50 µL of standard dilutions, samples, or sample background controls. A standard series was generated by direct dilutions with TG Assay Buffer in the wells, ranging from 0 to 10 nmol/well. The samples and sample background controls were also directly diluted 1:2 in the wells with TG Assay Buffer. Subsequently, 2 µL of Lipase was added to the standard

dilutions and samples. The background controls were supplemented with 2 µL TG Assay Buffer, resulting in a total of 52 µL per well. The plate was then put on a Belly Dancer to mix the solutions protected from light for 20 min. Meanwhile, a mastermix for the TG Reaction Mix was prepared according to Table 7.

Components	Amount/reaction (µL)
TG Assay Buffer	46
TG Probe	2
TG Enzyme Mix	2

Table 7: TG Reaction Mix for one reaction or one well

After incubation, 50 µL of the TG Reaction Mix was added to the standard dilutions, samples, and sample background controls, respectively. The solutions were protected from light and again mixed on the Belly Dancer for 60 min. Finally, the output was measured on an iMark Microplate Reader at λ = 550 nm.

The following Equation 1 shows how the yielded TG content per million cells was calculated. To force the calibration curve through the origin, the extinction of the blank, which was the standard dilution containing no TG, was subtracted from the extinctions of all standards. The extinction of the blank was further subtracted from the extinction of the samples and with the help of the calibration curve led to the concentration of nmol/well. Since all the wells contained only 25 µL sample and the total volume of the reactions was 50 µL, the received concentration had to be multiplied by 2, resulting in nmol/50 µL sample. To get the TG content of $1*10^{6*}$ cells, which are contained in 1 mL, a factor of 20 had to be taken into account. Hence, the final factor is 40.

$$c = \left(\frac{Ext_{Sample} - Ext_{Blank}}{k}\right) * 40$$

Equation 1

c	… TG content in $1*10^6$ cells (nmol/mL)
Ext_{Sample}	… Measured Extinction of the sample
Ext_{Blank}	… Measured Extinction of the standard dilution no TG
k	… Slope of the calibration curve (Ext/(nmol/well))
40	… Factor to yield nmol/mL

3.6 Western blot analysis

After cell lysis was performed, intracellular proteins were examined by Western blot analysis. First, the protein content of the lysates had to be determined to load each pocket on the SDS-PAGE with 30 µg to guarantee consistency. Through SDS-PAGE, proteins were then separated and followingly transferred to a nitrocellulose membrane to perform Western blot analysis.

3.6.1 Determining the protein concentration with Pierce BCA assay

The principle of this test is based on two steps: first, a biuret reaction takes place, reducing Cu^{2+} to Cu^{+} by chelation with proteins in an alkaline environment, leading to a light blue complex. Secondly, a chelate is formed by two molecules of bicinchoninic acid (BCA) with one Cu^{+}-ion, resulting in an intense purple color [58], which can be measured photometrically.

Reagent A, Reagent B, and a 2 g/mL Albumin Standard were part of the mentioned kit. Standard dilutions were measured in duplicates, the samples and the blank, which was the respective lysis buffer, were measured in triplicates.

First, a standard series ranging from 0 to 2000 µg/mL was set up, by diluting the 2 g/mL Albumin Standard with PBS. The working reagent was prepared by diluting Reagent B 1:50 with Reagent A, considering that each reaction needed 200 µL working reagent. Subsequently, 10 µL of each standard dilution or 2.5 µL sample was pipetted into a 96-well plate from Greiner Bio-One (Kremsmünster, Austria). The samples were supplemented with 7.5 µL PBS, before adding 200 µL working reagent to every reaction. After an incubation time of 30 min at 37 °C, the extinction was measured on an iMark Microplate Reader from Bio-Rad (Hercules, USA) at λ = 550 nm.

The extinction of the blank, which was the standard dilution containing no Albumin, was subtracted from all standard dilutions to gain a calibration curve through the origin. Further, the extinction of the used RIPA buffer, representing the blank of the samples, was subtracted from the extinctions of the samples. The concentration of the samples was then determined based on the calibration curve, as it is indicated by Equation 2. Furthermore, a dilution factor of 4 had to be noted, since the used volume of the sample was smaller than for the standards.

Thus, it was possible to load each slot of the SDS-PAGE with the same protein concentration of 30 µg. However, for cell fractionation, protein concentrations could not be established, since the blank, the corresponding lysis buffer, led to high background.

$$c = \left(\frac{Ext_{Sample} - Ext_{RIPA}}{k}\right) * 4$$

Equation 2

c	… Protein content of the lysates (µg/mL)
Ext_{Sample}	… Measured Extinction of the sample
Ext_{Blank}	… Measured Extinction of the RIPA lysis buffer
k	… Slope of the calibration curve (Ext/(µg/mL))
4	… Dilution factor

3.6.2 Separating cell proteins by SDS-PAGE

3.6.2.1 Electrophoresis buffer

As electrophoresis buffer, a Tris/Glycine buffer was used and prepared by diluting a 10x Tris/Glycine stock with ddH_2O. The contents for 1 L 10x Tris/Glycine were provided by Carl Roth (Karlsruhe, Germany) and are listed in Table 8.

Component	Amount
Tris	30 g
Glycine	144 g
SDS (10%)	100 mL

Table 8: Components of 1 L 10x Tris/Glycine stock

3.6.2.2 Gel production

The short plates, spacer plates, comb, Casting Frame and Stand were from Bio-Rad (Hercules, USA). Depending on the protein content, it was necessary to load different volumes of samples and therefore, a spacer of 0.75 mm, 1 mm, or 1.5 mm was used.

First, the plates were washed with ddH_2O and 70 % ethanol and placed into the casting frame and stand. Subsequently, the separation gel was mixed, as it is summarised in Table 9 for a 10 %, 0.75 mm thick gel, and poured. To prevent air bubbles and drying on the surface, 30 % isopropanol (Merck, Darmstadt, Germany) was put onto the separation gel. After 30 min, the gel was polymerized and the 30 % isopropanol was discarded, whereby any remains were washed away with ddH_2O. Then, the stacking gel was mixed according to Table 10 and poured onto the solid separation gel. A suitable comb was inserted between the plates and after 20 minutes the stacking gel was polymerized. Next, the gel cassette was either immediately used or wrapped in wet paper towels and stored at 4 °C (Gorenje, Velenje, Slovenia) for up to three days.

Component	Manufacturer	Amount (mL)
ddH_2O	-	2.05
Acrylamide/Bis-acrylamide (30 %)	Sigma-Aldrich (St. Louis, USA)	1.65
Tris-HCl (1.5 M, pH 8.8)	Carl Roth (Karlsruhe, Germany)	1.25
SDS (10 %)	Carl Roth (Karlsruhe, Germany)	0.05
TEMED	Bio-Rad (Hercules, USA)	0.005
Ammonium persulfate (10 %)	Sigma-Aldrich (St. Louis, USA)	0.016

Table 9: Components of a 10 % and 0.75 mm thick separation gel

Component	Manufacturer	Amount (mL)
ddH_2O	-	1.85
Acrylamide/Bis-acrylamide (30 %)	Sigma-Aldrich (St. Louis, USA)	0.40
Tris-HCl (0.5 M, pH 6.8)	Carl Roth (Karlsruhe, Germany)	0.75
SDS (10 %)	Carl Roth (Karlsruhe, Germany)	0.03
TEMED	Bio-Rad (Hercules, USA)	0.003
Ammonium persulfate (10 %)	Sigma-Aldrich (St. Louis, USA)	0.03

Table 10: Components of a 0.75 mm thick stacking gel

3.6.2.3 Sample preparation

As already mentioned, each slot was loaded with 30 µg protein and Table 11 shows the loaded volume per pocket for different gels.

Spacer (mm)	0.75	1.00	1.50
Volume/Slot (µL)	20	25	45

Table 11: Spacer and corresponding loaded volumes per slot

Depending on the protein concentration, different sample buffers were used. For high protein contents, a 2x Laemmli buffer (Sigma-Aldrich, St. Louis, USA) was used, and for low concentrations a 5x SDS Sample Buffer (Abcam, Cambridge, UK) to load higher volumes of lysates. The remaining volume was filled up with PBS and the mixture of lysates, sample buffer, and PBS was vortexed and down-spinned with a microcentrifuge from Carl Roth (Karlsruhe, Germany). Followingly, samples were heated to 95 °C in a Thermomixer for 5 min. In the meantime, the gel cassette was placed in a suitable electrophoresis chamber from Bio-Rad (Hercules, USA), which was filled with electrophoresis buffer. Subsequently, the samples were cooled down to room temperature and spun down with a microcentrifuge. Before loading the pockets, the comb was removed and the slots were washed with electrophoresis buffer. One pocket of the gel was loaded with BLUeye Prestained Protein Ladder from Sigma-Aldrich (St. Louis, USA) taking half the volume of the samples. After loading the remaining slots with the samples, the electrophoresis chamber was connected to the power supply from Bio-Rad (Hercules, USA). First, proteins were collected in the stacking gel for 10 min and 100 V and then separated in the separation gel for 80 to 100 min and 180 V.

3.6.3 Transfer of the proteins onto a nitrocellulose membrane

3.6.3.1 Transfer buffer

As transfer buffer, a Tris/Glycine buffer with 20 % methanol was used and prepared by diluting a 10x Tris/Glycine stock with ddH_2O and adding the appropriate amount of methanol from Carl Roth (Carlsruhe, Germany). The finished transfer buffer was stored at 4 °C. The contents for 1 L 10x Tris/Glycine are listed in Table 8 and were provided by Carl Roth (Karlsruhe, Germany).

3.6.3.2 Transfer preparation and transfer

The gel transfer cell, gel holder cassettes, cooling unit, and power supply were provided by Bio-Rad (Hercules, USA).

A 0.45 µm nitrocellulose membrane, NC membrane (Cytiva, Amersham, UK), and 3 mm Whatman filter paper (Sigma-Aldrich, St. Louis, USA), were cut according to the size of the gel. Shortly before the end of the gel electrophoresis, two sponges, two Whatman filter papers, and one nitrocellulose membrane were equilibrated in cold transfer buffer for one gel. As soon as the gel electrophoresis was done, the sandwich of the transfer was set up on in the gel

holder cassette with the soaked components as follows: sponge, Whatman filter paper, nitrocellulose membrane, gel, Whatman filter paper, and sponge. Before and after the gel was put on the nitrocellulose membrane, the sandwich was moistened with additional transfer buffer. To avoid air bubbles, an eprouvette was rolled over the filter paper on the gel. As soon as the sandwich was prepared, the gel holder cassette was closed and placed in the gel transfer cell, which was filled with cold transfer buffer. After the cooling unit was put into the gel transfer cell, it was connected to the power supply using 100 V for the transfer. For 0.75 and 1 mm gels, the transfer time lasted 80 min, and for 1.5 mm 100 min, whereby the cooling unit was renewed for a fresh one after 60 min.

3.6.3.3 Ponceau S staining

To examine the success of the transfer, the NC membrane was stained with a ponceau S solution (0.2 % in 3 % TCA) from Serva (Heidelberg, Germany).

As soon as the transfer was over, the sandwich was disassembled. The NC membrane was put in a suitable plastic container and was covered with ponceau S solution. After an incubation time of 5 to 7 min on the Belly Dancer, the solution was filled back in its bottle and the NC membrane was washed with ddH_2O until protein bands were visible. Therefore, it was assessable, if air bubbles or other factors disturbing the transfer were present. The staining also helped to cut the membrane into stripes which were then probed with different antibodies.

3.6.3.4 Washing buffer or TBS-T

For the washing buffer, TBS had to be prepared. The contents for 1 L of 10x TBS are listed in Table 12. All chemicals were from Carl Roth (Karlsruhe, Germany), and the used pH meter was from Hanna Instruments (Woonsocket, USA).

Component	Amount (g)
Tris	24.2
NaCl	84.8

adjusting the pH value to 7.4 with conc. HCl

Table 12: Components of 1 L 10x TBS

To obtain the washing buffer, 10x TBS was diluted at 1:10 with ddH_2O, adding 1 mL Tween20 (Sigma-Aldrich, St. Louis, USA) per liter of washing buffer.

3.6.4 Blocking and antibody probing

Before the NC membrane was incubated with the primary antibody (AB), it was blocked for 1 h on the Belly Dancer with 15 mL of TBS-T and 5 % milk (Skim Milk Powder from Sigma-Aldrich, St. Louis, USA) at room temperature. Subsequently, the membrane was washed for 5 min with washing buffer on the Belly Dancer and then incubated with the primary AB on the Belly

Dancer, overnight, protected from light, and at 4 °C. The following Table 13 summarises the primary ABs used for Western blotting and their manufacturer.

Targeting Protein	Source	Polyclonal/ Monoclonal	Dilution	TBS-T	Manufacturer
ApoO	Rabbit	polyclonal	1:250	5 % milk	Abcam
ApoE	Rabbit	polyclonal	1:1000	5 % milk	Sigma-Aldrich
CPT1A	Mouse	monoclonal	1:1000	5 % milk	Abcam
Nrf2	Mouse	monoclonal	1:1000	5 % milk	Abcam
PARP/Cleaved PARRP	Rabbit	polyclonal	1:1000	5 % milk	Cell Signaling
p-IκB	Mouse	monoclonal	1:1000	5 % milk	Cell Signaling
IκB	Mouse	monoclonal	1:1000	5 % milk	Cell Signaling
p-p65	Rabbit	polyclonal	1:1000	5 % BSA	Cell Signaling
p65	Rabbit	polyclonal	1:2000	5 % BSA	Cell Signaling
Lamin B1	Rabbit	polyclonal	1:1000	5 % BSA	Abcam
GAPDH	Rabbit	monoclonal	1:10000	5 % BSA	Abcam
TOMM20	Rabbit	monoclonal	1:2000	5 % milk	Abcam

Table 13: List of the primary antibodies used for Western blotting from Abcam (Cambridge, UK), Cell Signaling (Danvers, USA), or Sigma-Aldrich (St. Louis, USA)

After the incubation with the primary AB, the NC membrane was washed three times with washing buffer for 10 min on the Belly Dancer at room temperature. In the meantime, 15 mL of the species-specific HRP-linked secondary AB was prepared, by diluting it at 1:20000 in TBS-T with 5 % milk. To target ABs with the mouse as host species, a rabbit anti mouse IgG polyclonal secondary antibody conjugated to HRP (horse radish peroxidase) from Bio-Rad (Hercules, USA), and to target ABs with the rabbit as host species, a goat anti rabbit IgG polyclonal secondary antibody conjugated to HRP (horse radish peroxidase) from Cell Signaling (Danvers, USA), were used. Then, the NC membrane was covered in 15 mL of the secondary AB solution on the Belly Dancer for 1 h at room temperature and protected from light. Followingly, the NC membrane was washed again three times for 10 min on the Belly Dancer at room temperature.

3.6.5 Detection of proteins and image analysis

The detection solutions, Solution A (Luminol) and Solution B (Peroxide), were provided by Cytiva (Amersham, UK). For image analysis, a ChemiDoc Imager from Bio-Rad (Hercules, USA) was used.

First, a working solution was prepared, by mixing and vortexing Solution A with Solution B in a ratio of 1:1, all working steps protected from light. After the excess washing buffer of the NC membrane was drained, it was placed in a flat box and the working solution was added onto the membrane for an incubation time of 5 min. Then, the excess working solution was drained and the NC membrane was placed, protein side up, on a sample tray. For image analysis, the

sample tray was pushed into the CCD camera compartment, and a suitable exposure time was selected.

The captured images were evaluated with the software Image Lab from Bio-Rad (Hercules, USA) and the signal strength was determined, making it possible to calculate the relative ratios of observed proteins. The first term of Equation 3 shows that the signal intensity of the examined proteins had to be compared to the corresponding signal of the loading control, a protein that is unaffected by the treatments, such as GAPDH. This output had to be placed in relation to the intensity of the examined proteins of the treatment control, hence the group that was not exposed to a treatment, again compared to the signal of its loading control.

$$Relative\ Content\ (\%) = \left(\left(\frac{I_{Protein}}{I_{Loading\ Control}}\right) / \left(\frac{I_{Treatment\ Control}}{I_{Loading\ Control}}\right)\right) * 100$$

Equation 3

$I_{Protein}$ … Signal intensity of the examined Protein (Au)
$I_{Loading\ Control}$ … Signal intensity of the loading control (Au)
$I_{Treatment\ Control}$ … Signal intensity of the examined Protein of the treatment control (Au)

3.6.6 Stripping and re-blotting the membrane

To observe a second protein on the same NC membrane, ABs had to be stripped off when the primary ABs originated from the same species.

After image analysis, the NC membrane was washed for 5 min with washing buffer on the Belly Dancer at room temperature. In the meantime, the stripping buffer was prepared: 10x Re-Blot Plus Strong Solution from Merck Millipore (Burlington, USA) was diluted 1:10 with ddH_2O. Subsequently, the NC membrane was incubated with the stripping buffer for 15 min on the Belly Dancer at room temperature and washed again for 5 min with washing buffer. Then, the NC membrane was transferred into a new box and blocked two times with 15 mL of TBS-T with 5 % milk on the Belly Dancer at room temperature for 5 min. Finally, the NC membrane was washed for 5 min with washing buffer and incubated with the primary AB of interest.

3.7 Presentation of the results

Experiments were repeated in various combinations as described in *3.2.3 Treatment of cells*, Table 2 to Table 4, and in the *4 Results* section in the respective figure legends. The statistical significance of the results was not calculated because of the experimental character of this work and the lack of the same settings. For each experiment, LDH assays were performed to assess if measured effects are rather traced back to cytotoxic impacts or to the treatment itself. The photometrically LDH assay and NRR assay samples were measured in technical duplicates independently of the number of biological replicates.

The pictures of the Western blot analyses were evaluated with the software Image Lab from Bio-Rad (Hercules, USA) and as far as results could be compared, an overview will be provided with a heatmap. The outcomes of LDH assay, NRR assay, and TG quantifications were illustrated using GraphPad Prism 5. Error bars on the displayed graphs always represent the standard deviation (SD) of the mean for the respective number of samples.

4 Results

4.1 Testing of treatment conditions for HepG2 cells

In the beginning, it was important to assess the most accurate treatment for the control group. Therefore, a control experiment was conducted and cell integrity was examined both after 4 and 24 h of treatment. Despite carrying out the experiment in biological duplicates, standard deviations are shown in the following figures to better estimate the variation of the measured values.

4.1.1 Measuring cell integrity with NRR assay

First, the ability to accumulate neutral red dye into lysozymes was investigated. Therefore, HepG2 cells were pretreated with DMEM with 2 % BSA-FAF for 24 h, and then incubated with combinations of DMEM with OA, BSA-FAF, BSA-V, or growth medium (DMEM:F12 with 10 % FCS) at 37 °C before the overall functionality of cell organelles was examined. Figure 5 displays the outcome of the NRR assays after 4 (Figure 5A) and 24 h (Figure 5B).

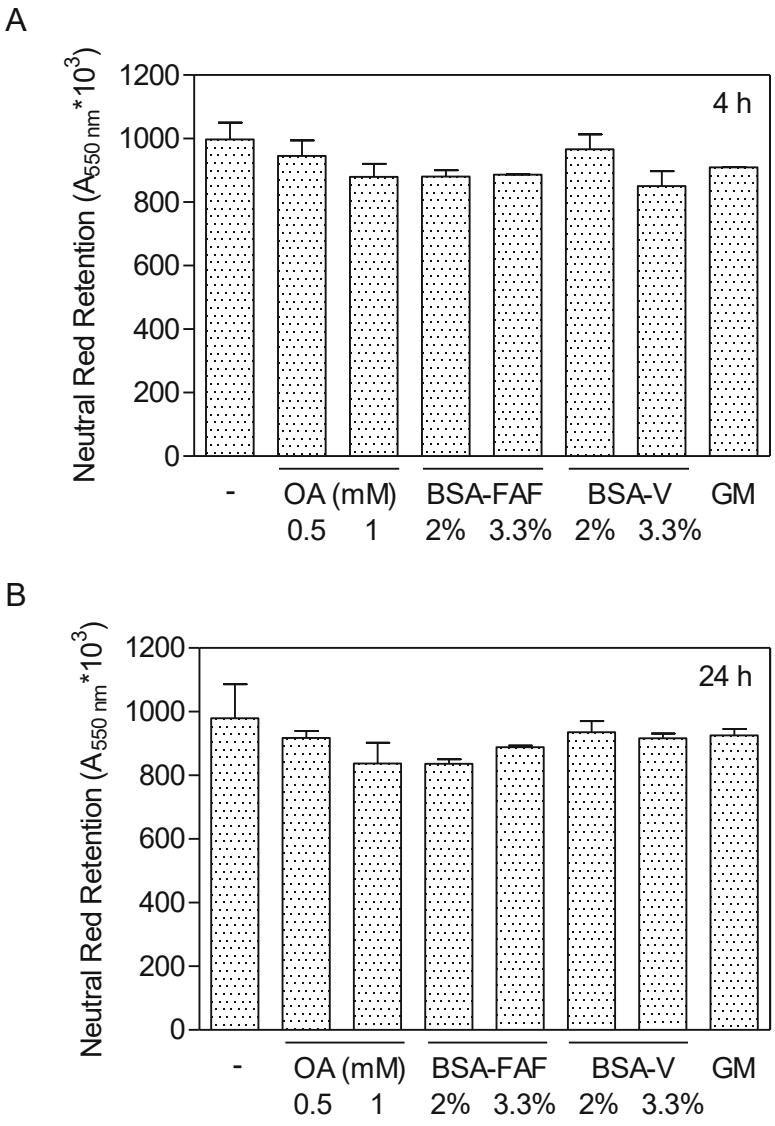

Figure 5: Influence of the treatment conditions on the integrity of HepG2 cells. Cells were pretreated with DMEM containing 2 % BSA-FAF for 24 h and then incubated with DMEM (Control) or DMEM with 0.5 and 1 mM OA, 2 and 3.3 % of BSA-FAF, 2 and 3.3 % of BSA-V or growth medium (DMEM:F12 with 10 % FCS) for 4 h (A) and 24 h (B), followed by determination of accumulated neutral red. Graphs show mean values +/- SD of one experiment performed in biological duplicates.

According to Figure 5A, only very small differences between the amount of accumulated dye are visible after 4 h of treatment. Cells treated with only DMEM and those treated with DMEM containing 2 % BSA-V showed the highest ability to take up neutral red, indicating that the lysozymes work the best with these treatment conditions.

As for Figure 5A, the differences in Figure 5B between the samples are small and the outcome after 24 h resembles the one after 4 h. Taking the standard deviations into account, it seems that all treatments, except for DMEM with 1 mM OA and with 2 % BSA-FAF, had a similar impact on the cells. Compared to DMEM, an approximate 15 % lesser accumulation of neutral red occurred by 1 mM OA and 2 % BSA-FAF.

When comparing the outcome of the neutral red retention of the cells which underwent a pretreatment and of the cells which were kept in growth medium (DMEM:F12 with 10 % FCS), it can be observed that serum starvation showed overall neither a positive nor negative effect on cell integrity.

4.1.2 Measuring cell integrity with LDH assay

Furthermore, the LDH release was investigated by LDH assay. Figure 6A and Figure 6B illustrate the obtained results after 4 and 24 h of treatment.

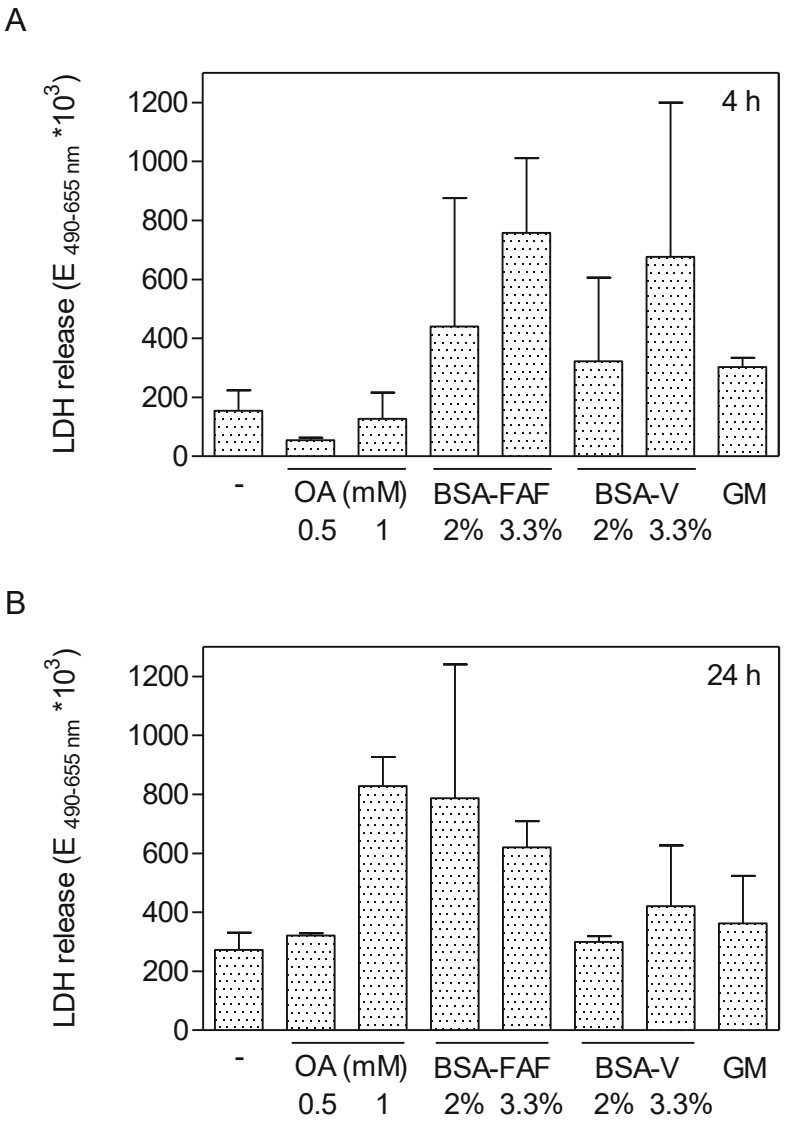

Figure 6: Influence of the treatment conditions on the LDH release of HepG2 cells. Cells were pretreated with DMEM containing 2 % BSA-FAF for 24 h and then incubated with DMEM (Control) or DMEM with 0.5 and 1 mM OA, 2 and 3.3 % of BSA-FAF, 2 and 3.3 % of BSA-V or growth medium (DMEM:F12 with 10 % FCS) for 4 h (A) and 24 h (B), followed by determination of LDH release. Graphs show mean values +/- SD of one experiment performed in biological duplicates.

When cell integrity was monitored with the LDH assay, bigger differences between the samples can be seen than for NRR assays (Figure 6). However, high standard deviations were achieved, making definite assumptions difficult, especially in Figure 6A for treatment medium

(DMEM) with BSA-FAF and BSA-V. Nevertheless, it is recognizable that the treatment with 0.5 mM OA led to the lowest number of damaged cells after 4 h of incubation (Figure 6A). Interestingly, the growth medium (DMEM:F12 with 10 %FCS) showed a higher LDH release than DMEM without BSA, with 0.5 mM and 1 mM OA. After incubation for 24 h (Figure 6B) the LDH release is elevated by the treatments with OA. Generally, this outcome complies with the corresponding NRR assay (Figure 5): the treatment medium with 1 mM OA seems to have the greatest negative impact on the cells.

Overall, it appears as if stressed cells release more LDH whereas the function of the cell organelles appears to be barely limited. At least, this applies to the lysozymes according to the NRR assays.

4.2 Quantification of intracellular triglyceride content

4.2.1 Impact of oleic acid (OA) on intracellular TG accumulation

To examine, if OA is appropriate to achieve a triglyceride accumulation mimicking NAFLD, HepG2 cells were pretreated with DMEM with 2 % BSA-FAF for 24 h and incubated with up to 1 mM of oleic acid for 24 h at 37 °C. Following, TG quantification and LDH assay were carried out.

4.2.1.1 TG quantification of HepG2 cells incubated with OA

The following Figure 7 illustrates the impact of OA on cellular TG concentration. The standard curves of three experiments were combined and the TG content was calculated using the resulting calibration curve.

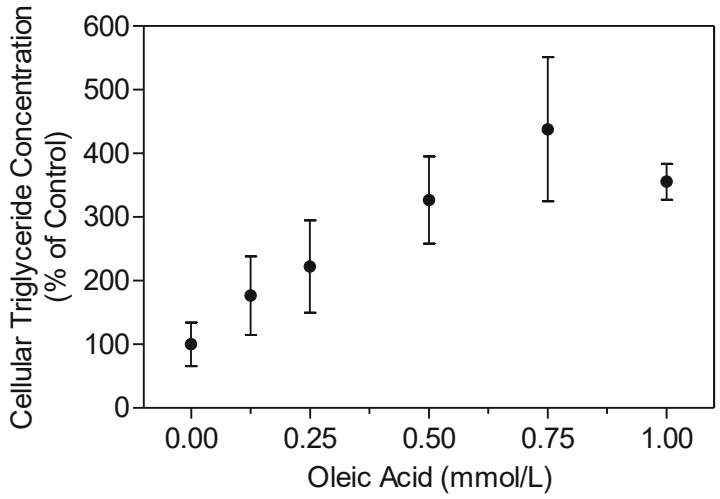

Figure 7: Effect of oleic acid on the cellular TG concentration of HepG2 cells. Cells were pretreated with pretreatment medium (DMEM) containing 2 % BSA-FAF for 24 h and incubated with treatment medium (DMEM with 2 % BSA-V (Control)) and up to 1 mM OA for 24 h, followed by determination of the intracellular triglyceride content. Data points show mean values +/- SD, from 2 to 3 (for Control and 0.5 mM OA) individual experiments.

As expected, the amount of TG amplified with rising oleic acid concentrations. According to Figure 7, intracellular lipid accumulation is approximately three times higher due to the incubation with 0.5 mM OA compared to the control. It seems that from 0.5 mM on, saturation is reached since 1 mM OA led to similar TG concentrations as 0.5 mM OA. However, the overall health condition of the cells was problematic at high OA concentrations. Thus, an LDH assay was performed with the supernatants of these experiments.

4.2.1.2 LDH assay of HepG2 cells incubated with OA

To assess the condition of the cells after exposure to an OA concentration gradient, LDH assay was performed with the corresponding supernatants. The result is shown in Figure 8.

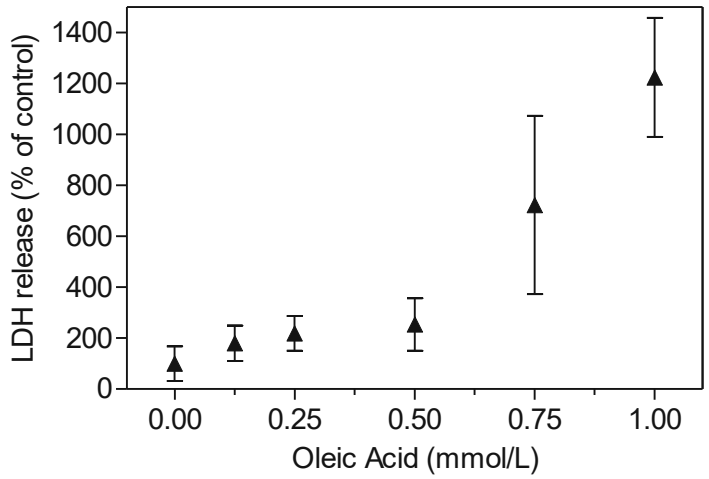

Figure 8: Influence of OA concentration gradient on the LDH release of HepG2 cells. Cells were pretreated with pretreatment medium (DMEM) containing 2 % BSA-FAF for 24 h and incubated with treatment medium (DMEM with 2 % BSA-V (Control)) and up to 1 mM OA for 24 h, followed by determination of LDH release. Data points show mean values +/- SD, from 2 to 3 (for Control and 0.5 mM OA) individual experiments.

Since the LDH release reflects the number of damaged cells, it is evident that more lysed cells were present with increasing OA concentrations as is displayed in Figure 8. Especially from 0.75 mM OA on, the LDH release rises rapidly. It can be seen that even at approximately the same levels of TG content (Figure 7), the LDH release is about six times higher for 1 mM OA than for 0.5 mM OA. This indicates that 0.5 mM OA led to a similar effect on lipid accumulation as 1 mM OA did, but cells released much less LDH. Hence, 0.5 mM OA plays a more important role in the following experiments than 1 mM OA because the processes inside the cells should be investigated when a lipid accumulation is achieved, but cells are still healthy, rather than examining events that occur during possible cell apoptosis.

4.2.2 Impact of pretreatment conditions on intracellular TG accumulation

One experiment was performed to examine the effect of no pretreatment, where cells were provided with fresh growth medium (DMEM:F12 with 10 %FCS), and results were compared to pretreatment with pretreatment medium (DMEM) containing 2 % BSA-FAF for 24 h. Before

the incubations with up to 1 mM OA for another 24 h at 37 °C, pretreated cells were washed once with PBS, and cells without pretreatment were washed twice to eliminate traces of FCS.

4.2.2.1 TG quantification of HepG2 cells with or without pretreatment

The outcome of the corresponding TG quantification can be taken from Figure 9.

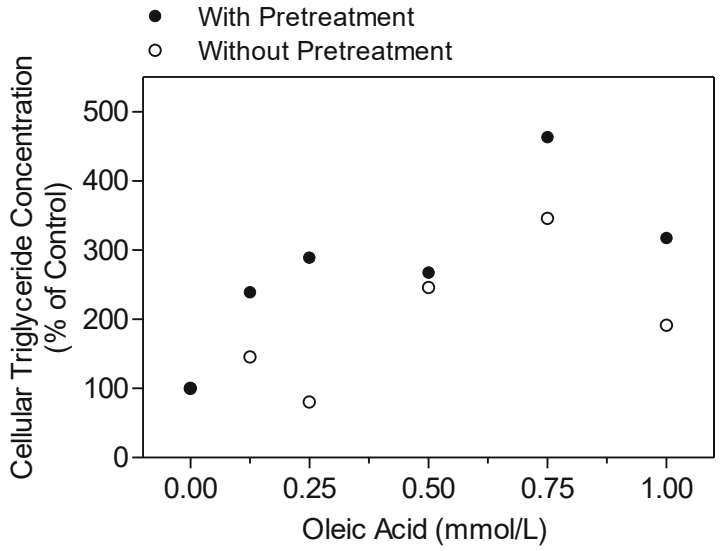

Figure 9: Influence of no pretreatment compared to 24 h pretreatment on the cellular TG concentration of HepG2 cells. Cells were pretreated with pretreatment medium (DMEM) containing 2 % BSA-FAF for 24 h (filled circles) or were instead provided with fresh growth medium (DMEM:F12 with 10 %FCS) for another 24 h (open circles). Both approaches were then incubated with treatment medium (DMEM with 2 % BSA-V (Control)) and up to 1 mM OA for 24 h, followed by determination of the intracellular triglyceride content. Data points show the results of one experiment performed in parallel for both conditions.

Figure 9 implies that both approaches, without pretreatment and with pretreatment of the cells with DMEM containing 2 % BSA-FAF led to an accumulation of intracellular triglycerides. For 0.25 mM OA, the values varied the most. However, lipid accumulation increased again by a factor of three for both versions at 0.5 mM OA compared to the control, and saturation might be reached with 0.5 mM OA on, as can be seen in Figure 7. Based on this experiment it is assumed that serum starvation of the cells for 24 h might generally increase triglyceride accumulation. To better assess the possible influence of the pretreatment compared to no pretreatment on the condition of the cells, LDH assays were conducted.

4.2.2.2 LDH assay of HepG2 cells with or without pretreatment

Supernatants for the experiment described above were used for the LDH assay, and the result is shown in Figure 10.

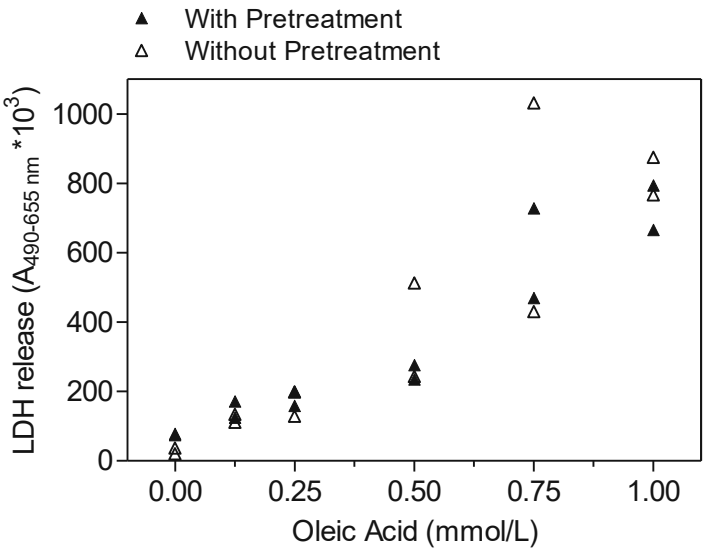

Figure 10: Influence of no pretreatment compared to 24 h pretreatment on the LDH release of HepG2 cells. Cells were pretreated with pretreatment medium (DMEM) containing 2 % BSA-FAF for 24 h (filled circles) or were instead provided with fresh growth medium (DMEM:F12 with 10 %FCS) for another 24 h (open circles). Both approaches were then incubated with treatment medium (DMEM with 2 % BSA-V (Control)) and up to 1 mM OA for 24 h, followed by determination of LDH release. Data points show biological duplication of one experiment performed in parallel for both conditions.

Based on Figure 10 the obtained values of no pretreatment are similar to those of 24 h pretreatment. Just as already displayed in Figure 8, it is visible that the LDH release increased slowly until 0.5 mM, except for one value, and then rapidly increases with 0.75 mM OA.

Overall, it is difficult to estimate if cells could also be incubated without pretreatment. The LDH assay, Figure 10, indicates that no pretreatment leads to similar results as for 24 h pretreatment. However, regarding the TG quantification, Figure 9, it seems that starving the cells by incubating them in serum-free medium for 24 h is advantageous for increasing the triglyceride content in the cells and therefore might be better to mimic conditions found in a fatty liver.

4.2.3 Impact of OA plus stress factors on intracellular TG accumulation

Since some of the following experiments were carried out with stress factors, and OA combined with stress factors, the question arose, if the presence of such substances influences lipid accumulation.

4.2.3.1 TG quantification of HepG2 cells incubated with OA plus stress factors

To detect possible effects of stress factors on triglyceride accumulation, TG quantification was performed. The outcome is displayed in Figure 11.

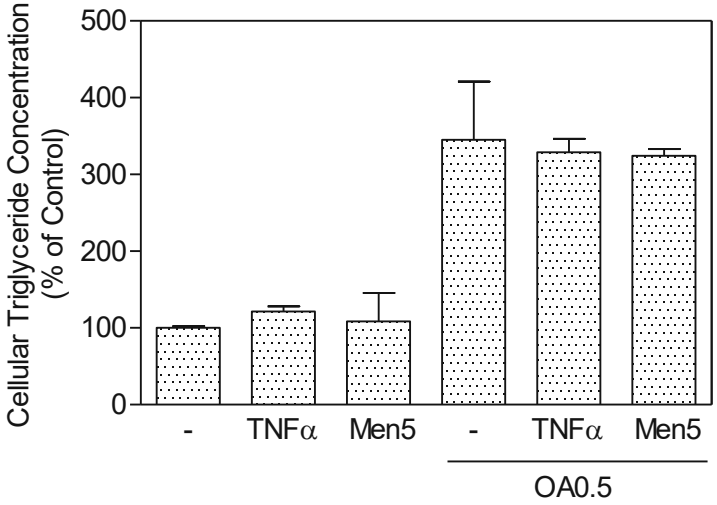

Figure 11: Effect of stress factors and OA plus stress factors on cellular TG concentration. Cells were not pretreated and therefore washed twice with PBS before incubating cells with treatment medium (DMEM with 2 % BSA-V, without L-glutamine (Control)), 100 ng/ml TNFα or 5 µM menadione (Men5) for 24 h in the absence or presence of 0.5 mM OA (OA0.5), followed by determination of the intracellular triglyceride content. Bars show means +/- SD of biological duplicates from one experiment.

Figure 11 demonstrates that TNFα and menadione, the used stress factors, did not influence the cellular TG content. As expected, and seen before, 0.5 mM OA showed a lipid accumulation by a factor of 3 compared to the control group (see Figure 7 and Figure 9). Furthermore, it can be recognized that the same lipid accumulation was achieved when TNFα or menadione was additionally present at 0.5 mM OA.

4.2.3.2 LDH assay of HepG2 cells incubated with OA plus stress factors

Again, concomitantly to this experiment, the LDH release was measured and the results are shown combined with further experiments in *4.5.2 LDH assay of HepG2 cells incubated with OA plus stress factors*, Figure 24.

4.3 Effect of OA on HepG2 cells

4.3.1 Western blot analysis of HepG2 cells incubated with OA

After it has been shown that the incubation with OA leads to an increased lipid content of HepG2 cells, the effect of an OA concentration dependency on the expression of various proteins, including ApoO, was examined by Western blot analysis.

4.3.1.1 Whole-cell lysates of HepG2 cells incubated with OA

Again, HepG2 cells were pretreated for 24 h with DMEM containing 2 % BSA-FAF and incubated without or with 0.125, 0.25, and 0.5 mM OA for 24 h at 37 °C. The cells of the control group were exposed to DMEM containing 2 % BSA-FAF. Then, whole-cell lysis was performed and proteins were examined by Western blot analysis. The following Figure 12 lists the observed proteins and shows the outcome of the Western blot analysis. For ApoO, ApoE, Nrf2,

CPT1A, and PARP, GAPDH was used as a loading control, and for the phosphorylated NF-κB proteins, the non-phosphorylated form, respectively. The corresponding relative values, calculated with Equation 3, can be taken from Table 14.

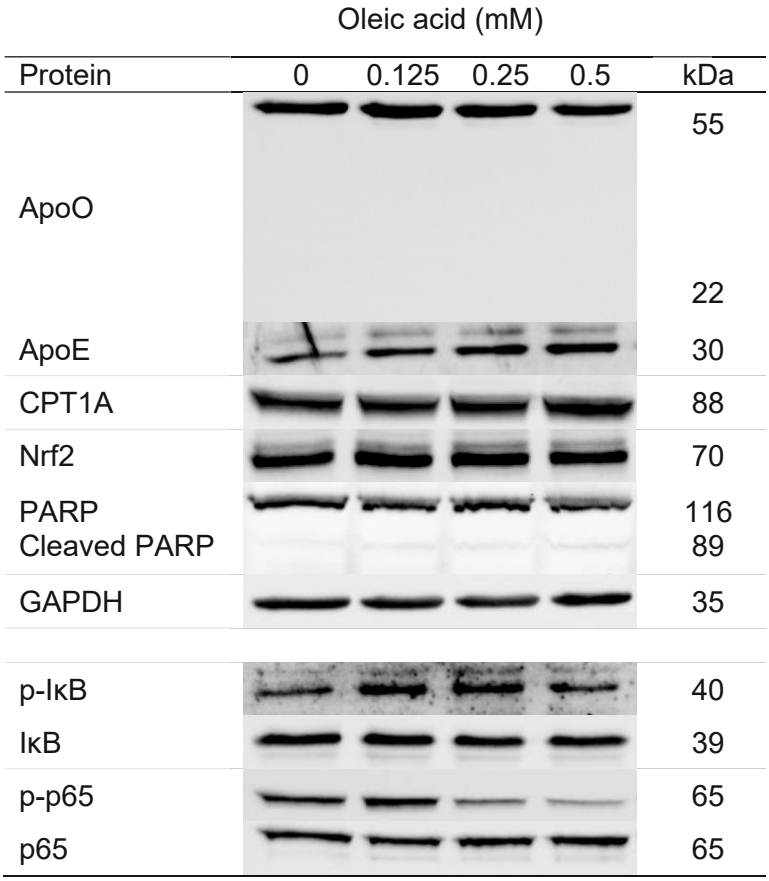

Figure 12: Effect of OA on ApoO, ApoE, CPT1A, Nrf2, PARP, and NF-κB proteins. HepG2 cells were pretreated with pretreatment medium (DMEM) containing 2 % BSA-FAF for 24 h and incubated with treatment medium (DMEM with 2 % BSA-FAF (Control)), 0.125, 0.25 and 0.5 mM OA for 24 h. Proteins were isolated in whole cell lysates followed by Western blot analysis using specific antibodies as described in *3.6.4 Blocking and antibody probing*, Table 13. The relative band intensities of the respective proteins from one experiment are depicted above.

	Oleic acid (mM)			
Protein	0	0.125	0.25	0.5
ApoO/GAPDH	100	145	137	67
ApoE/GAPDH	100	104	157	197
CPT1A/GAPDH	100	109	126	124
Nrf2/GAPDH	100	106	105	100
Cleaved PARP/PARP	5.2	6.7	6.0	8.4
p-IκB/IκB	100	165	165	99
p-p65/p65	100	139	42	24

Table 14: Effect of OA on ApoO, ApoE, CPT1A, Nrf2, PARP, and NF-κB proteins in HepG2 cells after 24 h. Relative band intensities were determined from Figure 12 and set in relation to the loading controls. Protein expression was then calculated with values from controls set as 100 % (see Equation 3). The relative intensities of the respective proteins from one experiment are listed above.

Based on Figure 12 and Table 14, it can be seen that the ApoO content increased with rising OA concentrations, except for 0.5 mM OA. Even though Lamant et al. suggested that also the non-glycosylated form of ApoO can be found at 22 kDa, only the glycosylated 55 kDa ApoO complex was detected.

It was proven that ApoO shows partial sequence homology to ApoE [19]. ApoE is the primary ligand for the LDL receptor and is essential in lipid metabolism [17]. As for ApoO, ApoE was more produced with elevated OA concentrations, which might be traced back to promoted lipid metabolism.

CPT1A is involved in lipid metabolism and fatty acid β-oxidation [59] and its levels appear to be upregulated by OA. Therefore, it can be assumed that β-oxidation is enhanced since more free fatty acids were present and metabolized.

Nrf2 is a transcription factor that binds to antioxidant response elements and is therefore crucial for the activation of such genes as a response to oxidative stress [60]. According to Figure 12 and Table 14, it seems that Nrf2 is unaffected by the treatments.

PARP represents a 116 kDa nuclear poly (ADP-ribose) polymerase, which is related to DNA repair as a reaction to environmental stress. However, it is rated among the main targets of caspase-3, and can be cleaved. Hence, PARP supports cell viability, but its cleavage marks cells undergoing apoptosis [61]. Full length PARP at 116 kDa can be seen for all incubations. However, the large fragment of PARP resulting from caspase-3 cleavage was also detected at 89 kDa, which indicates that cell apoptosis generally occurred. In Table 14 the cleaved fragment was set in relation to full length PARP whereby only small ratios were reached. Nevertheless, the cleaved fraction slightly increased with rising oleic acid concentrations, implying that apoptosis took place to a small extent.

NF-κB is a transcription factors involved in the regulation of genes linked to inflammation, cell proliferation and apoptosis. The transcription factor consists of a homo- or heterodimeric complex of different proteins, whereby the p65-p50 complex is the most common one [62]. The transcriptional activity is inhibited by IκB, which binds to NF-κB and thus keeps the complex in the cytoplasm. When IκB is phosphorylated, NF-κB is translocated to the nucleus, regulating gene expression. The activity of NF-κB complexes including p65 is positively regulated when the p65 subunit is phosphorylated [63]. Therefore, p-p65 and p-IκB can be seen as an indicator of the stress level of the cells. For p-IκB an increase was observed at 0.125 and 0.25 mM OA. Even if p-p65 first increased with 0.125 mM OA, it decreased with rising OA concentrations, implying that OA might have protective properties for the cells. On the other hand, activation of the NF-κB pathway could have occurred at an earlier time point and after 24 h a counter-regulation was monitored.

4.3.1.2 Cell fractionation of HepG2 cells incubated with OA

To have a better understanding of what is happening inside of the cells when they are exposed to OA, HepG2 cells were pretreated and treated as described for the whole cell lysates and cell fractionation was performed, separating cells into cytosolic, mitochondrial, and nuclear

fractions. The loading controls for the proteins of the fractions were represented by GAPDH, TOMM20, and Lamin B1, respectively. Figure 13 summarises the examined proteins and the pictures of the Western blot analysis. The corresponding relative values were calculated with Equation 3 and are listed in Table 15.

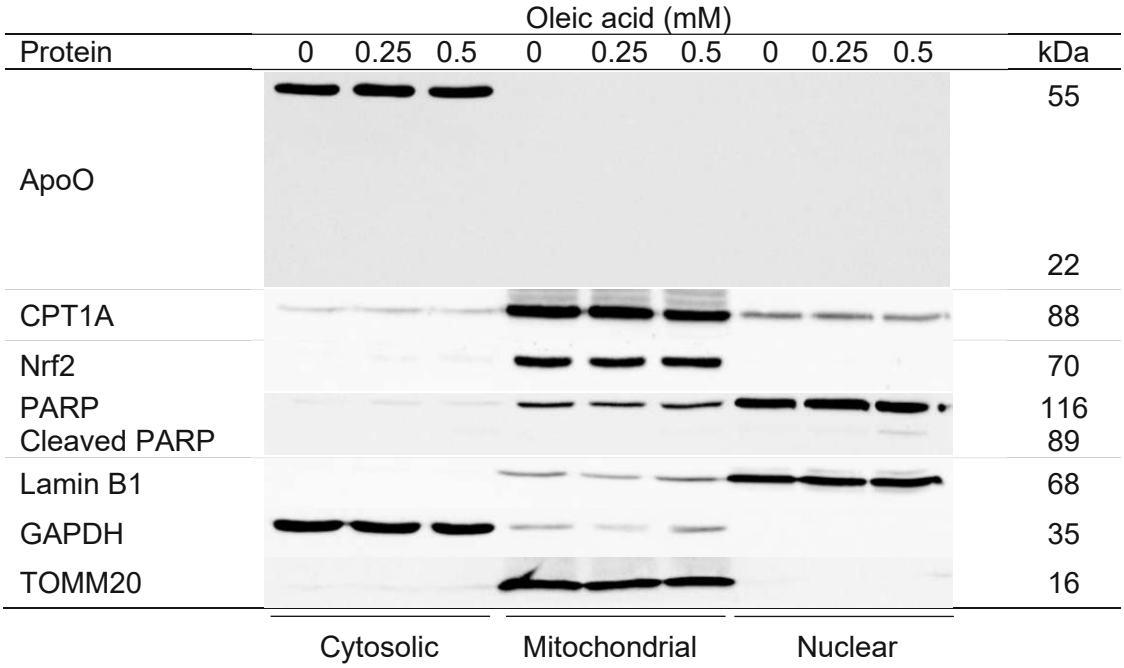

Figure 13: Effect of OA on ApoO, CPT1A, Nrf2, and PARP. HepG2 cells were pretreated with pretreatment medium (DMEM) containing 2 % BSA-FAF for 24 h and incubated with treatment medium (DMEM with 2 % BSA-FAF (Control)), 0.25 and 0.5 mM OA for 24 h. Proteins were isolated with an Abcam fractionation kit, followed by Western blot analysis using specific antibodies as described in *3.6.4 Blocking and antibody probing*, Table 13. The relative band intensities of the respective proteins from one experiment are depicted above.

		Oleic acid (mM)		
Protein	Fraction	0	0.25	0.5
ApoO/GAPDH	Cytosolic	100	158	114
CPT1A/TOMM20	Mitochondrial	100	113	92
Nrf2/TOMM20	Mitochondrial	100	125	158
Cleaved PARP/PARP	Nuclear	n.d.	n.d.	1.6

Table 15: Effect of OA on ApoO, CPT1A, Nrf2, and PARP in HepG2 cells after 24 h and isolation with an Abcam fractionation kit. Relative band intensities were determined from Figure 13 and set in relation to the loading controls. Protein expression was then calculated with values from controls set as 100 % (see Equation 3). The relative intensities of the respective proteins from one experiment are listed above.

Looking at Figure 13 and Table 15, it is apparent that the ApoO content increased with rising OA concentrations, as before (see *4.3.1.1 Whole-cell lysates of HepG2 cells incubated with OA*). Again the non-glycosylated form of ApoO, which is part of the MICOS complex [21], was not detected in the mitochondrial fraction. Only the glycosylated form was found in the cytosolic fraction.

CPT1A was mainly detected in the mitochondrial fraction since β-oxidation takes place in mitochondria. This time, the CPT1A content increased again by the treatment with 0.25 mM OA but decreased for 0.5 mM OA.

Since Nrf2 is a transcription factor, it was expected to find Nrf2 in the nuclear fraction. Instead, explicit bands can be seen in the mitochondrial fraction. In an unstressed environment, Nrf2 is bound to KEAP1, representing its inactive state. KEAP1 is primarily localized in the cytosol with small amounts in the nucleus and endoplasmic reticulum (ER) [64]. Furthermore, Abcam provided the information that ER proteins are mainly found in the mitochondrial fraction [65]. Thus, we conclude that the Nrf2 detected here reflects its KEAP1 anchored status of Nrf2 in ER. Contrary to *4.3.1.1 Whole-cell lysates of HepG2 cells incubated with OA*, Nrf2 was more produced with increased OA concentrations. However, it is negligible if it promoted the activation of antioxidant damage proteins because it was not found in the nuclear fraction and probably in its inactive form.

Full length PARP was detected for all treatments and was mainly found in the nuclear fraction. A faint band at 89 kDa for 0.5 mM OA can be seen, implying that cell apoptosis might have occurred. Regarding the Whole-Cell Lysates, cleaved fragments were visible by all treatments and it appears as if generally less PARP was cleaved this time, comparing Table 14 and Table 15.

Furthermore, the pictures of the cell compartment-specific loading control indicate that the fractionation was successful.

4.3.2 LDH assay of HepG2 cells incubated with OA

The effect of an oleic acid concentration gradient on the health condition of the cells was already described in *4.2.1.2 LDH assay of HepG2 cells incubated with OA*. To see if this outcome was representative, the measured values of all experiments with a treatment time of 24 h were combined. The corresponding result can be found in *9 Appendix*, Figure 25. Even if high standard deviations were reached for 0.75 and 1 mM OA, very similar LDH releases were measured for controls, 0.125, 0.25, and 0.5 mM OA. From 0.75 mM OA on, the LDH activity rises rapidly, probably referring to toxic OA concentrations. Generally, this outcome agrees with the previous one, which can be seen in Figure 8.

4.4 Effect of induced stress by TNFα and menadione on HepG2 cells

As several publications [19, 22, 24, 28,29] indicate, ApoO might play a role in stress responses. Hence, the effect of TNFα and menadione, which can activate the NF-κB pathway, on HepG2 cells was examined. Cells were pretreated with pretreatment medium (DMEM) without BSA for 2 h, followed by incubations with treatment medium (DMEM with 2 % BSA-FAF), 0.5 mM OA, 1 mM OA, 100 ng/mL TNFα, 5 µM menadione and 10 µM menadione for 24 h or with treatment

medium (DMEM with 2 % BSA-FAF), 1 mM OA, 100 ng/mL TNFα and 10 µM menadione for 4 h. With this, the main function of the NF-κB, which is to react as fast as possible, was considered and it was investigated if the exposure to TNFα and menadione led to traceable stress responses. For Western blot analysis, whole-cell lysates were generated and the health condition of the cells was further assessed by LDH assays with the corresponding supernatants.

Another experiment with stress factors was conducted, where cells were pretreated for 24 h with pretreatment medium (DMEM) containing 2 % BSA-FAF and incubated with treatment medium (DMEM with 2 % BSA-FAF), 1 mM OA, 100 ng/mL TNFα and 10 µM menadione for 24 h. The whole-cell lysates were investigated by Western blot analysis and are summarised in *9 Appendix* (see Figure 26 and Table 23)

4.4.1 Western blot analysis of HepG2 cells incubated with TNFα and menadione

Followingly, the pictures of the Western blot analysis of the experiment after 24 h incubation (described above) are shown in Figure 14. The corresponding relative values were calculated using Equation 3 and are summarised in Table 16.

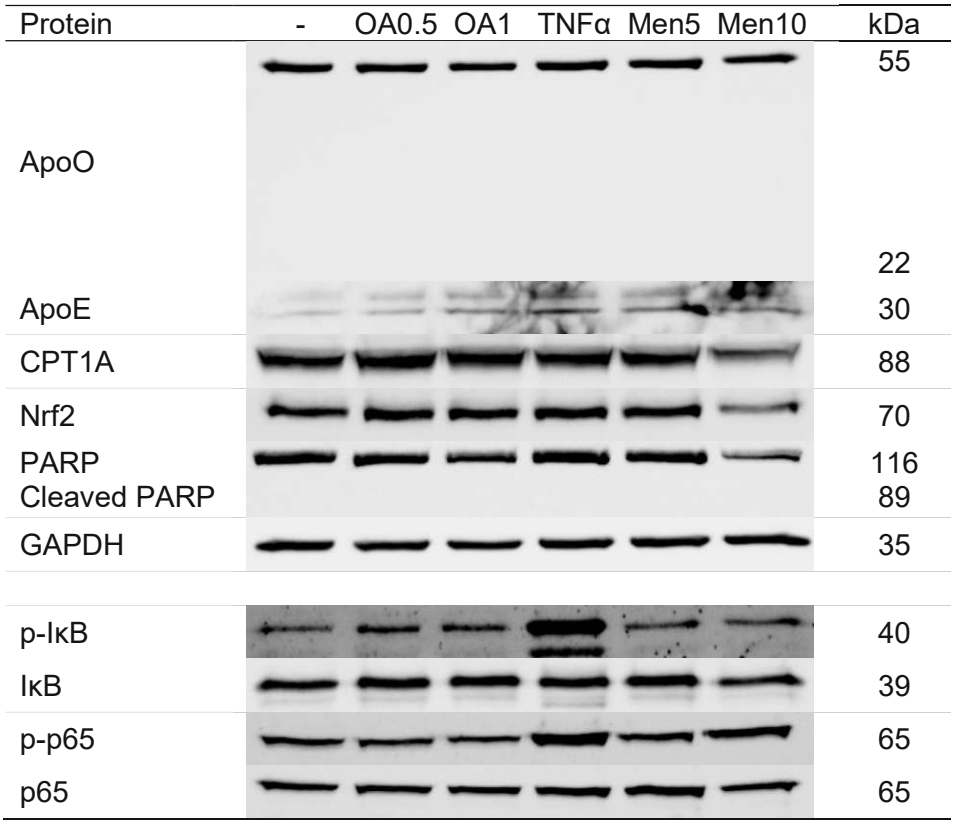

Figure 14: Effect of OA and stress factors on ApoO, ApoE, CPT1A, Nrf2, PARP, and NF-κB proteins. HepG2 cells were pretreated with pretreatment medium (DMEM) without BSA for 2 h and incubated with treatment medium (DMEM with 2 % BSA-FAF (Control)), 0.5 mM OA, 1 mM OA, 100 ng/mL TNFα, 5 µM menadione (Men5) or 10 µM menadione (Men10) for 24 h. Proteins were isolated in whole cell lysates followed by Western blot analysis using specific antibodies as described in *3.6.4 Blocking and antibody probing*, Table 13. The relative band intensities of the respective proteins from one experiment of two performed are depicted above.

Protein	-	OA0.5	OA1	TNFα	Men5	Men10
ApoO/GAPDH	100	121	106	120	109	80
ApoE/GAPDH	100	152	267	249	673	418
CPT1A/GAPDH	100	138	132	104	96	60
Nrf2/GAPDH	100	134	129	119	109	52
Cleaved PARP/PARP	n.d	n.d	n.d	n.d	n.d	n.d
p-IκB/IκB	100	118	138	1119	90	122
p-p65/p65	100	81	72	201	61	179

Table 16: Effect of OA and stress factors on ApoO, ApoE, CPT1A, Nrf2, PARP, and NF-κB proteins in HepG2 cells after 24 h. Relative band intensities were determined from Figure 14 and set in relation to the loading controls. Protein expression was then calculated with values from controls set as 100 % (see Equation 3). The relative intensities of the respective proteins from one experiment of two performed are listed above.

ApoO levels were slightly upregulated by all treatments, except for 10 µM menadione. The highest ApoO production was achieved by the incubation with 0.5 mM OA and TNFα. Regarding ApoE, an increase was determined by all treatments. However, due to the strong background, the effect is difficult to verify.

For Nrf2, other results than before were obtained. The outcome of the analysis of the whole-cell lysate of the OA dependency experiment (Figure 12, Table 14) suggests that Nrf2 was not much affected by the treatments containing OA. This time, both OA and TNFα led to a stronger increase.

As expected, the OA incubations elevated the CPT1A production. Through TNFα and 5 µM menadione, CPT1A appeared to be unaffected.

Regarding PARP, no cleavages were observed, and thus no apoptosis was detected. Before, cleavages for at least 0.5 mM OA were detected (see Figure 12, Figure 13). The stress factors TNFα and 10 µM menadione seem to activate the NF-κB pathway since their incubation led to an accumulation of p-IκB. Only 5 µM lowered the p-IκB content. As previously measured, lower p-p65 concentrations were established by OA (Table 14) and this time also by 5 µM menadione treatment. On the other hand, 10 µM menadione and TNFα reached a definite increase of p-p65.

Since the main function of the NF-κB pathway is to react as fast as possible, the effect of 1 mM OA, TNFα, and 10 µM menadione was additionally observed after 4 h of incubation. The pictures of the Western blot analysis are shown in Figure 15 and the relative intensities are summarised in Table 17.

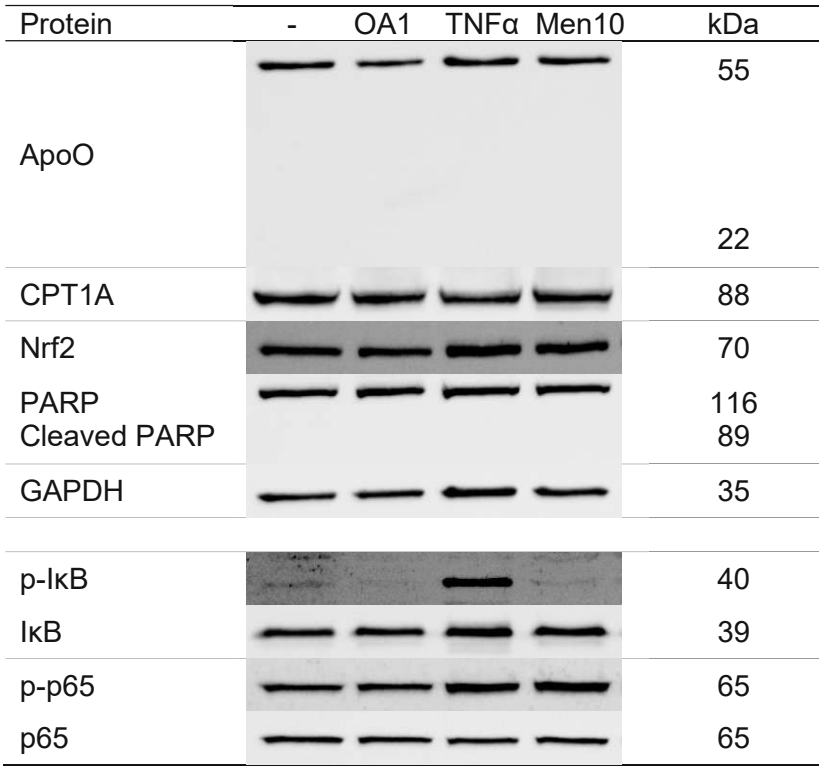

Figure 15: Effect of OA and stress factors on ApoO, CPT1A, Nrf2, PARP, and NF-κB proteins. HepG2 cells were pretreated with pretreatment medium (DMEM) without BSA for 2 h and incubated with treatment medium (DMEM with 2 % BSA-FAF (Control)), 1 mM OA, 100 ng/mL TNFα or 10 µM menadione (Men10) for 4 h. Proteins were isolated in whole cell lysates followed by Western blot analysis using specific antibodies as described in *3.6.4 Blocking and antibody probing*, Table 13. The relative band intensities of the respective proteins from one experiment are depicted above.

Protein	-	OA1	TNFα	Men10
ApoO/GAPDH	100	67	75	88
CPT1A/GAPDH	100	107	64	100
Nrf2/GAPDH	100	102	163	130
Cleaved PARP/PARP	n.d.	n.d.	n.d.	n.d.
p-IκB/IκB	100	50	743	51
p-p65/p-65	100	122	244	241

Table 17: Effect of OA and stress factors on ApoO, CPT1A, Nrf2, PARP, and NF-κB proteins in HepG2 cells after 4 h. Relative band intensities were determined from Figure 15 and set in relation to the loading controls. Protein expression was then calculated with values from controls set as 100 % (see Equation 3). The relative intensities of the respective proteins from one experiment are listed above.

Figure 15 and Table 17 indicate that the ApoO production was downregulated by all treatments after an incubation time of 4 h, which could lead to the assumption that ApoO might not be part of a quick stress response.

Regarding CPT1A, TNFα lowered its production, 1 mM OA and 10 µM menadione seemed to have no effect after 4 h of treatment.

The Nrf2 content was enhanced by the incubation with the stress factors and remained approximately at the same level by the OA treatment as the control, concluding that the stress factors might activate the expression of genes for antioxidant defense.

As the picture illustrates, no cleavage of PARP was detected, like after 24 h (see Figure 14). As expected, p-p65 levels were increased by all treatments, indicating a stress response. Due to the strong background of the picture of p-IκB, the relative intensities should be treated with caution. Nevertheless, since TNFα is a well-known inducer of NF-κB it seems that a quick stress response occurred during the incubation with TNFα, and a definite upregulation was detected by this treatment.

To better assess the differences between the incubation times, a heatmap, Figure 16, was created. Even though the second performed experiment with stress factors had a different pretreatment (see Figure 26, Table 23 in *9 Appendix*), the outcomes of this experiment and the ones shown above were also compared in the heatmap. Hence, differences in the protein production for 1 mM OA, TNFα, and 10 µM menadione are better visible.

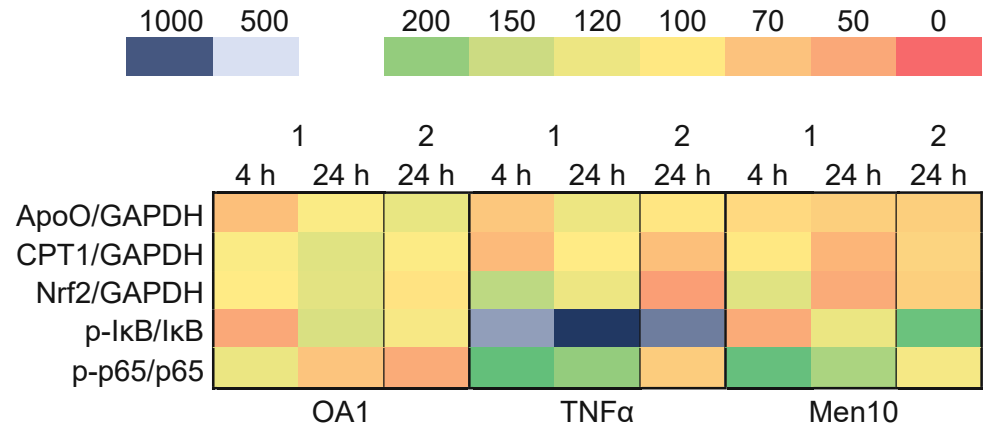

Figure 16: Heatmap of relative intensities of ApoO, Nrf2, CPT1A, and NF-κB proteins in HepG2 cells of two experiments. For one experiment (marked in the heatmap as "1"), cells were pretreated with pretreatment medium (DMEM) for 2 h and then incubated for 4 and 24 h. For the second experiment (marked in the heatmap as "2"), cells were pretreated with pretreatment medium (DMEM) containing 2 % BSA-FAF for 24 h and then incubated for 24 h. Cells were treated with treatment medium (DMEM with 2 % BSA-FAF (Control)), 1 mM OA, 100 ng/mL TNFα and 10 µM menadione (Men10) with DMEM containing 2 % BSA-FAF as treatment medium. Relative band intensities were taken from Table 16, Table 17, and Table 23 for experiment 1 after 24 h, experiment 1 after 4 h, and experiment 2 after 24 h, respectively.

Based on Figure 16, it can be seen that after 4 h of treatment, the ApoO content was reduced by all incubations. After 24 h, both experiments achieved similar outcomes: ApoO levels stayed approximately the same as the control or were slightly upregulated for 1 mM OA and TNFα, and were decreased by 10 µM menadione.

CPT1A levels were increased by 1 mM OA, implying that β-Oxidation was promoted, but the effect was only small for experiment 2. After 4 h and 24 h of incubation with stress factors, CPT1A production was reduced except for TNFα after 24 h for experiment 1. The decrease might be traced back to an amelioration of the oxidative stress inside the cells. β-Oxidation might be downregulated to avoid the production of intracellular reactive oxygen species and therefore further oxidative stress.

Regarding Nrf2, different results were obtained by the experiments. After 4 h, Nrf2 production was enhanced by the incubation with the stress factors. For experiment 1, Nrf2 creation was upregulated by 1 mM OA and TNFα after 24 h, while for experiment 2 a reduction was determined by TNFα and its expression seems to be unaffected by 1 mM OA. Nevertheless, both experiments led to a decrease of Nrf2 by the incubation with 10 µM menadione. Therefore, it might be assumed that after 4 h of treatment, oxidative stress is present by the stress factors and after 24 h cells regenerate over time at varying rates and a counter-regulation might be observed.

While after 4 h a possible protective effect of 1 mM OA is not present, it might have been after 24 h, since p-p65 was downregulated. As expected, the stress factors led to an increase of the p-p65 content after 4 h and 24 h for experiment 1. Surprisingly, for experiment 2, a decrease was detected by TNFα and only a slight increase by 10 µM menadione. As mentioned before, a counter-regulation might have been monitored, and different regeneration periods resulted in varied outcomes between experiments 1 and 2. The varying regeneration times might be traced back to the different pretreatments.

p-IκB showed a different course compared to p-p65. After 4 h, less p-IκB was detected than after 24 h. Nevertheless, similar trends were observed between experiment 1 and 2. Since IκB is phosphorylated before p65 during the cascade of the NF-κB pathway, a possible counter-regulation already occurred after 4 h, whereby the p-IκB content is already decreased, but p-p65 still increased. The results of p-IκB once more clarify that TNFα, a well-known NF-κB activator, caused the greatest stress response.

Overall, stress situations were successfully simulated by TNFα and menadione, as the p-p65 and p-IκB content (Figure 14, Figure 15, Figure 26) indicate. Regarding ApoO, it was shown that after 4 h of incubation, levels were decreased by all treatments. Therefore, it is neither formed due to lipid accumulation nor as a stress response. After 24 h of treatment, when the stress response seemed to decline, the ApoO content only slightly increased or stayed approximately at the same level as the control, except for 10 µM menadione. This might imply, that ApoO production is rather promoted when cells are not in an acute stress situation.

4.4.2 LDH assay of HepG2 cells incubated with TNFα and menadione

The results of the LDH assays after 4 h and 24 h of treatment are shown in Figure 17A and Figure 17B, respectively.

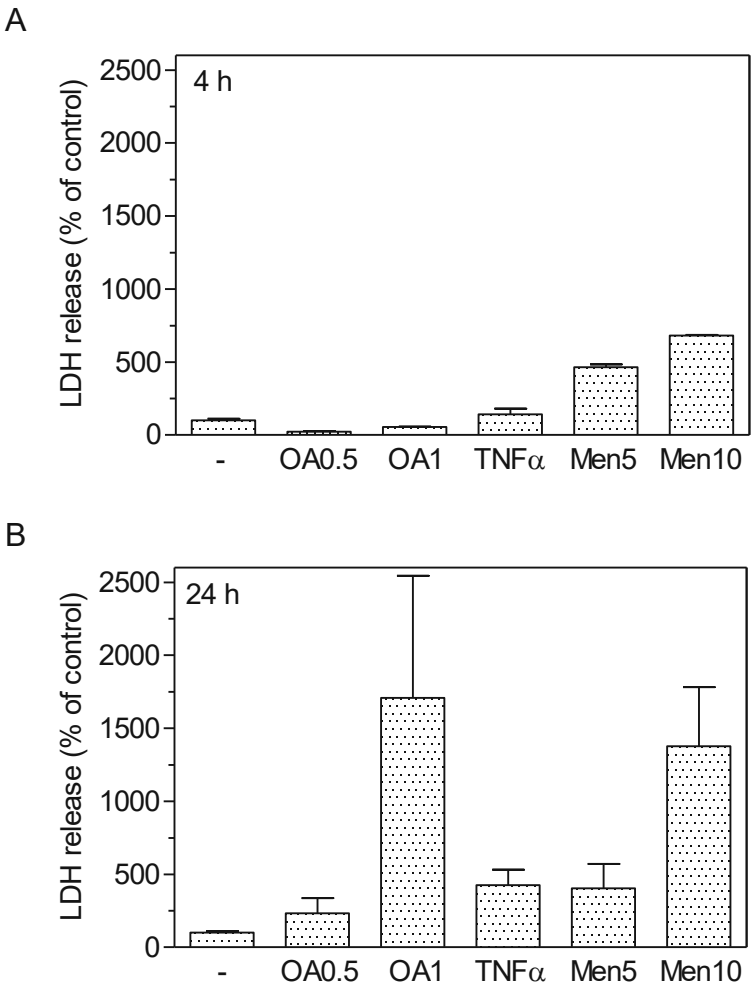

Figure 17: Effect of OA and stress factors on the LDH release of HepG2 cells after 4 (A) and 24 h (B). Cells were pretreated with pretreatment medium (DMEM) without BSA for 2 h, incubated with treatment medium (DMEM with 2 % BSA-FAF (Control)), 0.5 mM OA, 1 mM OA, 100 ng/mL TNFα, 5 µM menadione (Men5) or 10 µM menadione (Men10) for 4 (A) and 24 h (B), followed by determination of the LDH release. The experiment of 24 h treatment time was combined with another one, in which cells were pretreated with pretreatment medium (DMEM) with 2 % BSA-FAF for 24 h and incubated with treatment medium (DMEM with 2 % BSA-FAF (Control)), 1 mM OA, 100 ng/mL TNFα or 10 µM menadione (Men10) for 24 h. Bars show mean values +/- SD of biological duplicates from one experiment (A) and of two individual experiments (also in biological duplicates; B).

When taking a look at Figure 17A and Figure 17B, it is visible that lower LDH releases were detected after 4 h of treatment, compared to 24 h. Interestingly, the number of damaged cells is lower for the incubations including OA after 4 h than for the control group, even though an increased p-p65 content was identified by 1 mM OA (Table 17). On the other hand, a decreased production of p-p65 was established after 24 h incubation (Table 14, Table 16, and Table 23). Probably, cells were stressed due to the exposure to the treatment itself after 4 h, thus raising the p-p65 content and after 24 h, a possible protective mechanism could have lowered the p-p65 levels although the simultaneously lipotoxic effect that might be caused by 1 mM OA, damages the membranes. Another reason could be a counter-regulation after 24 h of p-p65 as stated above: inside the cells, a stress reaction occurs that decreases over time, and after 24 h, cells settle back to their normal state.

By comparing Figure 17A and Figure 17B it is additionally visible, that the LDH release increased the most for 1 mM OA over time due to the mentioned putative lipotoxicity. The effect of 5 µM menadione stayed approximately the same, and the one of TNFα on the LDH release rose over time. 10 µM menadione showed the highest number of damaged cells after 4 h of treatment which might be overtaken by 1 mM OA after 24 h. As for Figure 17B, the corresponding levels of p-p65 and p-IκB (Table 16) also indicate that the greatest stress response took place with TNFα and 10 µM menadione.

As seen before (Figure 8), the LDH release was increased by 1 mM OA compared to 0.5 mM OA, this time by a factor of about 7 after 24 h, indicating that this treatment leads to an even more toxic environment than the incubations with the stress factors, which might explain the cleaved band of PARP in Figure 26 only at 1 mM OA.

4.5 Effect of OA plus stress factors on HepG2 cells

As described above, it seems that OA might have a positive impact on the cells since the LDH release was even lower than for the control group after 4 h of incubation (Figure 17A), and the p-p65 content was decreased after 24 h of treatments containing OA compared to the control group (Table 14, Table 16 and Table 23). Hence, the question arose, if possible protective and anti-inflammatory effects are present when OA is incubated together with stress factors. Regarding lipid accumulation, Figure 11 implies that TG accumulation that occurs through the incubation with OA is not affected by the combination. To assess the processes inside HepG2 cells, Western blot analysis was conducted two times: first, with whole-cell lysates, and second after cell fractionation. For both experiments, cells were not pretreated and after two times of washing with PBS, incubated with treatment medium (DMEM with 2 % BSA-V (Control)), 0.5 mM OA, 100 ng/mL TNFα, 5 µM menadione, or 0.5 mM OA plus the stress factors for 4 and 24 h. Other than before, the treatment medium was not supplied with L-glutamine. Moreover, LDH assays with the corresponding supernatants were performed to investigate the condition of cells when exposed to the combination of OA and stress factors.

4.5.1 Western blot analysis of HepG2 cells incubated with OA plus stress factors

4.5.1.1 Whole-cell lysates of HepG2 cells incubated with OA plus stress factors

The effect of the combination of OA plus stress factors on cellular proteins were investigated by Western blot analysis. The obtained pictures after a treatment time of 4 h are shown in Figure 18 and the relative values are listed in Table 18.

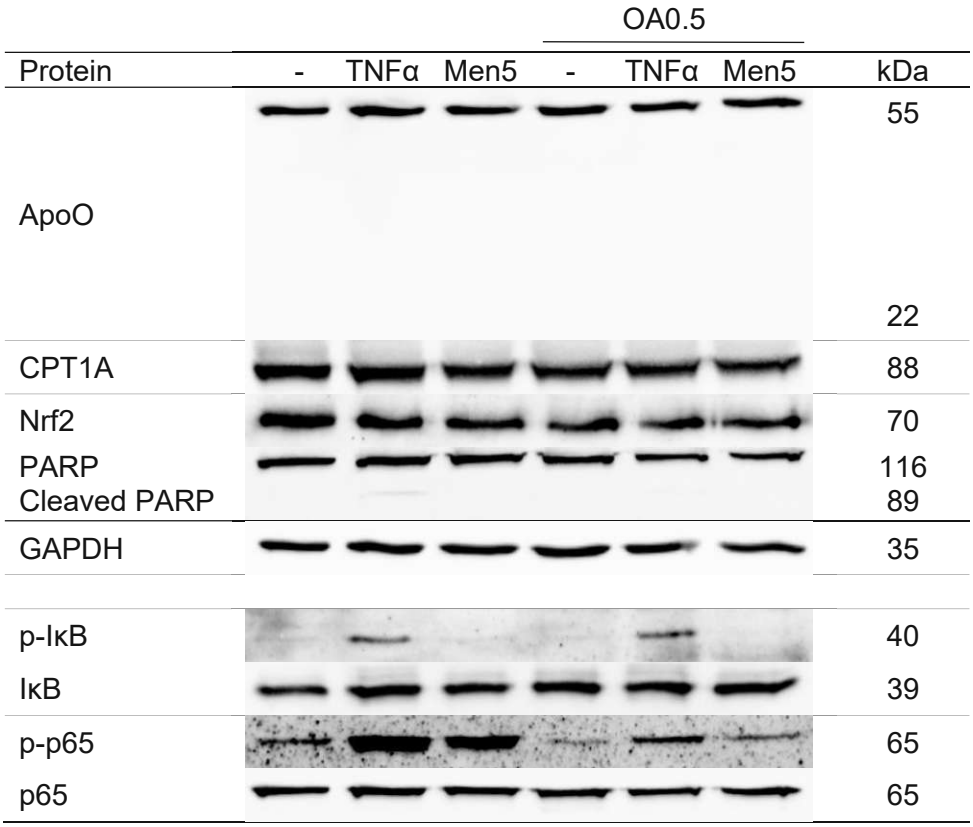

Figure 18: Effect of OA, stress factors, and OA plus stress factors on ApoO, CPT1A, Nrf2, PARP, and NF-κB proteins. HepG2 cells were not pretreated, washed two times with PBS, and incubated with treatment medium (DMEM with 2 % BSA-V, without L-glutamine (Control)), 100 ng/mL TNFα, 5 µM menadione (Men5), 0.5 mM OA, 0.5 mM OA plus 100 ng/mL TNFα or 0.5 mM OA plus 5 µM menadione for 4 h. Proteins were isolated in whole cell lysates followed by Western blot analysis using specific antibodies as described in *3.6.4 Blocking and antibody probing*, Table 13. The relative band intensities of the respective proteins from one experiment are depicted above.

				OA0.5		
Protein	-	TNFα	Men5	-	TNFα	Men5
ApoO/GAPDH	100	118	95	91	88	113
CPT1A/GAPDH	100	85	77	72	85	86
Nrf2/GAPDH	100	66	66	54	61	72
Cleaved PARP/PARP	n.d.	1.5	n.d.	n.d.	n.d.	n.d.
p-p65/p65	100	1187	599	32	176	67

Table 18: Effect of OA, stress factors, and OA plus stress factors on ApoO, CPT1A, Nrf2, PARP, and NF-κB proteins in HepG2 cells after 4 h. Relative band intensities were determined from Figure 18 and set in relation to the loading controls. Protein expression was then calculated with values from controls set as 100 % (see Equation 3). The relative intensities of the respective proteins from one experiment are listed above.

In contrast to the previous 4 h experiment where only decreased ApoO levels were detected (Table 17), the most ApoO was this time produced by the treatment with TNFα. Otherwise, its levels were decreased except for the combination of 0.5 mM OA and 5 µM menadione.

As seen before (Table 17), CPT1A levels were decreased by the incubations with the stress factors. But the content was also reduced by the treatments containing 0.5 mM OA, which was unexpected since it has been suggested that CPT1A production is promoted by lipid accumulation and is also enhanced by 1 mM OA after 4 h (Table 17).

Surprisingly, all treatments lowered the creation of Nrf2, which is contrary to Table 17, stating that 4 h of incubation with TNFα elevated the Nrf2 production.

According to the pictures in Table 15, PARP was only cleaved by the treatment with TNFα. However, the amount of cleaved PARP compared to full length PARP was only about 1.5 %, implying that cell apoptosis might have occurred to a small extent and the greatest environmental stress resulted from the treatment with TNFα.

This assumption can be maintained, when looking at p-p65 and p-IκB: the highest p-p65 level was determined by the well-known Nf-κB activator TNFα, and even though no relative intensities could be calculated for p-IκB, only bands at the two incubations with TNFα can be seen. For p-p65 it is even optically visible, that the presence of 0.5 mM OA decreased the p-p65 levels, even if stress factors were present, as the relative intensities confirm.

The following Figure 19 comprises the pictures of the Western blot analysis after 24 h and Table 19 summarises the corresponding relative values of the protein production.

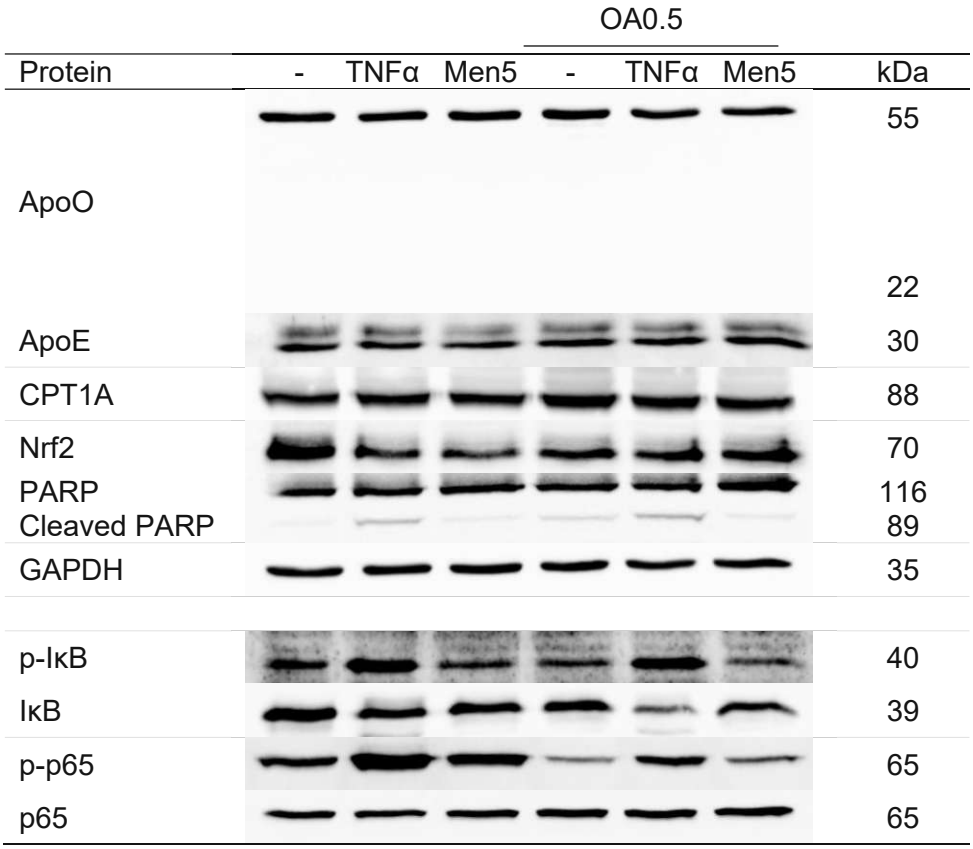

Figure 19: Effect of OA, stress factors, and OA plus stress factors on ApoO, ApoE, CPT1A, Nrf2, PARP, and NF-κB proteins. HepG2 cells were not pretreated, washed two times with PBS, and incubated with treatment medium (DMEM with 2 % BSA-V, without L-glutamine (Control)), 100 ng/mL TNFα, 5 µM menadione, 0.5 mM OA, 0.5 mM OA plus 100 ng/mL TNFα or 0.5 mM OA plus 5 µM menadione for 24 h. Proteins were isolated in whole cell lysates followed by Western blot analysis using specific antibodies as described in *3.6.4 Blocking and antibody probing*, Table 13. The relative band intensities of the respective proteins from one experiment are depicted above.

				OA0.5		
Protein	-	TNFα	Men5	-	TNFα	Men5
ApoO/GAPDH	100	88	92	104	89	69
ApoE/GAPDH	100	87	80	122	145	145
CPT1A/GAPDH	100	108	89	133	139	108
Nrf2/GAPDH	100	49	38	61	82	87
Cleaved PARP/PARP	4.7	10	3.3	8.2	16	4.3
p-IκB/ IκB	100	372	92	70	310	62
p-p65/p65	100	488	161	16	52	19

Table 19: Effect of OA, stress factors, and OA plus stress factors on ApoO, CPT1A, Nrf2, PARP, and NF-κB proteins in HepG2 cells after 24 h. Relative band intensities were determined from Figure 19 and set in relation to the loading controls. Protein expression was then calculated with values from controls set as 100 % (see Equation 3). The relative intensities of the respective proteins from one experiment are listed above.

According to Table 19, ApoO production was promoted the most by the treatment with 0.5 mM OA alone, as seen before in Table 16 and Table 23. However, the content was only slightly increased compared to the control. Furthermore, less ApoO was generated by the combination of 0.5 mM OA with 5 µM menadione than only for 5 µM menadione, even though it can be assumed that an increased lipid accumulation was achieved. Thus, it appears that ApoO levels were decreased by a stress response, even if an enhanced TG content is present. Lowered ApoO creation due to the incubation with stress factors was on one hand seen before (Table 23), but on the other hand, elevated levels were detected as well (Table 16). Therefore, the function of ApoO in stress responses after 24 h appears to remain unclear. Furthermore, no similarities to ApoE production were seen.

As expected, and seen before (Table 14 and Table 16), CPT1A levels appear to be raised by lipid accumulation, since the incubations containing 0.5 mM OA led to an increase.

Nrf2 was downregulated by all treatments, which is in accordance, with Table 23, but not with Table 16, where increased contents were achieved except for 10 µM menadione.

While after 4 h of treatment, only one faint cleaved band by the incubation with TNFα was detected (Figure 18), after 24 h a cleavage is visible by all incubations (Figure 19). Furthermore, based on the ratio of cleaved PARP to full length PARP (Table 19), no protective effect of OA can be seen, since it is higher for 0.5 mM OA than for the control, and for the combinations of OA with stress factors than the stress factors alone. Therefore, more cells seemed to undergo apoptosis when OA was present.

Optically, a decreased signal intensity of p-p65 due to incubations containing 0.5 mM OA compared to the respective samples without 0.5 mM OA can be determined in Figure 19, which can be confirmed, when examining the corresponding relative intensities (Table 19). This effect was also observable for p-IκB. Even though the signal for 0.5 mM OA with TNFα was increased compared to the control with OA alone, all values were lower in the presence of OA than in its

absence. These findings lead again to the assumption, that OA has protective and anti-inflammatory effects on the cells.

To gain a better overview of the effects of the incubation times with and without OA on cellular proteins, the following heatmap Figure 20 was created.

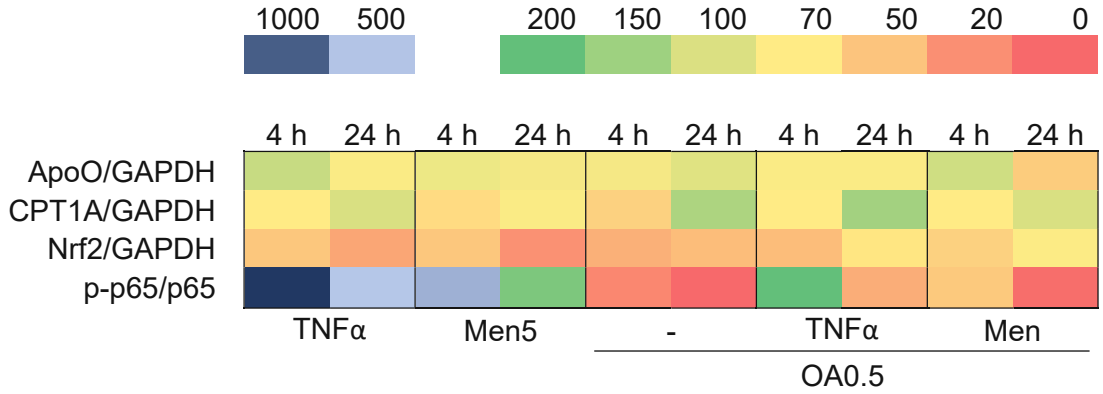

Figure 20: Heatmap of relative intensities of ApoO, Nrf2, CPT1A, and NF-κB proteins in HepG2 cells of one experiment. Cells were not pretreated, washed two times with PBS, and incubated with treatment medium (DMEM with 2 % BSA-V, without L-glutamine (Control)), 100 ng/mL TNFα, 5 µM menadione (Men5), 0.5 mM OA, 0.5 mM OA plus 100 ng/mL TNFα or 0.5 mM OA plus 5 µM menadione (Men5) for 24 h. Relative band intensities were taken from Table 18 and Table 19 for 4 h and 24 h of treatment, respectively.

Except for 0.5 mM OA combined with 5 µM menadione after 24 h, only small differences were detected for ApoO levels, as it is illustrated in Figure 20. As already mentioned, the highest ApoO amount after 4 h was reached by the treatment with TNFα and after 24 h by 0.5 mM OA. This could lead to the assumption that for short incubations, ApoO is rather formed due to a stress response, and for longer treatments due to lipid accumulation. However, this statement does not agree with the data stated above: in the heatmap, Figure 16, it is illustrated that ApoO levels were reduced by all treatments after 4 h, and Table 16 shows that after 24 h the incubations with 0.5 mM OA, and TNFα led to a similar increased ApoO production.

As expected, CPT1A production was promoted by the incubations containing OA after 24 h and stayed at approximately the same level as the control by treatments with the stress factors.

Except for the incubations of OA combined with stress factors, the Nrf2 content decreases over time. Generally, the Nrf2 levels were reduced compared to the control.

Figure 20 displays the reduction of p-p65 content over time for all treatments, by comparing 4 h with 24 h. Moreover, a possible protective and anti-inflammatory effect of OA can be seen, since the amount of p-p65 is decreased by OA and is also reduced by the combination of OA and the stress factors.

4.5.1.2 Cell fractionation of HepG2 cells incubated with OA plus stress factors

Finally, cell fractionation was performed. This time, cells were only separated in a cytosolic and a nuclear fraction, applying the Active Motif Kit (see *3.3.2.2 Active Motif Kit – Separation of cytosolic and nuclear fractions*). Cells were not pretreated and after two times of washing

with PBS, incubated with treatment medium (DMEM with 2 %BSA-V (Control)), 0.5 mM OA, 100 ng/mL TNFα, 5 µM menadione or 0.5 mM OA plus the stress factors for 4 and 24 h. Other than before, the treatment medium was not supplied with L-glutamine. The cellular protein production was then assessed by Western blot analysis and GAPDH was used as a loading control for the cytosolic, and Lamin B1 for the nuclear fraction. For the 24 h experiments, both stress factors and their combinations with 0.5 mM OA were observed. Due to a limited number of cells, only TNFα was used as a stress factor for the 4 h approach. The pictures after 4 h of incubation with TNFα are shown in Figure 21 and the relative values are listed in Table 20. The outcomes after 24 h with TNFα are shown in Figure 22 and Table 21, the results with 5 µM menadione can be found in Figure 23 and Table 22.

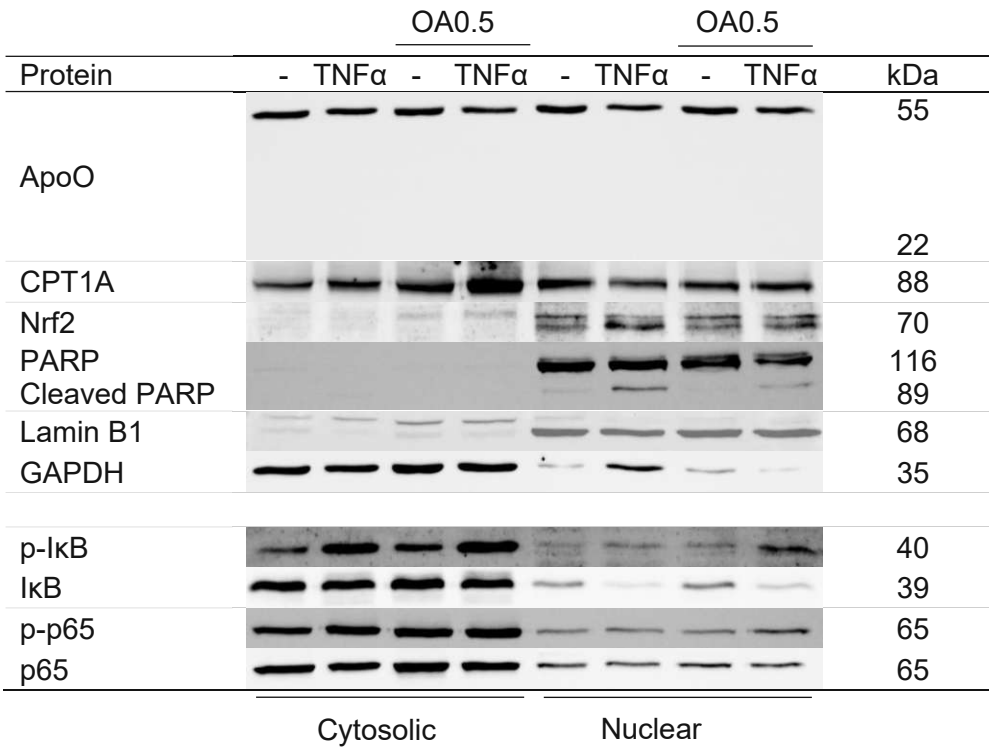

Figure 21: Effect of OA, TNFα, and OA plus TNFα on ApoO, CPT1A, Nrf2, PARP, and NF-κB proteins. HepG2 cells were not pretreated, washed twice with PBS, and incubated with treatment medium (DMEM with 2 % BSA-V (Control)), 100 ng/mL TNFα, 0.5 mM OA or 0.5 mM OA plus 100 ng/mL TNFα for 4 h. Proteins were isolated with an Active Motif Fractionation Kit, followed by Western blot analysis using specific antibodies as described in *3.6.4 Blocking and antibody probing*, Table 13. The relative band intensities of the respective proteins from one experiment are depicted above.

				OA0.5	
Protein	Fraction	-	TNFα	-	TNFα
ApoO/GAPDH	Cytosolic	100	95	69	49
ApoO/Lamin B1	Nuclear	100	80	95	66
CPT1A/GAPDH	Cytosolic	100	144	107	187
CPT1A/Lamin B1	Nuclear	100	79	73	73
Nrf2/Lamin B1	Nuclear	100	146	81	88
Cleaved PARP/PARP	Nuclear	0.7	7.3	0.5	5.6
p-IκB/ IκB	Cytosolic	100	679	127	965
p-p65/p65	Cytosolic	100	269	181	274

Table 20: Effect of OA, TNFα, and OA plus TNFα on ApoO, CPT1A, Nrf2, PARP, and NF-κB proteins in HepG2 cells after 4 h and isolation with an Active Motif Fractionation Kit. Relative band intensities were determined from Figure 21 and set in relation to the loading controls. Protein expression was then calculated with values from controls set as 100 % (see Equation 3). The relative intensities of the respective proteins from one experiment are listed above.

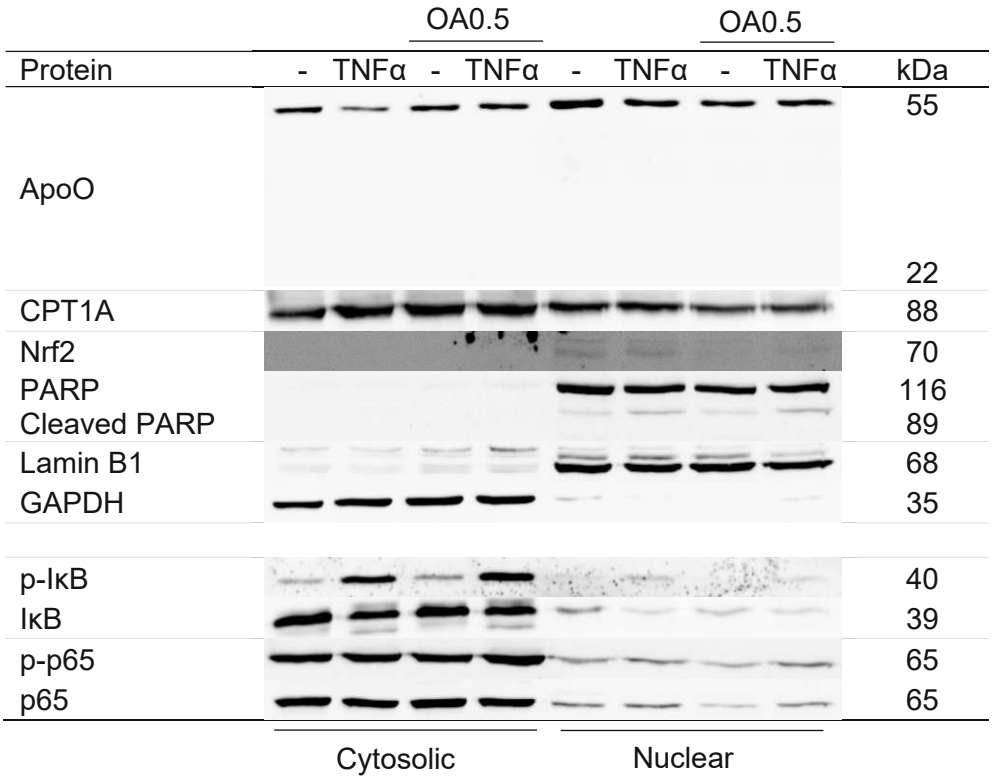

Figure 22: Effect of OA, TNFα, and OA plus TNFα on ApoO, CPT1A, Nrf2, PARP, and NF-κB proteins. HepG2 cells were not pretreated, washed twice with PBS, and incubated with treatment medium (DMEM with 2 % BSA-V (Control)), 100 ng/mL TNFα, 0.5 mM OA, or 0.5 mM OA plus 100 ng/mL TNFα for 24 h. Proteins were isolated with an Active Motif Fractionation Kit, followed by Western blot analysis using specific antibodies as described in *3.6.4 Blocking and antibody probing*, Table 13. The relative band intensities of the respective proteins from one experiment are depicted above.

				OA0.5	
Protein	Fraction	-	TNFα	-	TNFα
ApoO/GAPDH	Cytosolic	100	27	45	50
ApoO/LaminB1	Nuclear	100	64	39	63
CPT1A/GAPDH	Cytosolic	100	89	68	65
CPT1A/Lamin B1	Nuclear	100	108	76	120
Cleaved PARP/PARP	Nuclear	1.6	4.7	2.6	6.4
p-IκB/ IκB	Cytosolic	100	1162	165	1602
p-p65/p65	Cytosolic	100	131	97	214

Table 21: Effect of OA, TNFα, and OA plus TNFα on ApoO, CPT1A, Nrf2, PARP and NF-κB proteins in HepG2 cells after 24 h and isolation with an Active Motif Fractionation Kit. Relative band intensities were determined from Figure 22 and set in relation to the loading controls. Protein expression was then calculated with values from controls set as 100 % (see Equation 3). The relative intensities of the respective proteins from one experiment are listed above.

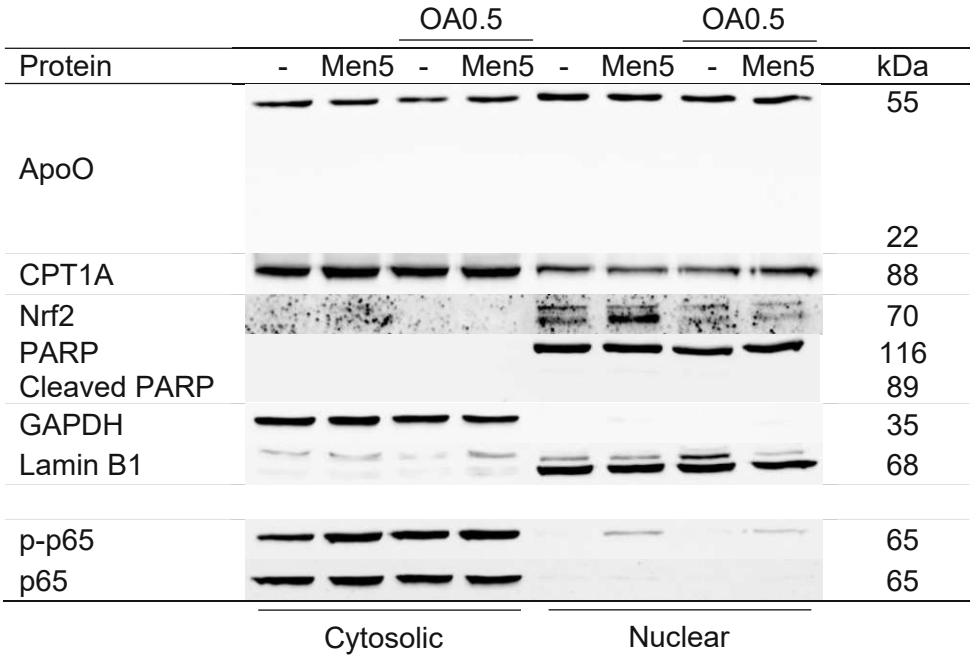

Figure 23: Effect of OA, menadione, and OA plus menadione on ApoO, CPT1A, Nrf2, PARP, and NF-κB proteins. HepG2 cells were not pretreated, washed twice with PBS, and incubated with treatment medium (DMEM with 2 % BSA-V (Control)), 5 µM menadione (Men5), 0.5 mM OA, or 0.5 mM OA plus 5 µM menadione (Men5) for 24 h. Proteins were isolated with an Active Motif Fractionation Kit, followed by Western blot analysis using specific antibodies as described in *3.6.4 Blocking and antibody probing*, Table 13. The relative band intensities of the respective proteins from one experiment are depicted above.

				OA0.5	
Protein	Fraction	-	Men5	-	Men5
ApoO/GAPDH	Cytosolic	100	86	77	147
ApoO/Lamin B1	Nuclear	100	100	81	97
CPT1A/GAPDH	Cytosolic	100	126	149	208
CPT1A/Lamin B1	Nuclear	100	89	88	170
Cleaved PARP/PARP	Nuclear	0.2	0.3	0.3	n.d.
p-p65/p65	Cytosolic	100	178	189	319

Table 22: Effect of OA, menadione, and OA plus menadione on ApoO, CPT1A, Nrf2, PARP, and NF-κB proteins in HepG2 cells after 24 h and isolation with an Active Motif Fractionation kit. Relative band intensities were determined from Figure 23 and set in relation to the loading controls. Protein expression was then calculated with values from controls set as 100 % (see Equation 3). The relative intensities of the respective proteins from one experiment are listed above.

As seen in the pictures, Figure 21 to Figure 23, glycosylated ApoO and CPT1A were unexpectedly not only found in the cytosolic but in the nuclear fraction as well. However, the respective loading controls were detected as anticipated. Therefore, it can be assumed that the fractionation after 4 and 24 h was successful. Since there is no additional mitochondrial fraction, proteins of the mitochondria, such as CPT1A, were also found in the nuclear fraction. In previous experiments in our lab, it was observed that membrane proteins are generally found in the nuclear fraction when using the Actif Motive Kit, which follows the data shown. To avoid this, it could be helpful to distinguish between more cell fractions. However, the applied kit with only separation into cytosolic and nuclear fractions was chosen to have a clearer opinion if the NF-κB pathway is activated (see below).

Based on Table 20, the ApoO production after 4 h of incubation was downregulated by all treatments for both the cytosolic and nuclear fractions. For the whole-cell lysates, similar results, except for TNFα (Table 18) were obtained. Just as for 4 h, after 24 h of treatment (Table 21 and Table 22), the ApoO content, which was found in the cytosolic fraction, was decreased by all treatments, except for 0.5 mM OA combined with 5 µM menadione. For the nuclear fraction, it stayed either at the same level as the control or was reduced as well. This would imply, that the ApoO production was neither promoted by stress, nor by lipid accumulation. Compared to the whole-cell lysates, similar results were obtained, apart from 0.5 mM OA, which led to a slight rise in the ApoO amount (Table 19).

For CPT1A, distinct results were acquired after 4 h of incubation. Its levels were elevated by all treatments in the cytosolic fraction, and reduced in the nuclear fraction, as for the whole-cell lysates (Table 18). After 24 h, the effect on CPT1A remains unclear: during the experiment with TNFα as a stress factor (Table 21), CPT1A levels were lowered by all treatments in both fractions, except for the ones with TNFα in the nuclear fraction. The attempt with 5 µM menadione (Table 22), showed that the content of CPT1A was enhanced by all treatments in the cytosolic fraction, but decreased in the nuclear fraction, except for 0.5 mM OA plus 5 µM menadione. For the whole-cell lysates (Table 19), the amount of CPT1A was only slightly elevated by TNFα and 0.5 mM OA plus 5 µM menadione, lowered by 5 µM menadione and increased by 0.5 mM OA and 0.5 mM OA plus TNFα.

When compared with all previous experiments, the Nrf2 signal was faint and located in the non-cytosolic fraction for both after 4 and 24 h (Figure 21 to Figure 23). However, it is questionable, if Nrf2 was indeed found in the nucleus since Nrf2 was previously detected in the mitochondrial fraction, which portends that Nrf2 was in its inactive form (Figure 13). Other than for the whole-cell lysates after 4 h (Table 18), the amount of Nrf2 was not reduced by all incubations but was also elevated by the treatment with TNFα. This might indicate, that cells were exposed to oxidative stress, which was not present when cells were additionally

incubated with 0.5 mM OA. Within 24 h of treatment, the obtained pictures of Nrf2 could not be quantified. Nevertheless, it can be seen that more Nrf2 was produced by the control group, TNFα and 5 µM menadione, compared to the incubations with OA, which is contrary to the results of the whole-cell lysates after 24 h (Table 19)

Regarding PARP, a faint cleavage is visible by all treatments after 4 h. In Figure 21 it seems that the treatment with TNFα led to the highest portion of cleaved PARP, which is confirmed by the ratio of cleaved PARP to full length PARP in Table 20 and follows the result of the whole-cell lysates (Figure 21 and Table 20). Furthermore, a possible protective and anti-inflammatory effect of OA might be reflected by the ratios, since the incubation with OA resulted in a lower number of cleavages than the control, which can also be seen by the OA combined with TNFα compared to TNFα alone. After 24 h and for the approach with TNFα as stress factors, cleaved PARP was detected by all incubations (Figure 22), whereas with 5 µM menadione only faint bands were visible (Figure 23). Contrary to 4 h of treatment (Table 20), no positive effects of OA might be present in the experiment with TNFα after 24 h according to the ratio of cleaved PARP to full length PARP, since more PARP was cleaved by OA compared to the control, and OA plus TNFα compared to TNFα. Due to the little portion of cleaved PARP in the approach with 5 µM menadione after 24 h, no assumptions regarding positive effects of OA can be made.

Surprisingly, the indicators for stress, the phosphorylated NF-κB proteins, were not located in the nuclear, but in the cytosolic fraction, both after 4 and 24 h. This indicates that the proteins were not regulating gene transcription at the time examined. Contrary to the whole-cell lysates (Table 20), the p-p65 production was promoted by all treatments after 4 h and reached its peak during the incubation with 0.5 mM OA plus TNFα. Even the content at 0.5 mM OA was increased compared to the control. The same applies to p-IκB. Thus, positive effects of OA might have been reflected by PARP, but not by the NF-κB proteins after 4 h of treatment. Even though the whole-cell lysates showed that OA might have anti-inflammatory effects after 24 h (Table 19), such effects were not observed for the cell fractionation based on the p-p65 levels of OA combined with stress factors compared to the stress factors alone (Table 21 and Table 22). Furthermore, no protective effect of OA after 24 h was observed, since the p-p65 content of 0.5 mM OA was higher or similar compared to the control (Table 21 and Table 22), which is also in contrast to the outcome of the whole-cell lysates (Table 19). The same applies to the measured p-IκB signal after 24 h for the experiment with TNFα (Table 21)

To better assess, if OA has positive properties on the cells, LDH assays of the supernatants of the corresponding whole-cell lysates and lysates after cell fractionation were performed and evaluated.

4.5.2 LDH assay of HepG2 cells incubated with OA plus stress factors

To achieve a representative result, the outcomes of different LDH assays were combined. For the 4 h incubation, the following three experiments were consulted: whole-cell lysates and cell fractionation, which included stress factors combined with OA (see *3.2.3.4 Addition of OA plus stress factors*, Table 4), and the whole-cell lysates of the approach containing stress factors (see *3.2.3.3 Addition of stress factors*, Table 3). Regarding 24 h incubations, the just referred experiments plus two further were evaluated: the combination of stress factors with OA, which was used to determine TG quantification (see *3.2.3.4 Addition of OA plus stress factors*, Table 4), and the whole-cell lysates of the approach containing stress factors (see *3.2.3.3 Addition of stress factors*, Table 3), the results of which are shown in *9* Appendix (Figure 26, Table 23). It has to be considered that the OA combination experiments and the stress factor attempts had different pretreatment times. While the first had no pretreatment at all, the latter was exposed to a pretreatment of 2 h with pretreatment medium (DMEM). Furthermore, the treatment medium of the OA combination experiments was not supplemented with L-Glutamine, and consisted of DMEM with 2 % BSA-V, while the treatment medium of the approaches with the stress factors contained DMEM with 2 % BSA-FAF.

Even though different experiments were combined, it has to be noted that the stress factor experiment could only be conducted for values at 0.5 mM OA, TNFα, 5 µM menadione and the control. Moreover, it was not possible to investigate 0.5 mM OA plus 5 µM menadione in the cell fraction experiment after 4 h treatment time. Therefore, the number of experiments varied.

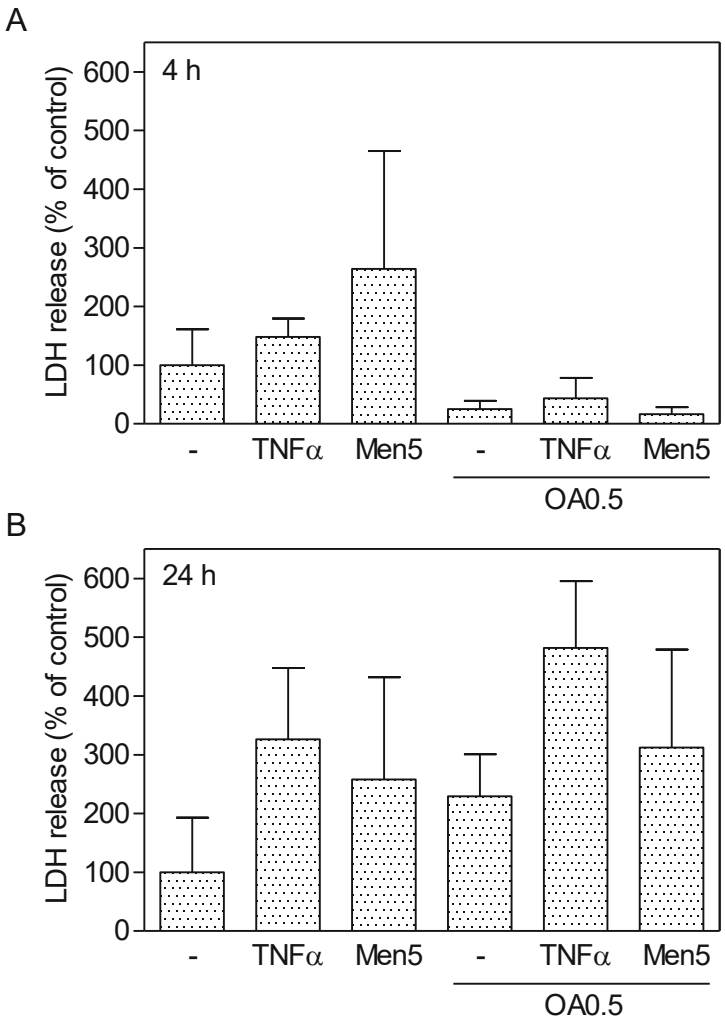

Figure 24: Effect of OA, stress factors, and OA plus stress factors on the LDH release of HepG2 cells after 4 (A) and 24 h (B). For the 4 h approach, three experiments were combined. Two of them had no pretreatment and cells were instead washed twice with PBS. Followingly, cells were incubated with treatment medium (DMEM with 2 % BSA-V (Control)), 100 ng/mL TNFα, 5 µM menadione (Men5), 0.5 mM OA, 0.5 mM OA plus 100 ng/mL TNFα or 0.5 mM OA plus 5 µM menadione (Men5). One of them was performed as duplicates and the other one was a single approach and was not incubated with 5 µM menadione and 0.5 mM OA plus 5 µM menadione. The third experiment of the 4 h approach was performed as duplicates, had a pretreatment of 2 h with DMEM, and cells were incubated with treatment medium (DMEM with 2 % BSA-FAF (Control)), 100 ng/mL TNFα, 5 µM menadione (Men5) or 0.5 mM OA. For the 24 h approach, five experiments were combined. Three of them had no pretreatment and cells were instead washed twice with PBS. Followingly, cells were incubated with treatment medium (DMEM with 2 % BSA-V (Control)), 100 ng/mL TNFα, 5 µM menadione (Men5), 0.5 mM OA, 0.5 mM OA plus 100 ng/mL TNFα or 0.5 mM OA plus 5 µM menadione (Men5). One of them was performed as a single approach, the other two as duplicates. Two of the five experiments of the 24 h approach were performed as duplicates and had a pretreatment of 2 h with DMEM and cells were incubated with treatment medium (DMEM with 2 % BSA-FAF (Control)), 100 ng/mL TNFα, 5 µM menadione (Men5) or 0.5 mM OA. Bars show mean values +/- SD of three individual experiments for Control, TNFα and OA0.5 (A), two individual experiments for Men5 and OA0.5+TNFα (A), one experiment for OA0.5+Men5 (technical duplicates, A), five individual experiments for Control, TNFα and Men5 (B), four individual experiments for OA0.5 (B) and three individual experiments for OA0.5+TNFα and OA0.5+Men5 (B).

Despite the variations due to the experimental approaches, Figure 24 illustrates that the LDH release of 0.5 mM OA is lower after 4 h than after 24 h. Furthermore, Figure 24A shows that the LDH release of the control is higher than that by OA, indicating a positive effect of OA. These outcomes were also recognized in Figure 17A. Moreover, it appears as if OA has anti-inflammatory properties since the LDH release is reduced by the combination of OA with stress

factors compared to the stress factors alone (Figure 24A). The possible protective and anti-inflammatory effect of OA that is reflected by the LDH release after 4 h, rather matches with the outcomes of the Western blot analysis of the corresponding whole-cell lysates (see *4.5.1.1 Whole-cell lysates of HepG2 cells incubated with OA plus stress factors)* than after cell fractionation. Contrary, the LDH assay after 24 h seems to confirm the result of the Western blot analysis of the cell fractionation (see *4.5.1.2 Cell fractionation of HepG2 cells incubated with OA plus stress factors).* After 24 h it is observable, that all treatments led to an LDH release higher than the control. Nevertheless, the LDH release of the exposure to 0.5 mM OA was lower than that to TNFα and 5 µM menadione, as seen before in Figure 17B. However, no protective effect of 0.5 mM OA can be interpreted.

5 Discussion

To combat the increasing prevalence of NAFLD and its consequences, a closer look has to be taken at its pathogenesis and its connection to lipid metabolism and apolipoproteins. Various publications link ApoO to lipid metabolism and NAFLD. However, it is still uncertain if ApoO fulfills protective roles or if it promotes disorders. Hence, the connection between ApoO and overnutrition as well as oxidative stress was examined to better assess the function of ApoO.

First of all, an optimal experimental environment was investigated to avoid distortions through cytotoxic impacts (Figure 5, Figure 6). Using the investigated optimal conditions, DMEM plus 2 % BSA-V, lipid accumulation through OA was determined, mimicking NAFLD. However, no optimal pretreatment conditions and periods were established. Nevertheless, the effect of no pretreatment compared to 24 h pretreatment was examined regarding LDH release and TG accumulation. While the LDH release showed similar results (Figure 9), the TG quantification indicated that the TG deposition was lower for no pretreatment than for 24 h pretreatment (Figure 10). Thus, the effect of serum starvation on cytotoxicity and TG accumulation remains unclear, whereby 24 h pretreatment seems to positively affect the latter. Furthermore, the experiments with the combinations of OA plus stress factors contained no L-glutamine to cut out this energy source and force cells to use OA-BSA instead. Even though no abnormities were observed regarding cell cytotoxicity or LDH release, it is not known how it might have influenced the cells. Further experiments are required to determine optimal pretreatment conditions and the requirement of L-glutamine during the treatments.

Overall, only small effects were observed regarding ApoO protein production. Contrary, Wu et al. measured a 2-fold increase of ApoO after incubating HepG2 cells with 1 mM OA [24]. Weijler et al. exposed cells to 2 mM OA, whereby a 7.2-fold fat accumulation, determined by quantification of Oil Red O staining, was reached, and ApoO transcript levels were 1.6-fold elevated [26]. In this study, we achieved approximately a 3-fold intracellular triglyceride increase both through 0.5 mM and 1 mM OA (Figure 7). However, we decided to focus on 0.5 mM OA, since LDH release indicated that cytotoxicity is higher by the incubation with 1 mM OA than with 0.5 mM OA (Figure 8). If higher OA concentrations were applied, other ApoO contents than in this study might have been measured. But the goal was to observe the role of ApoO in NAFLD-like conditions, and not in a cytotoxic environment, in which cell apoptosis might occur. Nevertheless, the ApoO production was slightly elevated in all experiments by the incubation with 0.5 or 1 mM OA after 24 h, except for 0.5 mM OA for the experiment with an OA concentration gradient (Table 14), and the cell fractionation of OA combined with stress factors (Table 21, Table 22). After 4 h of treatment with 0.5 and 1 mM OA, all protocols showed a decrease in the ApoO generation. Since the extent of lipid accumulation after 4 h was not

measured, it could only be assumed that ApoO production is promoted by the lipid accumulation that appears through incubation with OA after 24 h.

Wu et al. also treated HepG2 cells for 24 h with 100 ng/mL TNFα, a well-known activator of the NF-κB pathway, and detected a 2.5-fold rise in ApoO protein production. Hence, it is indicated that the ApoO generation is affected by inflammatory stimuli [24]. In this study, an increase in the ApoO content by TNFα was detected only once after 24 h of incubation (Table 16). The same applies to a treatment time of 4 h: TNFα led to enhanced ApoO levels only once (Table 18). To further investigate the connection between inflammatory responses and ApoO generation, we tested the effect of menadione, which leads to the formation of intracellular reactive oxygen species (ROS). ROS can inter alia be formed during fatty acid oxidation and can activate the NF-κB pathway. 10 µM menadione led to a decrease in ApoO production, both after 4 and 24 h of incubation, while 5 µM menadione resulted in different ApoO levels. After 24 h of treatment, the ApoO content was once slightly elevated (Table 16), and otherwise stayed at the same level as the control or was reduced. For 4 h incubation time, only one value was obtained, which also revealed a decrease (Table 18). Overall, no clear results were obtained and thus assumptions of the influence of stress factors on ApoO production could not be concluded.

Combining the assumptions of Wu et al [24] that ApoO production in HepG2 cells is affected by exposure to lipid accumulation and inflammation, cells were exposed to 0.5 mM OA plus 100 ng/mL TNFα or 5 µM menadione. After both 4 and 24 h treatment time, ApoO levels were reduced by OA plus TNFα (Table 18 to Table 21). The combination of OA with menadione after 24 h of incubation led on the one hand to a decreased ApoO production (Table 19) and on the other hand to an enhanced generation according to the cytosol fraction of the cell fractionation (Table 22). 4 h treatment time resulted in an elevated ApoO production (Table 18). Again, more experiments need to be conducted to obtain a clearer picture.

Nevertheless, a protective and anti-inflammatory effect of 0.5 mM OA on HepG2 cells might have been revealed through the incubations of OA plus stress factors. The outcome of the Western blot analysis of the whole-cell lysates led to decreased contents of p-p65 both after 4 h and 24 h of incubation, just as for p-IκB after 24 h, when 0.5 mM OA was present (Table 18, Table 19). Moreover, the corresponding LDH assay showed that after 4 h of treatment less LDH was released, comparing both the cells incubated with 0.5 mM OA to the control and OA plus stress factors to just stress factors, respectively (Figure 24A). However, this is contrasted to the results of the Western blot analysis after the cell fractionation, which displayed increased p-p65 and p-IκB levels after 4 and 24 h by the presence of 0.5 mM OA (Table 20, Table 21). Furthermore, the LDH assay also reflected no positive effects of 0.5 mM OA after incubation for 24 h (Figure 24B). Thus, the question arises, which experiment reflects

the actual impact of OA on the cells. The effect of OA could be time-dependent, as would have been illustrated by the LDH assays (Figure 24). However, the whole-cell lysates indicate protective effects of OA both after 4 and 24 h of treatment (Table 18, Table 19). In contrast, the data gained from cell fractionation implies that there is no positive impact on the cells neither after 4 nor 24 h (Table 20, Table 21). Chen et al. also reported positive effects of OA on HepG2 cells, showing that OA weakens cell apoptosis, oxidative stress, endoplasmic reticulum stress, impaired mitochondrial function, and inflammation induced by saturated palmitic acid [66]. Furthermore, the difficulty of reflecting *in vitro* metabolic disorders, and thus high plasma concentrations of fatty acids, is also described by Alsabeeh et al. They claim that saturated FAs, like palmitate and stearate, can trigger apoptosis in HepG2 cells, which was not observed for monounsaturated palmitoleate or oleate [54], the salts and ester of oleic acid. Taken together, it is questionable, whether OA should be used to mimic NAFLD if positive effects that distort the reflection of NAFLD are present.

Tian et al. inserted an adenoviral vector expressing human *APOO* (Ad-hApoO) and a vector without the sequence of the target gene as a control (Ad-CON) into L02 cells, a human hepatoma cell line. When cells were then exposed to 0.8 mM OA, increased deposition of lipid droplets was determined by Oil Red O staining. Furthermore, they observed that cells transfected with Ad-hApoO displayed more lipids than with Ad-CON, which might imply that overexpression of *APOO* inhibits FAO. Moreover, mice were transfected with the vectors and it was proven that FAO genes – containing the gene encoding for CPT1 – were significantly reduced in the liver of mice with the Ad-hApoO vector. Thus, the assumption that overexpression of *APOO* impairs FAO is supported. Other genes that are part of adipogenesis and *de novo* lipid synthesis were also significantly elevated [27]. Looking at the measured CPT1A relative intensities of this study, it was found that CPT1A protein production always increased with the raise of ApoO levels, except for the following experiments: 0.5 mM OA for the 24 h experiment with OA concentration gradient (Table 15), 5 µM menadione for the 24 h experiments with stress factors (Table 16), TNFα and OA plus menadione for the 4 h experiment with OA plus stress factors (Table 18). Therefore, according to our results, it seems that FAO was not affected by upregulated ApoO levels as is reflected by the CPT1A content. However, it has to be noted that the protein production of ApoO was only slightly elevated. Hence, it is unknown whether higher contents of ApoO would have led to a decreased CPT1A production.

Instead of obtaining decreased CPT1A contents for raised ApoO levels, increased CPT1A production was observed by the incubations with OA after 24 h, except for 0.5 mM OA for the experiment with OA concentration gradient (Table 15), 0.5 mM OA for the cell fractionation of OA plus TNFα (Table 21) and 0.5 mM OA for the nuclear fraction of the cell fractionation of OA

plus menadione (Table 22). Otherwise, the increase of CPT1A is likely traced back to the lipid accumulation caused by the incubation with OA, since more free fatty acids are present and are therefore metabolized. After 4 h incubation time, no assumptions can be made due to the lack of consistency of observed CPT1A intensities. However, as mentioned before, it was not observed to what extent lipid accumulation occurred after 4 h of treatment.

Regarding cell fractionations, calculated values should not be used as definite numbers, since the purpose of the cell fractionation was to gain insight into ongoing processes including locations of the proteins rather than quantifying protein contents. Therefore, the Active Motif Kit seemed to be sufficient due to its ability to locate the phosphorylated NF-κB proteins, which unfortunately were found in the cytosolic fraction instead of the nuclear fraction. However, there was no clear fraction for membrane and mitochondrial proteins, leading to the detection of ApoO and CPT1A both in the cytosolic and nuclear fractions. Hence, the relative intensities lose significance, since it is not known how the proteins were separated and which fraction reflected the actual protein levels. The Abcam Kit on the other hand led to a better separation into cytosolic, mitochondrial, and nuclear fractions. However, an additional loading control and a more time-consuming sample preparation are required. For both kits, it was not possible to establish the protein concentrations by Pierce BCA assay due to the high background of the sample buffers. Thus, it is difficult to compare the relative intensities with other experiments. Moreover, it should be considered that less protein is present in the nuclear fraction than in the cytosolic fraction, which contributes to the problem of relative intensities.

Another difficulty was interpreting the values measured after 4 h. As already stated, the intracellular TG content was only determined after 24 h, but not after 4 h. Furthermore, it has to be noted that even though activations by e.g. phosphorylation occur rapidly within several minutes, protein production takes longer. Thus, the NF-κB pathway might be activated after 4 h or even much earlier, but the effect on the protein production might be observable later on. This reflects the overall problem of the applied methods: only certain time points can be assessed, but happenings between them can only be assumed. This might explain the different outcomes after 4 h of treatment. However, they could also simply reflect the distribution of the measured values and thus of the applied methods.

Regarding the used methods, it has to be considered that all measured values were first compared to the loading control and then set in relation to the control group of each experiment. Imperfections occurring during the incubation of the cells, sample preparation, and analysis of the controls can distort reality and therefore affect the measured relative intensities. Furthermore, it should be kept in mind that there is no guarantee that the values produced by the loading control are truly reflecting the biology of the cells.

Taken together, it is challenging to estimate both the effects of overnutrition – simulated by increased TG levels through incubation with OA – and oxidative stress – caused by TNFα and menadione – on ApoO protein production. Several factors have to be taken into account: problems with the quantification of Western blot analysis (e.g. appropriate controls), inconsistency of experiments and therefore lack of repeated measurements, the unknown effect of pretreatment and depletion of L-glutamine, and challenges in cell culture (e.g. finding a balance between lipid accumulation and lipotoxicity). Nevertheless, non-alcoholic steatosis and stress situations were successfully simulated and quick assays were found to assess cytotoxicity.

To conclude, we suppose that investigating the impacts of overnutrition and oxidative stress on apolipoprotein O has the potential to reveal possible connections to human health in general and NAFLD.

6 Outlook

For this master thesis, a new way of reflecting the pathobiochemistry of NAFLD was studied, and within this context, ApoO was investigated. HepG2 cells were incubated with *(i)* OA, to reach triglyceride accumulation as in NAFLD, *(ii)* TNFα and menadione, two stress factors that can directly or indirectly activate the NF-κB pathway, and *(iii)* combinations of OA plus stress factors. Overall, only small effects on ApoO protein production were observed and ApoO might be formed due to lipid accumulation. Regarding the NAFLD model, the following proposals are given to investigate in the future:

- Replace oleic acid treatment with palmitic acid or combinations of both to overcome possible protective effects of oleic acid on the cells. Since palmitic acid is a saturated fatty acid that can trigger lipotoxicity, low concentrations should be applied.
- Observe the long-term effects of oleic acid on the cells by raising the incubation time to e.g. 48 h. Probably, stronger effects can be seen by longer lipid accumulation.
- Optimize pretreatment conditions by testing the impact of different pretreatment times and BSA variations on cell integrity (LDH and NRR assay).
- Test the effect of L-glutamine starvation on cell integrity (LDH and NRR assay).
- Repeat the experiments for representative results and estimate, whether distributions can be traced back to imperfect handling or the applied methods themselves.
- Test the enzymatic degradation of LDH by measuring the LDH release directly after the treatment time and after a certain period stored at -20 °C to gain the most accurate reflection of true biology.
- Observe the level of cytotoxicity not only by LDH release but also by measuring cell apoptosis and mitochondrial reactive oxygen species, e.g. by flow cytometry. Hence, the fact that stressed cells produce more LDH and thus release more LDH than non-stressed cells for equal membrane damage can be considered.
- Determine the TG accumulation after exposure to oleic acid for 4 h to assess when lipid depositions occur.

7 Abbreviations

APO	Apolipoprotein
AB	Antibody
ACS	Acute coronary syndrome
Belly Dancer	Stovall Belly Dancer Shaker
BSA	Bovine serum albumin
BSA-FAF	Bovine serum albumin fatty acid free
BSA-V	Bovine serum albumin fraction V
CF	Cell fractionation
CLB	Complete Lysis Buffer
CM	Chylomicron
CoA	Coenzyme A
CPT1	Carnitine palmitoyltransferase-1
CPT2	Carnitine-palmitoyltransferase-2
CRAT	Carnitine acetyl-transferase
CROT	Carnitine-octanolyltransferase
ddH_2O	Double-distilled water
DMEM	Dulbecco's Modified Eagle's Medium
DNL	*De novo* lipogenesis
ER	Endoplasmic reticulum
FA	Fatty acid
FCS	Fetal calf serum
FFA	Free fatty acid
FAO	Fatty acid oxidation
GAPDH	Glyceraldehyde 3-phosphate dehydrogenase
GM	Growth medium
HB	Hypotonic Buffer
HCC	Hepatocellular carcinoma
HDL	High density lipoprotein
HRP	Horseradish peroxidase
IDL	Intermediate density lipoprotein
IκB	Inhibitor of nuclear factor-kappa B
LDH	Lactate dehydrogenase
LDL	Low density lipoprotein
Lp(a)	Lipoprotein(a)
LPL	Lipoprotein lipase
Men	Menadione
Men5	Menadione 5 µM
Men10	Menadione 10 µM
MetS	Metabolic syndrome
MTTP	Microsomal triglyceride transfer protein
n.d.	Not detected
NAFL	Non-alcoholic fatty liver
NAFLD	Non-alcoholic fatty liver disease
NASH	Non-alcoholic steatohepatitis
NC	Nitrocellulose
NF-κB	Nuclear factor-kappa B
Nrf2	Nuclear factor erythroid-derived 2-like 2
OA	Oleic acid-albumin
OA0.5	Oleic acid-albumin 0.5 mM
OA1	Oleic acid-albumin 1 mM
p65	Transcription factor p65
p-IκB	Phosphorylated IκB
p-p65	Phosphorylated p65
PARP	Poly (ADP-ribose) polymerase

PBS	Phosphate Buffered Saline
PBS/PI	Phosphate Buffered Saline /Phosphatase Inhibitors
PIC	Protease inhibitor cocktail
ROS	Reactive oxygen species
SD	Standard deviation
SDS-PAGE	Sodium dodecylsulfate polyacrylamide gel electrophoresis
TEMED	N, N, N', N'-Tetramethylethylene-diamine
TG	Triglycerides
TNFα	Tumor necrosis factor alpha
TOMM20	Translocase of outer mitochondrial membrane 20
Tris	Tris(hydroxymethyl)aminomethane
T2DM	Type 2 diabetes mellitus
VLDL	Very low density lipoprotein
WB	Western blot analysis
WCL	Whole-cell lysates

8 References

(1) Jonas, A.; Phillips, M. C. In *Biochemistry of lipids, lipoproteins and membranes*; Elsevier, 2008.

(2) Schwandt, P. *Handbuch der Fettstoffwechselstörungen: Dyslipoproteinämien und Atherosklerose; Diagnostik, Therapie und Prävention; mit 193 Tabellen*; Schattauer Verlag, 2007.

(3) Díaz-Aragón, A.; Ruiz-Gastélum, E.; Álvarez-López, H. Knowing the basic mechanisms of lipid metabolism. *Cardiovascular and Metabolic Science* **2021,** *32* (S3), 147.

(4) Kwiterovich Jr, P. O. The metabolic pathways of high-density lipoprotein, low-density lipoprotein, and triglycerides: a current review. *The American journal of cardiology* **2000,** *86* (12), 5.

(5) Heeren, J.; Scheja, L. Metabolic-associated fatty liver disease and lipoprotein metabolism. *Molecular metabolism* **2021,** *50*, 101238.

(6) Lilley, L. L.; Collins, S. R.; Snyder, J. S.; Savoca, D. *Pharmacology and the Nursing Process7: Pharmacology and the Nursing Process*; Elsevier health sciences, 2014.

(7) Evans, R.; Frayn, K. N. Human metabolism: a regulatory perspective. **2019**.

(8) Ridgway, N.; McLeod, R. *Biochemistry of lipids, lipoproteins and membranes*; Elsevier, 2008.

(9) Heinrich, P. C.; Müller, M.; Graeve, L. *Löffler/Petrides Biochemie und Pathobiochemie*; Springer-Verlag, 2014.

(10) Kliegman, R.; Stanton, B.; St Geme, J.; Schor, N.; Behrman, R.; Elsevier, Philadelphia, PA, USA, 2019.

(11) Vasudevan, D. M.; Sreekumari, S.; Vaidyanathan, K. *Textbook of biochemistry for medical students*; Jaypee brothers Medical publishers, 2019.

(12) Ren, L.; Yi, J.; Li, W.; Zheng, X.; Liu, J.; Wang, J.; Du, G. Apolipoproteins and cancer. *Cancer medicine* **2019,** *8* (16), 7032.

(13) Mehta, A.; Shapiro, M. D. Apolipoproteins in vascular biology and atherosclerotic disease. *Nature Reviews Cardiology* **2022,** *19* (3), 168.

(14) Das, M.; Gursky, O. Amyloid-forming properties of human apolipoproteins: sequence analyses and structural insights. *Lipids in Protein Misfolding* **2015**, 175.

(15) Wu, C. L.; Zhao, S. P.; Yu, B. L. Intracellular role of exchangeable apolipoproteins in energy homeostasis, obesity and non-alcoholic fatty liver disease. *Biological Reviews* **2015,** *90* (2), 367.

(16) Waisundara, V. Y.; Jovandaric, M. Z. *Apolipoproteins, Triglycerides and Cholesterol*; BoD–Books on Demand, 2020.

(17) Yin, Y.; Wang, Z. ApoE and neurodegenerative diseases in aging. *Aging and Aging-Related Diseases* **2018**, 77.

(18) Tran, T. T.; Corsini, S.; Kellingray, L.; Hegarty, C.; Le Gall, G.; Narbad, A.; Müller, M.; Tejera, N.; O'Toole, P. W.; Minihane, A.-M. APOE genotype influences the gut microbiome structure and function in humans and mice: relevance for Alzheimer's disease pathophysiology. *The FASEB Journal* **2019,** *33* (7), 8221.

(19) Lamant, M.; Smih, F.; Harmancey, R.; Philip-Couderc, P.; Pathak, A.; Roncalli, J.; Galinier, M.; Collet, X.; Massabuau, P.; Senard, J.-M. ApoO, a novel apolipoprotein, is an original glycoprotein up-regulated by diabetes in human heart. *Journal of Biological Chemistry* **2006,** *281* (47), 36289.

(20) Nielsen, L. B.; Bartels, E. D.; Bollano, E. Overexpression of apolipoprotein B in the heart impedes cardiac triglyceride accumulation and development of cardiac dysfunction in diabetic mice. *Journal of Biological Chemistry* **2002,** *277* (30), 27014.

(21) Koob, S.; Barrera, M.; Anand, R.; Reichert, A. S. The non-glycosylated isoform of MIC26 is a constituent of the mammalian MICOS complex and promotes formation of crista junctions. *Biochimica et Biophysica Acta (BBA)-Molecular Cell Research* **2015,** *1853* (7), 1551.

(22) Yu, B.-l.; Wu, C.-l.; Zhao, S.-p. Plasma apolipoprotein O level increased in the patients with acute coronary syndrome. *Journal of lipid research* **2012,** *53* (9), 1952.

(23) Overbaugh, K. J. Acute coronary syndrome. *AJN The American Journal of Nursing* **2009,** *109* (5), 42.
(24) Wu, C.-L.; Zhao, S.-P.; Yu, B.-L. Microarray analysis provides new insights into the function of apolipoprotein O in HepG2 cell line. *Lipids in health and disease* **2013,** *12* (1), 1.
(25) Schmidinger, B.; Weijler, A. M.; Schneider, W. J.; Hermann, M. Hepatosteatosis and estrogen increase apolipoprotein O production in the chicken. *Biochimie* **2016,** *127*, 37.
(26) Weijler, A. M.; Schmidinger, B.; Kapiotis, S.; Laggner, H.; Hermann, M. Oleic acid induces the novel apolipoprotein O and reduces mitochondrial membrane potential in chicken and human hepatoma cells. *Biochimie* **2018,** *147*, 136.
(27) Tian, F.; Wu, C.-l.; Yu, B.-l.; Liu, L.; Hu, J.-r. Apolipoprotein O expression in mouse liver enhances hepatic lipid accumulation by impairing mitochondrial function. *Biochemical and biophysical research communications* **2017,** *491* (1), 8.
(28) Turkieh, A.; Caubère, C.; Barutaut, M.; Desmoulin, F.; Harmancey, R.; Galinier, M.; Berry, M.; Dambrin, C.; Polidori, C.; Casteilla, L. Apolipoprotein O is mitochondrial and promotes lipotoxicity in heart. *The Journal of clinical investigation* **2014,** *124* (5), 2277.
(29) Liu, Y.; Xiong, Z.; Zhou, W.; Chen, Y.; Huang, Q.; Wu, Y. Role of apolipoprotein O in autophagy via the p38 mitogen-activated protein kinase signaling pathway in myocardial infarction. *Clinics* **2022,** *77*, 100046.
(30) Mostofa, M. G.; Tran, M.; Gilling, S.; Lee, G.; Fraher, O.; Jin, L.; Kang, H.; Park, Y.-K.; Lee, J.-Y.; Wang, L. MicroRNA-200c coordinates HNF1 homeobox B and apolipoprotein O functions to modulate lipid homeostasis in alcoholic fatty liver disease. *Journal of Biological Chemistry* **2022,** *298* (6).
(31) Jiang, Z. G.; Robson, S. C.; Yao, Z. Lipoprotein metabolism in nonalcoholic fatty liver disease. *Journal of biomedical research* **2013,** *27* (1), 1.
(32) Polyzos, S. A.; Goulis, D. G.; Giouleme, O.; Germanidis, G. S.; Goulas, A. Anti-obesity Medications for the Management of Nonalcoholic Fatty Liver Disease. *Current Obesity Reports* **2022**, 1.
(33) Paik, J. M.; Henry, L.; De Avila, L.; Younossi, E.; Racila, A.; Younossi, Z. M. Mortality related to nonalcoholic fatty liver disease is increasing in the United States. *Hepatology communications* **2019,** *3* (11), 1459.
(34) Ludwig, J.; Viggiano, T. R.; Mcgill, D. B.; Oh, B. Mayo Clinic Proceedings, 1980; p 434.
(35) Wang, J.; He, W.; Tsai, P.-J.; Chen, P.-H.; Ye, M.; Guo, J.; Su, Z. Mutual interaction between endoplasmic reticulum and mitochondria in nonalcoholic fatty liver disease. *Lipids in Health and Disease* **2020,** *19* (1), 1.
(36) Friedman, S. L.; Neuschwander-Tetri, B. A.; Rinella, M.; Sanyal, A. J. Mechanisms of NAFLD development and therapeutic strategies. *Nature medicine* **2018,** *24* (7), 908.
(37) Drenth, J. P.; Schattenberg, J. M. The nonalcoholic steatohepatitis (NASH) drug development graveyard: established hurdles and planning for future success. *Expert Opinion on Investigational Drugs* **2020,** *29* (12), 1365.
(38) Huang, D. Q.; El-Serag, H. B.; Loomba, R. Global epidemiology of NAFLD-related HCC: Trends, predictions, risk factors and prevention. *Nature Reviews Gastroenterology & Hepatology* **2021,** *18* (4), 223.
(39) Elfawy, H. A.; Das, B. Crosstalk between mitochondrial dysfunction, oxidative stress, and age related neurodegenerative disease: Etiologies and therapeutic strategies. *Life sciences* **2019,** *218*, 165.
(40) Li, J.; Wang, T.; Liu, P.; Yang, F.; Wang, X.; Zheng, W.; Sun, W. Hesperetin ameliorates hepatic oxidative stress and inflammation via the PI3K/AKT-Nrf2-ARE pathway in oleic acid-induced HepG2 cells and a rat model of high-fat diet-induced NAFLD. *Food & Function* **2021,** *12* (9), 3898.
(41) Simpson, D. S.; Oliver, P. L. ROS generation in microglia: understanding oxidative stress and inflammation in neurodegenerative disease. *Antioxidants* **2020,** *9* (8), 743.
(42) Taguchi, K.; Yamamoto, M. The KEAP1–NRF2 system as a molecular target of cancer treatment. *Cancers* **2020,** *13* (1), 46.
(43) Ramadass, V.; Vaiyapuri, T.; Tergaonkar, V. Small molecule NF-κB pathway inhibitors in clinic. *International journal of molecular sciences* **2020,** *21* (14), 5164.

(44) Perla, F. M.; Prelati, M.; Lavorato, M.; Visicchio, D.; Anania, C. The role of lipid and lipoprotein metabolism in non-alcoholic fatty liver disease. *Children* **2017,** *4* (6), 46.
(45) Jakab, J.; Miškić, B.; Mikšić, Š.; Juranić, B.; Ćosić, V.; Schwarz, D.; Včev, A. Adipogenesis as a potential anti-obesity target: A review of pharmacological treatment and natural products. *Diabetes, Metabolic Syndrome and Obesity: Targets and Therapy* **2021,** *14*, 67.
(46) Schlaepfer, I. R.; Joshi, M. CPT1A-mediated fat oxidation, mechanisms, and therapeutic potential. *Endocrinology* **2020,** *161* (2).
(47) Adeva-Andany, M. M.; Carneiro-Freire, N.; Seco-Filgueira, M.; Fernández-Fernández, C.; Mouriño-Bayolo, D. Mitochondrial β-oxidation of saturated fatty acids in humans. *Mitochondrion* **2019,** *46*, 73.
(48) Ku, C. W.; Tan, Z. W.; Lim, M. K.; Tam, Z. Y.; Lin, C.-H.; Ng, S. P.; Allen, J. C.; Lek, S. M.; Tan, T. C.; Tan, N. S. Spontaneous miscarriage in first trimester pregnancy is associated with altered urinary metabolite profile. *BBA clinical* **2017,** *8*, 48.
(49) Grabner, G. F.; Xie, H.; Schweiger, M.; Zechner, R. Lipolysis: cellular mechanisms for lipid mobilization from fat stores. *Nature Metabolism* **2021,** *3* (11), 1445.
(50) Su, X.; Peng, D. The exchangeable apolipoproteins in lipid metabolism and obesity. *Clinica chimica acta* **2020,** *503*, 128.
(51) Cholankeril, R.; Patel, V.; Perumpail, B. J.; Yoo, E. R.; Iqbal, U.; Sallam, S.; Shah, N. D.; Kwong, W.; Kim, D.; Ahmed, A. Anti-diabetic medications for the pharmacologic management of NAFLD. *Diseases* **2018,** *6* (4), 93.
(52) Borenfreund, E.; Puerner, J. A. Toxicity determined in vitro by morphological alterations and neutral red absorption. *Toxicology letters* **1985,** *24* (2-3), 119.
(53) abcam. Neutral Red Assay Kit - Cell Viability/Cytotoxicity (ab234039), https://www.abcam.com/neutral-red-assay-kit-cell-viability--cytotoxicity-ab234039.html, accessed on July 17, 2022
(54) Alsabeeh, N.; Chausse, B.; Kakimoto, P. A.; Kowaltowski, A. J.; Shirihai, O. Cell culture models of fatty acid overload: Problems and solutions. *Biochimica et Biophysica Acta (BBA)-Molecular and Cell Biology of Lipids* **2018,** *1863* (2), 143.
(55) Lothar, T. Clinical Laboratory Diagnostics 2020, https://www.clinical-laboratory-diagnostics-2020.com/index.html, accessed on September 10, 2022
(56) AG Scientific. LDH Cytotoxicity Assay Kit, https://agscientific.com/products/enzymes/d-l-enzymes/ldh-cytotoxicity-assay-kit-400-assays.html, accessed on July 22, 2022
(57) abcam. Triglyceride Assay Kit - Quantification (ab65336), https://www.abcam.com/triglyceride-assay-kit-quantification-ab65336.html, accessed on July 17, 2022
(58) ThermoFisher Scientific™. Pierce™ BCA Protein Assay Kit, https://www.thermofisher.com/order/catalog/product/23225, accessed on July 22, 2022
(59) abcam. Anti-CPT1A antibody [8F6AE9], https://www.abcam.com/cpt1a-antibody-8f6ae9-ab128568.html, accessed on August 12, 2022
(60) abcam. Anti-Nrf2 antibody [3G7] ab89443, https://www.abcam.com/nrf2-antibody-3g7-ab89443.html, accessed on August 12, 2022
(61) Cell Signaling. PARP Antibody #9542, https://www.cellsignal.com/products/primary-antibodies/parp-antibody/9542, accessed on August 12, 2022
(62) abcam. Recombinant Anti-NF-kB p65 antibody [E379] (ab32536), https://www.abcam.com/nf-kb-p65-antibody-e379-ab32536.html, accessed on August 12, 2022
(63) ThermoFisher Scientific™. Phospho-NFkB p65 (Ser529) Monoclonal Antibody (B33B4WP), PE, eBioscience™, https://www.thermofisher.com/antibody/product/Phospho-NFkB-p65-Ser529-Antibody-clone-B33B4WP-Monoclonal/12-9863-41?ef_id=EAIaIQobChMI2rfyls65-QIVAeR3Ch0nWQATEAAYASAAEgImb_D_BwE:G:s&s_kwcid=AL!3652!3!278928573340!!!g!!!1454324556!63404918784&cid=bid_pca_frg_r01_co_cp1359_pjt0000_bid00000_0se_gaw_dy_pur_con&gclid=EAIaIQobChMI2rfyls65-QIVAeR3Ch0nWQATEAAYASAAEgImb_D_BwE, accessed on August 12, 2022

(64) Watai, Y.; Kobayashi, A.; Nagase, H.; Mizukami, M.; McEvoy, J.; Singer, J. D.; Itoh, K.; Yamamoto, M. Subcellular localization and cytoplasmic complex status of endogenous Keap1. *Genes to Cells* **2007,** *12* (10), 1163.

(65) abcam. Cell Fractionation Kit - Standard (ab109719), https://www.abcam.com/cell-fractionation-kit-standard-ab109719.html?pageNumber=2&productWallTab=ShowAll&PageSize=10&SortOrder=VoteDesc, accessed on August 25, 2022

(66) Chen, X.; Li, L.; Liu, X.; Luo, R.; Liao, G.; Li, L.; Liu, J.; Cheng, J.; Lu, Y.; Chen, Y. Oleic acid protects saturated fatty acid mediated lipotoxicity in hepatocytes and rat of non-alcoholic steatohepatitis. *Life sciences* **2018,** *203*, 291.

9 Appendix

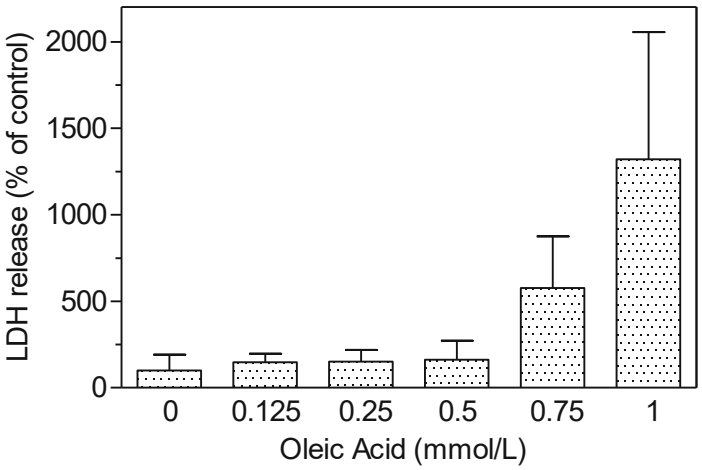

Figure 25: Combined LDH release values of all experiments after 24 h treatment. Cells were pretreated 24 h for five experiments and 2 h for one experiment with pretreatment medium (DMEM) containing 2 % BSA-FAF. For three experiments, cells were not pretreated and instead washed twice with PBS and the treatment medium contained no L-glutamine. Followingly, cells were exposed to a treatment with the treatment medium consisting of DMEM with 2 % BSA-V for the three experiments without pretreatment and the two experiments with 24 h pretreatment. The remaining experiments contained DMEM with 2 % BSA-FAF as treatment medium. All experiments except one with no pretreatment were measured in biological duplicates. Bars show mean values +/- SD of nine individual experiments for Control, four individual experiments for 0.125, 0.25 and 1 mM OA, eight individual experiments for 0.5 mM OA, and two individual experiments for 0.75 mM OA.

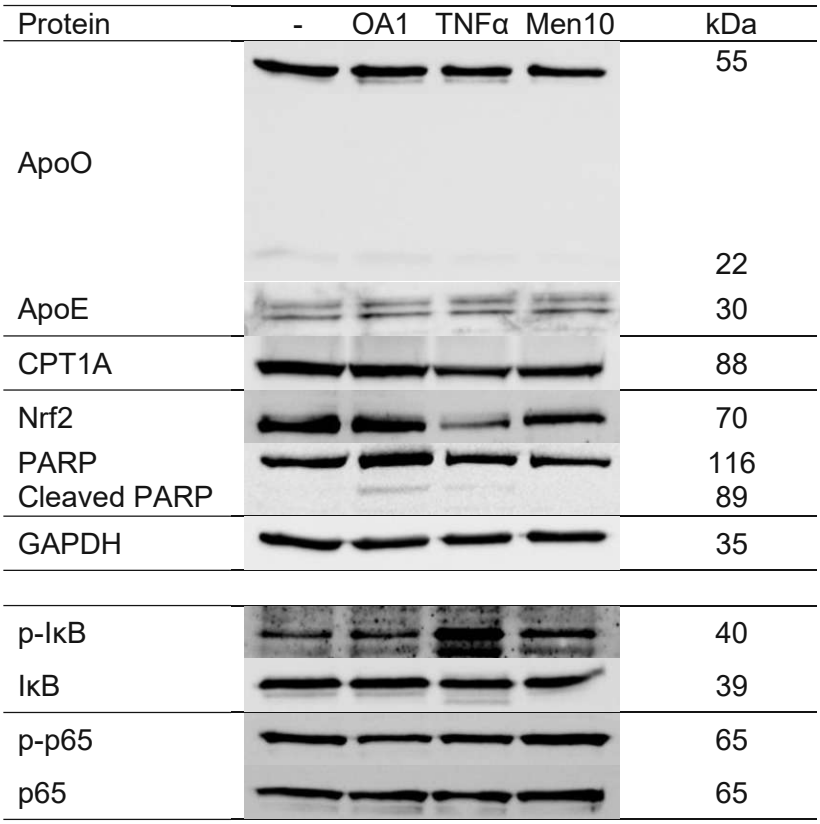

Figure 26: Effect of OA and stress factors on ApoO, ApoE, CPT1A, Nrf2, PARP and NF-κB proteins. HepG2 cells were pretreated with pretreatment medium (DMEM) with 2 % BSA-FAF for 24 h and incubated with treatment medium (DMEM with 2 % BSA-FAF (Control)), 1 mM OA, 100 ng/mL TNFα or 10 µM menadione for 24 h. Proteins were isolated in whole cell lysates followed by Western blot analysis using specific antibodies as described in *3.6.4 Blocking and antibody probing*, Table 13. The relative band intensity of the respective proteins from one experiment of two performed are depicted above.

Protein	-	OA1	TNFα	Men10
ApoO/GAPDH	100	123	98	79
ApoE/GAPDH	100	129	107	117
CPT1A/GAPDH	100	105	69	84
Nrf2/GAPDH	100	97	42	79
Cleaved PARP/PARP	n.d.	4.5	3.3	n.d.
p-IκB/ IκB	100	109	864	236
p-p65/p65	100	52	79	111

Table 23: Effect of OA and stress factors on ApoO, ApoE, CPT1A, Nrf2, PARP and NF-κB proteins in HepG2 cells after 24 h. Relative band intensities were determined from Figure 26 and set in relation to the loading controls. Protein expression was then calculated with values from controls set as 100 % (see Equation 3). The relative intensities of the respective proteins from one experiment of two performed are listed above.

9.2 List of Tables

9.3 List of Figures